The Dissertation Committee for Megan Davis-Fields Certifies that this is the approved version of the following Dissertation:

The Role of Mechanical Properties in Infections

Committee:

Vernita Gordon, Supervisor

Bryan Davies

Lauren Ehrlich

Laura Suggs

The Role of Mechanical Properties in Infections

by

Megan Davis-Fields

Dissertation

Presented to the Faculty of the Graduate School of

The University of Texas at Austin

in Partial Fulfillment

of the Requirements

for the Degree of

Doctor of Philosophy

The University of Texas at Austin

August 2018

Dedication

To my family: To my Mom for her unwavering comfort and encouragement through the best and worst of times. To my Dad for inspiring even a portion of his passion and drive in me. To Amy for being my best friend who can offer the wisdom I need to hear. To Nick for instilling in me an unyielding sense of humor so I can laugh through anything. And last but not least, to Leia who I know will never read this because, well, she's a dog, but on whose unknowing, furry shoulders rested my day to day happiness and joy. I would never be here without my family and their unconditional love and support.

Acknowledgements

I first and foremost would like to acknowledge my always-amazing lab mates Kristin, Layla, Karishma, Jacob, Chris, Orrin, Jaime, and everyone else who passed through our lab. Thank you for your friendship, the overly long lunches and coffee breaks, and the help making my science what it is today. To Dr. Gordon, thank you for being one of the world's most understanding PIs and trying to teach me that my humor doesn't need to be so self-deprecating. I'd like to thank my committee, Dr. Bryan Davies, Dr. Lauren Ehrlich, Dr. Laura Suggs, and Dr. Marvin Whiteley. Without your input and guidance, my projects would have never progressed and succeeded in the ways they did. To Dr. Ruth Buskirk and Mrs. Teresa Coomaraswamy, thank you for helping me discover my love of teaching and sharing science with anyone willing to listen.

I'd also like to sincerely thank everyone in my cohort. I gained friends and scientific peers that became family. I'd especially like to acknowledge Alfire, Rasheen, Gizelle, Jessica, Courtney, Amanda, and Natasha for being the greatest group of friends and lady scientists. To my Microbiology compatriots Alex and Justine, the classes, presentations, and research were so much more enjoyable with great colleagues like you. I had the best support system and friends back home, encouraging me everyday. I'd lastly like to especially thank the person who was so integral to my graduate school career, Kristin Kovach. Thank you for your patience with my never-ending questions, for teaching me Physics, for dog-sitting, for your support, and for being such a dear friend and the best lab wife ever. I couldn't have done it without you.

Abstract

The Role of Mechanical Properties in Infections

Megan Davis-Fields, Ph.D.

The University of Texas at Austin, 2018

Supervisor: Vernita Gordon

Pseudomonas aeruginosa is an opportunistic human pathogen that forms antibiotic resistant and immune system resistant biofilms leading to chronic infections in immunocompromised patients. In Cystic Fibrosis patients, these decades-long infections evolve to produce more biofilm matrix polymers resulting in chemical benefits and unknown physical benefits. Using oscillatory bulk rheology, I measured the changing mechanical properties resulting from these evolutionary adaptations. This revealed that mechanical properties conferred to the biofilm were unique to each different matrix polymer and that during these long-term infections, retained and enhanced biofilm mechanical toughness. Enhanced toughness may aid in resistance to the immune system, therefore I created a new method to explore the limitations of neutrophil phagocytosis based on the mechanical properties of the target of engulfment. I found that mechanical properties of large, abiotic, viscoelastic targets directly influence the success of neutrophil phagocytosis and that stiffer targets with higher elastic modulus have a decreased likelihood of being successfully engulfed by neutrophils.

Table of Contents

List of Tables

List of Figures

Chapter 1: Introduction

1.1 Overview

Biophysics is a branch of science concerned with the application of physical principles and methods to biological problems. Biological problems are often considered and explored in a context solely of biological phenomena and biological answers; however, more context is needed to fully evaluate these problems. Physical interactions influence biological development and resulting biological systems have physical properties. Physical and biological phenomena influence each other, and that influence is often overlooked. One such system where biological and physical properties collide is in bacterial biofilms.

Bacterial biofilms are complex biological systems with intertwined chemical, physical, and biological properties. *Pseudomonas aeruginosa,* an opportunistic human pathogen, is responsible for chronic infections where the bacteria are protected within their biofilm. The bacteria are constantly evolving during infections, allowing us to study the beneficial mutations they gain. These mutations have been studied for their alteration in biological properties, but my dissertation will focus on the physical, mechanical changes to the biofilm over the course of infection and whether these changes could be beneficial in evading neutrophil phagocytosis. The chapters will discuss methods to measure biofilm mechanics, changes to biofilm mechanics during infection, and a new way to assess the ability of neutrophils to engulf large targets of varying mechanics.

In my introduction, I will cover in brief the background of biofilms, *Pseudomonas aeruginosa*, and neutrophils.

1.2 BIOFILMS

1.2.1 Biofilm Background

Bacterial biofilms are aggregates of bacteria surrounded by a matrix of extracellular polymeric substances, EPS. When embedded within a biofilm, bacteria can more easily adhere to each other and to surfaces [1]. Communication and structural organization of the bacteria within the biofilm facilitates these single-cell organisms living as a community. As bacteria switch from a planktonic to a sessile lifestyle, there are corresponding regulatory changes that alter gene production [2]. These gene changes tend to increase the production of EPS material and decrease production of motility factors [3]. The increase of EPS within a biofilm aids the bacteria in trapping nutrients and decreases the efficacy of antibiotics[4]. Due to the nature of biofilms, bacteria within a biofilm are inherently difficult to remove from surfaces or clear from the body.

1.2.2 Biofilms and Health

Annually, biofilm infections affect 17 million Americans, cause at least 550,000 American deaths, and cost the US healthcare system billions of dollars [5-7]. Mature biofilm infections have higher resistance to antimicrobials and the host immune defense than do their genetically-identical planktonic counterparts [8-11]. Mechanical removal is often required to clear biofilm infections, because they resist antibiotics as well as other antimicrobials and evade the host immune defense. The mechanical integrity of the biofilm matrix leads to antibiotic resistance since the stable spatial arrangement of bacteria gives rise to differentiated microenvironments with phenotypic antibiotic resistance; indeed, mechanical breakup of biofilms can render bacteria more susceptible to

antibiotics [12,13]. Debridement, the mechanical scraping-away of biofilm, is part of the standard-of-care for chronic wounds and has been shown to induce a brief window of increased antibiotic susceptibility for the biofilm remaining in the wound [14]. Thus, biofilms' mechanical integrity and their response under mechanical agitation are tightly linked to medical impact and possibilities for treatment [15].

1.3 *PSEUDOMONAS AERUGINOSA*

1.3.1 *Pseudomonas aeruginosa* Overview

Pseudomonas aeruginosa is a Gram-negative, non-fermenting bacterium that is an opportunistic human pathogen and by far the best-characterized, most widely-studied model organism for biofilm formation. The widespread use of *P. aeruginosa* as a model organism for biofilm formation has two principle causes. First, *P. aeruginosa* readily forms biofilms on a large variety of surfaces (and multicellular, biofilm-like aggregates in liquid suspension) and under a wide range of growth conditions, including on contact lenses, in water treatment facilities and pipes, and on oil spills [16]. Second, *P. aeruginosa* biofilm infections are an important factor that detrimentally affect the outcome for patients with implants or medical devices, chronic obstructive pulmonary disease, chronic wounds, and cystic fibrosis (CF) [1,17].

P. aeruginosa is an opportunistic pathogen responsible for up to 10% of acquired nosocomial infections [18]. Patients with diabetes are particularly vulnerable to the development of chronic wounds, which can cost, per patient, tens of thousands of dollars per year [6]. Chronic wounds are characterized by a lack of healing, which largely results from infection by bacterial biofilms

dominated by *P. aeruginosa* and *Staphylococcus aureus* - these can even lead to amputation [10]. In patients with chronic obstructive pulmonary disease, *P. aeruginosa* acquisition is associated with exacerbation and can lead to long-term infection [19].

1.3.2 Cystic Fibrosis and *Pseudomonas aeruginosa* Infections

Cystic Fibrosis is a genetic disease caused by a mutation in the *CFTR* gene, resulting in mutations in the cystic fibrosis transmembrane conductance regulator [20]. This protein is an ion channel that allows movement of negatively charged ions across the membranes of cells that produce mucus, sweat, and saliva [21]. This mutation significantly affects the lungs of CF patients wherein the ion channel no longer moves chloride ions and therefore there is reduced movement of water. This leads to an increase in thick, viscous mucus and cilia in the respiratory tract can no longer facilitate movement of the mucus [21]. The thick mucus provides a hospitable environment for *P. aeruginosa* biofilms [22].

P. aeruginosa is the leading proximate cause of death in CF patients and these infections can persist in the lungs for decades. CF sputum is nutrient-rich with carbon sources that help support and sustain bacterial growth [23]. By adulthood, 80% of CF patients have long-term infections of *P. aeruginosa* within their lungs [24]. In these and in additional cases of *P. aeruginosa* biofilm infection as mentioned above, the biofilm is able to resist immunological and antibiotic clearance. During these long-term infections, *P. aeruginosa* adapts to its environment, not only adapting to live in human lungs, but also adapting to antibiotic treatments and the body's immune response.

1.4 *P. aeruginosa* Biofilm and Its Evolution

Decades-long infections of *P. aeruginosa* biofilms in the lungs of CF patients are convenient natural models for what biofilm characteristics contribute to fitness. It has been shown that during these long-term infections, *P. aeruginosa* evolves to increase polysaccharide production [25-27]. Along with genetic mutations due to adaptation during infection, throughout the life cycle of the biofilm, there are corresponding gene changes within the community of bacteria that correspond to the transition from planktonic to the sessile state of living and again before dispersal of the bacteria is triggered.

Planktonic bacteria are coated in sticky extracellular polysaccharides (EPS) that promote surface adhesion [28]. In a mature biofilm, bacteria are embedded in a polymer matrix, which, for *P. aeruginosa*, can contain up to three distinct EPS materials, Pel, Psl, and alginate as well as extracellular DNA (eDNA) and proteins [29-36].

1.4.1 Cylic-di-GMP in *P. aeruginosa*

The production of these polysaccharides is controlled by a global regulator within *P. aeruginosa* called cyclic-di-GMP. Cyclic-di-GMP is an intracellular chemical signal used by many species to regulate gene expression for biofilm initiation [37]. Levels of cyclic-di-GMP increase when planktonic *P. aeruginosa* adhere to a surface [3,4,38]. Without cyclic-di-GMP, bacteria that otherwise form robust biofilms within 12 hours instead make no biofilm whatsoever over at least 72 hours of culturing [39].

1.4.2 Psl

Polysaccharide synthesis locus of *P. aeruginosa* is composed of 15 co-transcribed genes which code for the polysaccharide Psl [40]. Psl is a galactose and mannose rich polysaccharide [41]. Only 11 of 15 of the Psl genes are required for functional Psl production which is necessary for initiation of the biofilm and maintaining structural integrity of the biofilm [42]. Overproduction of Psl leads to increased intercellular adhesion and surface attachment [43]. Psl has helical distribution across *P. aeruginosa* cells to aid in intercellular adhesion in early stage biofilms and is located around the periphery of late-stage mushroom-structured biofilms. It is important to note that these mushroom structures are likely an *in vitro* artifact. Psl has been shown to stimulate a positive feedback regulatory cycle by stimulating cyclic-di-GMP production, which in turn increases production of Psl and other biofilm matrix components [44].

Not only is Psl important for the structural integrity of *P. aeruginosa* biofilms, but it is also important in the resistance of *P. aeruginosa* to antibiotics and the immune system. In early stages of biofilm development, Psl helps bind to and prevent the diffusion of tobramycin, an antibiotic commonly used to treat *P. aeruginosa* infections in CF patients, potentially by electrostatically binding to the antibiotic [45]. Psl also decreases the likelihood of phagocytosis of planktonic *P. aeruginosa*, likely by preventing the binding of complement protein to the bacterial surface [46].

Within CF patients, there is an increased likelihood of *P. aeruginosa* becoming a Rugose Small Colony Variant, or RSCV [47]. These RSCVs are defined that way due to their phenotypic appearance. RSCVs are known to have an increased amount of Psl within their biofilms. It has been shown that during

long-term infections in CF patients, *P. aeruginosa* does indeed evolve to increase production of Psl in an unknown post-transcriptional method.

1.4.3 Pel

Until 2015, the composition of Pel was unknown and less was known about this polysaccharide of the *P. aeruginosa* biofilm matrix. In 2015, it was discovered that Pel is composed of partially acetylated galactosamine and glucosamine sugars [48]. Pel is a positively charged polysaccharide and associates with negatively charged extracellular DNA (eDNA) in the biofilm matrix. Pel and eDNA were known to be spatially segregated within the *in vivo* biofilm structures and it is now known that Pel is present in the same regions as eDNA [48]. The linkage of eDNA and Pel can compensate for the loss of Psl in the biofilm mushroom. Due to the more recent discovery of Pel's composition and role in the biofilm, little is known about its role in clinical infections.

While Psl is generally thought of as the primary mediator of surface attachment for *P. aeruginosa* biofilms, Pel promotes the bacteria to lie flat on the surface [28]. It does so by aiding Psl in making short-ranged, localized adhesive forces. Adhesion and lying flat on the surface are promoted through Psl and Pel, respectively, but Psl can do so without the presence of Pel.

1.4.4 Alginate

P. aeruginosa's third EPS polysaccharide is alginate. Alginate is not a factor in the commonly used wild-type lab strain, PAO1, but is an important presence in chronic *P. aeruginosa* infections in CF patients [33]. During the course of infection, *P. aeruginosa* biofilms often convert to a mucoid phenotype, characterized by an increase in alginate production [49]. This conversion is usually

due to an insertion or mutation in *mucA*. In CF infections, production of alginate is known to increase over time; more alginate is associated with poorer outcomes for patients because alginate chemically protects the biofilm [50,51]. Alginate protects the bacteria by binding to reactive oxygen species (ROS) produced by neutrophils, the immune cell that causes the most prominent response to *P. aeruginosa* infections in the lung of CF patients [52]. Without the ability to kill the bacteria, the continued production of ROS in turn causes significant damage to host tissue, resulting in poorer outcomes for patients.

1.4.5 *P. aeruginosa* and the Immune System

As mentioned above, EPS components of the biofilm matrix help P. aeruginosa avoid clearance by antibiotics and the immune system. Bacteria within a biofilm are innately more resistant to clearance due to properties such as electrostatic binding between polymers and antibiotics. Lungs from CF patients infected with P. aeruginosa have shown that the biofilms are surrounded by neutrophils, part of the innate immune response, but that neutrophils cannot penetrate into the biofilm [53,54]. One theory is that in clinical patients, the increased alginate makes the environment too viscous to allow for chemotaxis by neutrophils, however, effective phagocytosis by neutrophils of bacteria from periphery of the biofilm has never been observed either.

It is likely that while the EPS components do exert some chemical protection over the biofilm, there is an overlooked mechanical aspect of protection in biofilm infections. While it has been shown that mechanical breakup of biofilms renders them more susceptible to clearance, there is less known about the changes in mechanics and potential mechanical benefits of being

within a biofilm. Phagocytosis, one of the main ways a neutrophil can kill a pathogen, is inherently a physical process with limitations. In the next section, I will discuss the basics of neutrophils, phagocytosis, and their known and possible limitations.

1.5 NEUTROPHILS

1.5.1 Neutrophil Overview

Neutrophils are an integral part of a human's innate immune response. They are typically short-lived cells that are the first responders to foreign particles. When a human is healthy, the body produces a billion neutrophils/kg each day in the bone marrow and up to 10 billion during infection [55]. Neutrophils are produced in the bone marrow where they mature and are then released into the blood stream where they can travel to the site of infection. There are conflicting points of view as to whether neutrophils circulate for hours or days within the body.

Neutrophils play an integral role in controlling infection while also releasing signaling factors to attract macrophages to the site of infection. Neutrophils are primed to respond to infections by constitutively expressing adhesion molecules that bind immediately upon activation by foreign particles. Neutrophils are often referred to as the "first responders" to the site of infection due to their constant presence in the blood stream and ability to reach the site of infection [56]. Neutrophils also respond to sterile injuries. The well-known neutrophil chemoattractants, formyl peptides, are produced by both bacteria and damaged mitochondria [57]. A neutrophil's ability to quickly clear infection is an asset to the host, but due to a risk of host damage by the inflammatory response, neutrophil cell death is a highly regulated[58]. It is known that macrophages, another innate phagocytic cell, induce apoptosis of neutrophils and engulf them [55] . There is also some debate about neutrophils circulating back to bone marrow or out to the spleen and liver to die in the absence of infection.

Much of the debate surrounding neutrophils is due to the lack of thorough studies of the cell type. *In vivo* studies are difficult and results are often gathered at discrete time points, not in a continuously observable manner. Neutrophils are difficult to work with and large amounts of their characteristics are actually inferred from studies of macrophages, another phagocytic cell that is part of the innate immune system. Much of the knowledge of phagocytosis is based on macrophages, so the information given in some of the following sections will necessarily reflect results of those studies. There are very likely corollaries between neutrophil and macrophage functions, but there is a greater need for neutrophil-specific studies to help elucidate any unique functions of a cell so integral to the innate immune response.

1.5.2 Neutrophil Non-phagocytic Pathogen Clearance

Neutrophils are professional phagocytes but employ a number of other mechanisms to help control infections. Neutrophils are a part of a category of white blood cells called granulocytes, which also includes basophils, eosinophils, and mast cells. Neutrophils make up ~60% of circulating white blood cells[59]. Granulocytes are characterized by the presence of granules in their cytoplasm. Neutrophils contain multiple types of granules containing anti-microbial peptides. Azurophilic peptides such as defensins and elastase, are the strongest of these peptides and are contained within the primary granule [60]. Upon activation, granules fuse with the cell membrane or with the phagosome, the vacuole in which a pathogen is enveloped and killed once it is engulfed through successful phagocytosis, and release their anti-microbial peptides [61] . These granules can

also be found on neutrophil extracellular traps, another mechanism by which neutrophils can trap and kill pathogens.

One of the more recently elucidated mechanisms of neutrophil-mediated pathogen clearance is neutrophil extracellular traps, known as NETs [62]. The process of NET formation, or netosis, begins with decondensation of chromatin that is released into extracellular space, forming the backbone of the NETs. Anti-microbial peptides released from granules are distributed into these NETs to facilitate the killing of trapped pathogens. It is widely agreed that neutrophils do produce NETs, but it was first thought that netosis, the formation of these NETs, inevitably led to cell death. It is now believed that there are multiple types of netosis including “suicide netosis” which leads to cell death, and “vital netosis” that may not [63]. It has been suggested that “vital netosis” is fast-acting but less efficient while the classical netosis pathway that leads to cell death is more efficient. During “vital netosis” NET proteins and DNA are released through exocytosis and it is mitochondrial DNA that is released; however, it has not been confirmed that neutrophils stay alive after this process despite their intact membrane. The classical pathway of netosis is triggered by the production of reactive oxygen species (ROS) by neutrophils wherein the membrane of the neutrophil ruptures and nuclear DNA, along with granular proteins, are released.

Reactive oxygen species are produced in massive quantities by neutrophils upon activation [64]. Both netosis and ROS production are useful methods in clearing infections resistant to phagocytosis, but ROS can also cause extensive damage to host cell tissue if prolonged and unregulated. Upon activation, neutrophils produce an oxidative burst of ROS generated by membrane-bound NADPH (Nicotinamide adenine dinucleotide phosphate-

oxidase/Nox2) [65,66]. ROS are released extracellularly and within the phagosome to aid in pathogen destruction and also serve to activate granule release and netosis as mentioned above [63]. Extracellular ROS will damage DNA leading to bacterial death, but it also harms host DNA and causes an increase in potentially beneficial mutations for the bacteria. Pathogens have also found ways to protect themselves from ROS, such as the ability of alginate species' in *P. aeruginosa* and *Burkholderia cenocepecia* to scavenge ROS [52].

1.5.3 Neutrophil Phagocytosis

Phagocytosis is the process by which neutrophils and other phagocytic immune cells, mainly macrophages, engulf and clear infections. The foreign particle or invading pathogen is engulfed by the cell membrane into the phagosome at which point granules fuse with the phagosome releasing their anti-microbial contents leading to the death of the bacteria. Neutrophils can recognize pathogens through pattern recognition receptors (PRRs) or through opsonin binding. Neutrophil opsonin binding is facilitated through Fc receptors and their recognition of antibodies or integrins and their recognition of complement-coated particles [67].

1.5.4 Evasion of Neutrophil Phagocytosis

Microbes have evolved ways to avoid neutrophil phagocytosis. *P. aeruginosa* bacterial cells are coated with Psl that reduces opsonin binding which in turn prevents neutrophil binding and uptake [46]. Bispecific antibodies against proteins that aid *P. aeruginosa* in evasion of neutrophil phagocytosis can help overcome this resistance mechanism; however, studies showing this only looked at planktonic bacteria [68].

P. aeruginosa within a biofilm is known to be resistant to phagocytosis, but the entire mechanism is still unclear. Neutrophils can easily engulf particles smaller than 10μm [69] . Planktonic bacteria are around 1μm and are readily taken up by neutrophils, but biofilms, on average, are much larger than the 10μm threshold of readily-engulfed targets. It was recently shown that neutrophils were able to use trogocytosis, a process also called "nibbling," to kill *Trichomonas vaginalis* [70]. *T. vaginalis* is a large, highly motile pathogen and its 10-15μm diameter allows it to surpass the size of particles neutrophils can engulf during phagocytosis. Neutrophils were able to kill the parasite in this phagocytic-independent and Net-independent method by taking bites, leading to the death of the parasite [70].

Phagocytosis has known size limitations but there are likely undiscovered ways that neutrophils can clear large particles and infections. When biting fragments off of a particle or injury, neutrophils have to exert the mechanical stress needed to break off bites. Inevitably, there will be mechanical limitations on the neutrophil's ability to break apart its target. Bacteria such as *P. aeruginosa* have the ability to alter their EPS and biofilm matrix content to change the mechanical properties of the biofilm, potentially surpassing this threshold of neutrophil's mechanical ability to breakup a target.

1.5.5 Mechanical Limitations of Neutrophil Phagocytosis

In order to engulf particles, neutrophils must drastically alter their cell shape. This imposes mechanical limitations on the extent of phagocytosis. Shape and size of the phagocytic target are known to impact the initiation and completion of phagocytosis.

Non-spherical shapes have been shown to prevent phagocytosis in macrophages independent of particle size [71] . It is still unknown if neutrophils behave the same way. The ability of macrophages to complete phagocytosis was dependent on the shape of the particle; shape was measured as the tangent angle of the initial point of contact between macrophage and particle. All particles were smaller than 12.5μm but if the actin network in macrophages could not form a structure with which to properly build an actin network, the cell spread across the particle instead of engulfing it.

Target size determines the success of engulfment by a neutrophil when particle volume exceeds cell volume. Size-dependent engulfment ability is generally measured with stiff spherical particles [69] [72] . When the neutrophil cannot engulf these large particles, phagocytosis stalls. Stalled, incomplete phagocytosis is referred to as frustrated phagocytosis. Completion of phagocytosis is crucial not only for limiting ROS damage to the host as mentioned above, but also in limiting time for bacterial virulence factors that damage neutrophils, such as pyocyanin and rhamnolipids produced by *Pseudomonas aeruignosa*, to be made and secreted [73,74].

The mechanical components neutrophils must overcome have been posited by Herant *et al.* and are as follows: 1) rapid alteration of cell morphology and cytoskeletal resistance 2) a rapid increase in surface area, during which villi in the neutrophil's cell membrane are unfolded 3) adhesion to the phagocytic target and 4) the protrusive force of the leading edge of the phagocytic cup, the invagination of the neutrophil membrane driven by actin. They postulated that neutrophils can exert an attractive force of 1kPa on its phagocytic target. They also showed that neutrophils are unable to engulf particles over roughly 10μm,

the relative size of a neutrophil [69]. Taken together, theoretically a phagocytic target that is too large and too hard would lead to frustrated phagocytosis

1.6 Dissertation Objectives

During long-term biofilm infections, we found the bacterial adaptations lead to changes in mechanical properties of the bacterial biofilms. There is little understanding of how the mechanical properties of the biofilm are conferred and what potential benefits these mechanical properties may confer to bacteria. Further, neutrophil mechanics are vastly understudied in general and in relation to macrophages. Without a more clear understanding of neutrophil mechanics, it will be nearly impossible to determine ways to target biofilm mechanics to make them more susceptible to breakup and effective neutrophil clearance. My dissertation seeks to expand upon the current knowledge and methods of measuring mechanical properties in both biofilms and neutrophils, potentially elucidating new mechanical targets to aid in the clearance of biofilms by the immune system.

Chapter 2 elaborates on current methods utilized to measure the mechanics of bacterial biofilms and some of the known mechanical properties of biofilms that was previously published by our lab [75]. Chapter 3 will detail a study measuring the mechanical properties of *P. aeruginosa* based on EPS production and the change in mechanical properties throughout long-term infections [76]. In chapter 4, I will discuss the development of new ways to measure the ability of neutrophils to engulf pieces broken off of large targets with varied mechanical properties to determine the ability of neutrophils to break off and engulf fragments of these large particles. Chapter 5 will briefly summarize the

conclusions and impact of this dissertation and look ahead to potential future studies to expand upon the work presented here.

Chapter 2: Methods in the biophysical study of the mechanics of bacterial biofilms[1]

2.1 INTRODUCTION

Biofilms are developmentally-dynamic communities of sessile microbes that adhere to each other and, often, to other structures in their environment. The cohesive mechanical forces binding microbes to each other confer mechanical and structural stability on the biofilm and give rise to biofilm viscoelasticity. The adhesive mechanical forces binding microbes to other structures in their environment can promote biofilm initiation and mechanosensing that leads to changes in biological activity. Thus, physical mechanics is intrinsic to characteristics that distinguish biofilms from free-swimming or free-floating microbes in liquid culture. These knowledge gaps arise, in part, from the challenges associated with experimental measurements of microbial and biofilm biomechanics. Here, I review extant experimental techniques for measuring biofilm mechanics and their most-salient findings to date. At the end of this review I indicate areas where significant advances in the state-of-the art are heading.

Microscopy observations of biofilms grown in our lab and others show discrete bacteria suspended in a continuous matrix, with the bacterial volume fraction well below 50% [76] [77]. For this reason, the matrix is the primary determinate of the mechanical properties of *P. aeruginosa* biofilms and other

[1] This chapter is adapted from **75** Vernita D Gordon, M. D.-F., Kristin Kovach, and Christopher A Rodesney. Biofilms and mechanics: a review of experimental techniques and findings. *Journal of Physics D: Applied Physics* **50** (2017). All authors contributed equally.

biofilms with low volume fraction of bacteria. This is not universal and biofilms of other species, with higher microbial volume fraction, could have very different mechanics. This is because bacteria and yeast are much stiffer than aqueous polymer matrices – the measured moduli for both Gram-negative and Gram-positive bacteria typically range from a few MPa to several hundred MPa [78,79].

Biofilms are viscoelastic materials, behaving similarly to polymer gels. Studying biofilms from a mechanical standpoint allows us to consider such behaviors as elastic modulus, yielding behavior, and energy dissipation in the system. While an understudied facet of biofilm properties, the mechanical strength and malleability allows biofilms to survive and adapt to many environments, from human bodies to industrial filters and pipes. *Staphylococcus aureus*, a pathogen responsible for many medical implant infections and endocarditis, is exposed to continuous and laminar flows in these scenarios. The viscoelasticity of the *S. aureus* biofilms allows the bacteria to stay attached to surfaces even under high fluid shear [80] . *S. aureus* microcolonies can roll under flow; this may be essential for dispersal of nonmotile bacteria.

Recent reviews provide a discussion of different approaches to measuring biofilm mechanics and a list of biofilm mechanical properties for a wide variety of species, although this list is dominated by *P. aeruginosa* studies [81 82]. Numerous methods have been applied to study biofilm mechanics. These methods can be categorized into both flow and static assays, as follows: flow assays are done in the presence of flowing nutrients, allowing for a continuous time-series of measurements that allow dynamic properties to be studied; static assays are done without an ongoing supply of nutrients so that measurements are taken at specific time points where growth is no longer occurring.

2.2 STATIC ASSAYS

2.2.1 Atomic Force Microscope

While there is great utility in Atomic Force Microscopes (AFM) for studying single cell bacteria, this small-scale technique can also be useful for studying the mechanics of the surface of a biofilm. AFM allows measurement of the mechanical properties of biofilms with high spatial resolution, in principle much less than the size of a single bacterial cell. In a reductionist view, the smallest fundamental unit of the biofilm [83] would be two cohering cells. We have recently used AFM to measure the cohesive forces and energies between pairs of bacteria with different patterns of EPS expression and have found that the strength of inter-bacterial cohesive interactions varies greatly with the type of EPS produced [76]. However, these bacteria were not in a biofilm state, and our bulk rheology on biofilms grown from the same bacterial strains showed that the mechanical properties of isolated bacterial pairs do not always have a straightforward mapping onto biofilm mechanics (see below under Static Assay: Bulk Rheology). Other researchers have used an AFM, functionalized with a microbead, to measure the adhesive and viscoelastic properties of biofilms with different levels of lipopolysaccharide production [84].

AFM has also been used to study the cohesive energy of biofilms by using the cantilever tip to abrade the surface of the biofilm. By measuring the energy dissipated as the AFM cantilever is scraped over the biofilm, a total cohesive energy measurement is obtained for the volume abraded. In this study, *P. aeruginosa* biofilms were found to have increasing cohesive strength deeper within the biofilm, from 0.1nJ/μm3 on the surface to 2.05nJ/μm3 within the

biofilm. Adding calcium to the biofilms during growth increases biofilm cohesive energy, a result that has been seen in other studies of P. aeurginosa biofilms [85].

2.2.2 Microindentation

Another method similar to the AFM is the measurement of cohesive or tensile strength using a microcantilever. These devices are often custom-made for the measurement of biofilm mechanics. By measuring the deflection of a cantilever, simple stress and strain measurements can be obtained based off of the deformation of the biofilm of interest. These measurements have been done on a wide array of biofilms, such as *P. aeruginosa* [86], *S. epidermidis* [86], *P. fluorescens* [87], *S. mutans* [88], and mixed-species biofilms [89].

In *P. aeruginosa*, biofilm cohesive strength was measured from 1kPa to 16kPa depending on the speed of the measurement, size of biofilm growth, and whether or not the biofilm was intact [86] [89]. *S. epidermidis* biofilms were somewhat weaker, only testing from 0.9kPa to 1.4kPa [86]. Biofilms *of S. mutans* bacteria were stronger like *P. aeruginosa* biofilms with strengths measured from 1kPa up to 10kPa [88]. A mixed species biofilm of return activated sludge (RAS) was the strongest of all biofilms measured, with strengths reaching 206kPa, while some were as weak as 0.4kPa [89]. The strength of the *P. fluorescens* was reported differently than the other biofilm measurements. In this microcantilever experiment, the biofilms had adhesive strengths from 0.1 to 1 J/m2, thus a value more classically considered as a surface tension or stiffness [87].

A benefit of the microcantilever measurement is that it can be performed on intact biofilms at an array of sizes that are clinically relevant for human infections, ~10 to 102 microns. In addition, growth is not restricted to

unidirectional flow cell. Aggarwal *et al*. have used a rotating disk reactor for growth, which results in more isotropic biofilm structures.

2.2.3 Bulk Rheology

A classic method for studying the mechanics of viscoelastic systems is bulk rheological studies using a rheometer (Figure 2.1). Bulk rheology uses large amounts of material (on the order of milliliters). Experiments with rheometers can be used in both steady state or oscillatory mode. Viscoelastic materials, including biofilms, have both an elastic (or solid-like) and viscous (or liquid-like) response to strain deformation, meaning they both store and dissipate energy when a strain is applied. Oscillatory mode allows for the complex viscoelastic modulus, G*=G'+iG'', which gives the elastic and viscous moduli G' and G'', to be measured directly [90-92] (Figure 2.1). The measure of the material's response to stress with time is proportional to the rate of deformation.

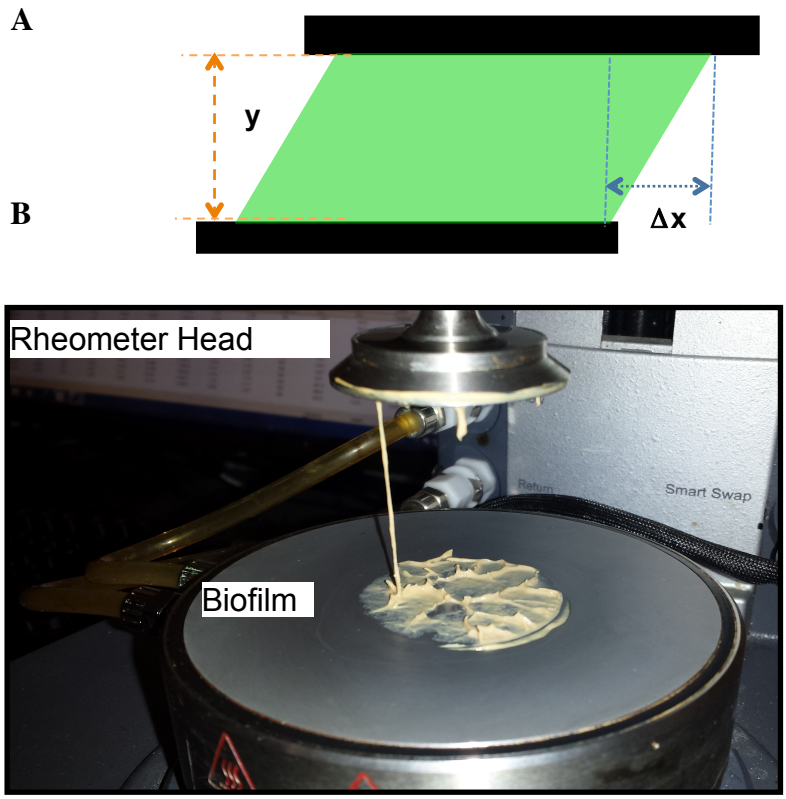

Figure 2.1 Rheology schematic and biofilm on rheometer

(A) Rheology schematic. The rheometer tool applies a shear strain ε = Dx/y = ε0·sin(ωt) to the biofilm, where ω = angular frequency of oscillation and t = time. The resulting shear stress response, σ = σ0·sin(ωt + δ) = ε0·[G' sin(ωt) + G'' cos(ωt)], gives the elastic modulus G' and the viscous modulus G''. (B) Biofilm that has been measured using a parallel-plate rheometer tool, as described in [93]. This picture was taken after the rheology measurement when the rheometer head was retracted. Biofilm adheres to both the upper and lower plates.

Another measure of the viscoelasticity of a material is creep compliance J. The creep compliance characterizes how the material's strain deformation ε(t) changes over time as a constant stress σ_0 is applied; generally, $J = \frac{\varepsilon(t)}{\sigma_0}$..

By measuring the elastic and viscous modulus over a range of strains and frequencies, much can be determined from a material of interest. If a material is highly time-dependent in its stress response, then the frequency sweep of the material will reveal dramatic changes over a range of frequencies. A strain sweep can be used to determine a material's yield point at a given frequency of interest. This allows measurements of energy required cause a material to yield, as energy is simply the integral of stress over strain to the point of material yield.

Two main methodologies for studying biofilms via bulk rheology have been used. In one method, the EPS components are isolated from the bacteria and their mechanics are tested. This method has been used successfully to probe the viscoelasticity of EPS material and how those polymers respond to the addition of divalent calcium ions [94]. The other method utilizes biofilm grown on many agar plates in order to achieve the amount of biofilm necessary for rheological study [92]. We have used this method to measure distinctive mechanical properties that arise from different EPS materials and show that biofilm mechanics evolve within the lungs of cystic fibrosis patients [76].

2.3 Flow Assays

2.3.1 Flow Shear

A common method for studying the growth and properties of biofilms is using flow assays with time-lapse microscopy. In such experiments, a biofilm is

seeded and grown inside a channel in which nutrients are continually flowed over the growing biofilm. Flow assays allow for a continuous supply of nutrients for the bacteria as well as a way to modulate the forces experienced by a growing biofilm. Biofilm mechanics can be evaluated because the shear rate within the channel is known, and thus the response to the biofilm to varying shear rates can be determined through image analysis of the biofilm deformation. Stoodley e*t al*. and Rupp *et al.* have done flow rheological measurements on biofilms of *P. aeruginosa*, *S. aureus*, and mixed species [80] [91]. The results of these measurements gave shear moduli, G, in the range of a couple to tens of Pascals.

A benefit of this method of measurement is that the data is taken *in situ* as the biofilm grows in the channel, meaning the biofilm maintains any heterogeneity and complexity it creates in growth. A pitfall of this method is that the biofilm is grown under shear, and so may select for genes in response to shear flow. Also, the strain of the biofilm is measured via the deformation of "streamers" growing off of the biofilm. As biofilms are heterogeneous, measuring the rheology of the streamer is not the full picture of biofilm mechanics or polymer contribution to mechanics.

However streamer creation itself is also of interest as it has been seen that streamers can cause more rapid clogging in a flow channel in *P. aeruginosa* biofilms, which has an impact in medical devices or industrial pipes. When biofilms form on the walls of a channel, the streamers that reach around a corner cause clogs more quickly than the biofilms that are simply growing on the flat walls of the channel. As such, a biofilm's ability to form biofilms that grow long, ductile streamers can cause the biofilm to become more damaging in a health or environmental application [95]. Studies on multi-species biofilms show that under

turbulent flow, these biofilms form streamers and ripple-like structures which are likely important in biofilm dispersal [96] [97].

2.3.2 Passive and Active Microrheology

Another method that can utilize flow cell chambers is microrheology. Microrheology is a powerful tool for probing local mechanical response. In this method, beads are added to the biofilm throughout growth. The beads can be glass, steel, or any other material that is easily visualized within the biofilm matrix under a microscope.

Passive microrheology uses thermally-driven motion of beads to probe their local microenvironment (Figure 2.2A). The motion of the beads is imaged under the microscope and software [98] identifies bead positions. For an elastic solid, the mean square displacement (MSD) $\langle \mathbf{r}^2 \rangle$ of a bead will plateau at a value that depends on the bead size, a, and the elastic modulus of the microenvironment, thus: $\langle \boldsymbol{r}(t)^2 \rangle = \frac{2k_BT}{3\pi a G_0}$, where k_BT is the thermal energy. This approach can be extended to characterize viscous as well as elastic properties and has been used to characterize biofilms of *E. coli* and *P. aeruginosa* [83] [99]. The creep compliance of *P. aeruginosa* biofilms was found to be around 10^{-4} Pa^{-1} and to be dynamically variable by changes in what type of EPS was produced [83]. One group has succeeded in the challenging task of using the bacteria themselves as passive tracers to measure the viscoelasticity of *S. aureus* and *P. aeruginosa* biofilms [100].

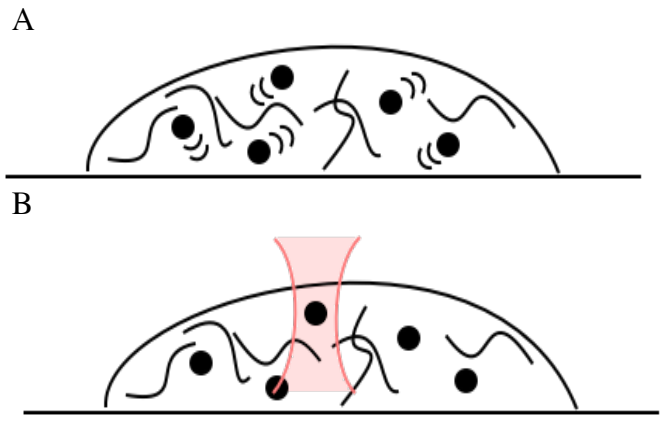

Figure 2.2: Microrheology schematic

Microrheology measures local mechanics by measuring the displacement of tracers. (A) In passive microrheology, displacement arises from Brownian motion driven by thermal energy, kBT. (B) In active microrheology, displacement arises from a directed, externally-applied force. For ease of illustration, this schematic shows an optical trap applying a force. Magnetic trapping can also be used and will not be confounded by the high optical density of biofilms, as well as being able to apply higher forces than optical trapping.

Some biofilms are too stiff for passive microrheology to be an effective probe of mechanics. In such situations, active microrheology becomes the better tool. Active microrheology uses magnetic or optical tweezers to move beads imbedded in the extracellular matrix (Figure 2.2B). By applying force on the tracer bead, the strain response to this stress can be determined – this measures the mechanics of the biofilm [101].

Since microrheology probes the local region around a bead, this method can be used to probe biofilm heterogeneity. Biofilms are inherently heterogeneous, in structure, metabolism, genetics, and polysaccharide production [102-104]. As bacterial interactions with antibiotics and immune cells is primarily on a smaller scale, learning the heterogeneous distribution of mechanics and polymers is certainly of interest to efficiently attacking a biofilm via mechanical removal.

2.4 Current questions and Future Directions

2.4.1 Overview

Some biofilms are too stiff for passive microrheology to be an effective probe of mechanics. In such situations, active microrheology becomes the better tool. Active microrheology uses magnetic or optical tweezers to move beads imbedded in the extracellular matrix (Figure 2.2B). By applying force on the tracer bead, the strain response to this stress can be determined – this measures the mechanics of the biofilm [101].

Since microrheology probes the local region around a bead, this method can be used to probe biofilm heterogeneity. Biofilms are inherently heterogeneous, in structure, metabolism, genetics, and polysaccharide

production [102-104]. As bacterial interactions with antibiotics and immune cells is primarily on a smaller scale, learning the heterogeneous distribution of mechanics and polymers is certainly of interest to efficiently attacking a biofilm via mechanical removal.

2.4.2 Physical Interpretations of Biofilm Mechanics

It is well-known that increasing the concentration of polymer (c) in a gel will increase the gel's elasticity, $G' \propto cA$, where A is a scaling factor that is 2.25 for entangled polymer in good solvent [105]. This is a physical effect that does not depend on polymer chemistry. However, we have shown that increasing Pel and alginate production does not increase the elasticity of *P. aeruginosa* biofilms, whereas increasing Psl production does stiffen biofilms [76]. Thus, understanding the molecular mechanisms by which specific matrix components give rise to specific biofilm mechanics is essential both to understanding the physical origins of biofilm mechanics and to devising targeted strategies for disrupting biofilm mechanics. For this, it should be possible to leverage a large body of physical-chemistry work that connects the molecular chemistry of constituent polymers with the macroscale mechanical properties of bulk materials [92].

For example, in the case of Psl, we attribute mechanical changes to cross-linking by the protein CdrA, which arises because of the specific, mannose-rich chemistry of Psl [76]. Future investigations of this system, and of other biofilm systems where cross-linking might contribute to biofilm elasticity, could be guided by rubber elasticity theory, in which $G' \sim c/M_c$. Here, c is polymer concentration and M_c is the polymer molecular weight between cross-links [106,107]. For another example, we have shown that increased Pel production increases the yield strain

of *P. aeruginosa* biofilms. Others have recently shown that cationic Pel binds with anionic extracellular DNA [48] and we have speculated that this may result in a double-network structure [76]. Rheological signatures of a double-network gel vary with the molecular interactions stabilizing the gel and can include strain hardening for 2-component systems but not for 1-component systems, non-monotonic dependence of yield stress on crosslinking density (set by the concentrations of Pel and DNA), and increase of yield strain with increasing contour length of the softer component of the network [108].

2.4.3 Potential Benefits Arising From Better Understanding of Biofilm Mechanics

Knowledge of the roles played by mechanics in the biofilm life-cycle has the potential to reveal mechanics-oriented approaches to preventing or remediating biofilms. Such approaches are especially appealing in the face of rising antibiotic resistance because mechanical properties and mechano-responsive biology are orthogonal to mechanisms of antibiotic activity and resistance. Some EPS types are made by more than one biofilm-forming species, such as alginate that is produced in both *P. aeruginosa* and *Burkholderia cenocepecia* biofilms [52]. This suggests the possibility of mechanics-targeting strategies for biofilm disruption that are not species-specific but rather oriented toward what type(s) of EPS dominate the matrix. The mechanics of biofilms will be an important factor in determining how biofilms break up, disperse, and seed new biofilms under mechanical perturbation, such as flow in industrial settings. Predicting and possibly controlling biofilm dispersal would allow for more efficient clearance. Knowing what mechanical cues activate virulence or biofilm initiation, and how these cues are sensed, would open the

possibility for preventing bacteria from sensing the cue, thus disrupting virulence upregulation and/or biofilm formation from their inception.

2.4.4 Need for Improved, Standardized Approaches to Measurement

One prevalent issue with the current understanding of biofilm mechanics is that it is difficult, perhaps impossible, to meaningfully compare measurements from different research groups, or even within the same group, that use different growth conditions, bacterial strains, and measurement techniques.

Another issue with the current state of biofilm mechanics studies is the lack of *in vivo* measurement techniques. *In vitro* studies allow for more control over experimental conditions and much easier access to the biofilm. However*, in vitro* biofilm structures are very different from in vivo biofilm structures [109 110 53 111] . It is likely that the mechanical properties of biofilms grown and measured *in vivo* would deviate from the mechanical properties of biofilms grown and measured *in vitro.*

There are methods, such as AFM and microrheology, which allow biofilms to remain intact and preserve structural integrity and microenvironments while probing local mechanics. There are also approaches for characterizing biofilms *in vivo* and *ex vivo* – for example, mouse models for chronic wounds and explanted human lung tissue [53 111]. However, mechanical measurements have not yet been applied to these more clinically-relevant biofilms. Until the state-of-the-art includes measurements of the mechanics of biofilms grown *in vivo*, it will be difficult if not impossible to determine what mechanical characteristics actual biofilm infections have and to distinguish the roles of genetics versus environment in biofilm mechanics.

2.4.5 Lack of Knowledge of How Polymicrobial Interactions Impact Biofilm Mechanics

Most studies of biofilm mechanics have been done on single-species biofilms. However, most real-world biofilms contain multiple microbial species. Inter-species interactions are known to produce synergies, and some reported synergies are at least suggestive of changes in the adhesive and/or cohesive properties of biofilm bacteria. Synergy in biofilms of the oral cavity includes enhanced coaggregation and protection [112] [113], and mixed-species cultures in aquatic systems grow biofilms that are more robust and protective to bacteria than are biofilms grown from single-species cultures [114]. Moreover, different species of bacteria can have both beneficial and harmful interactions, which can lead to a bacterial fight-and-flight response [115]. This leads to optimal distances between bacterial species, creating microstructures and environments within the biofilm. The changes in matrix composition, aggregation and growth, and biofilm organization that accompany a transition from single to multi-species biofilms could well lead to changes in biofilm mechanics. This area is entirely uninvestigated, yet knowledge of how polymicrobial interactions impact biofilm mechanics and mechanical vulnerabilities would be widely applicable.

Chapter 3: Evolutionary adaptations of biofilms infecting cystic fibrosis lungs promote mechanical toughness by adjusting polysaccharide production[2]

3.1 INTRODUCTION

As stated in the introduction chapter, *P. aeruginosa* biofilms chronically infect Cystic Fibrosis patients. These strains have been isolated from patients and have lead to the ability to study how *P. aeruginosa* adapts *in vivo* to living within the host and evading antibiotic and immune system treatments. It is well known that alginate production is increased during long-term infections and leads to worse patient outcomes. It was also recently discovered that the production of Psl increases [25].

Why it could be advantageous for *P. aeruginosa* to produce more than one type of EPS is not thoroughly understood and is a topic of active research. Most thought on this topic has focused on distinct chemical properties of the different EPS materials and the possibility that having redundancy in biofilm-matrix production capability could allow one EPS to act as a backup if a bacterial line lost the ability to produce a primary EPS [48,93,116].

Our studies employ biofilms grown from clinical bacterial isolates from CF patients and biofilms grown from genetically-manipulated lab strains. Here, we show for the first time that changes in polysaccharide production can increase the mechanical toughness of biofilms, which is equivalent to increasing the energy cost of overcoming the material integrity of the biofilm. Furthermore, different EPS materials accomplish this in different ways. Increased Pel or

[2] The chapter adapted from **76.** Kovach, K. Davis-Fields, M. *et al*. , Evolutionary adaptations of biofilms infecting cystic fibrosis lungs promote mechanical toughness by adjusting polysaccharide production, *npj Biofilms and Microbiomes,* 2017. I am co-first author on this paper and contributed equally with K. Kovach.

alginate increase the yield strain of the biofilm; yield strain measures how far the biofilm can be deformed before mechanical failure, or yielding, begins. In contrast, Psl increases the elastic modulus, so that more energy is required per unit deformation. Psl increases the elastic modulus only when it is co-produced with CdrA, a protein that binds to Psl [117].

We use two techniques to explore the mechanical properties of our biofilms. The first tool is a bulk rheometer, which provides the standard way to characterize complex fluids. The second tool is atomic force microscopy (AFM), which lets us measure directly the energy required to pull two bacteria apart. We find that increased Psl results in a greater energy cost expended to separate two bacteria. Energy of de-cohesion increases because increased Psl production increases both the distance over which the inter-bacterial cohesion force is exerted and the maximum value of that force, and thus the mechanical work of separation. Increasing cohesion lengthscale is directly analogous to the tactics used to design greater toughness into engineering materials [118]. These experiments provide the first direct measurements of inter-bacterial cohesion.

3.2 RESULTS

3.2.1 Explanation of Reported Results

Previous measurements of *P. aeruginosa* biofilm moduli have reported ranges of values that vary over orders of magnitude (from a few Pa to tens or hundreds of kPa) [84,91,92,119,120]. It is not clear to what degree this reflects differences between bacterial strains versus differences resulting from measurement techniques or culturing conditions. To circumvent this problem, we quantify changes in the toughness, which is the energy cost to cause the biofilm

to yield, the plateau elastic modulus G′, the yield strain ε_Y, and the yield stress σ_Y associated with changes in polymer expression by taking ratios to compare a clinical isolate that has evolved in the lung of a CF patient with its initially-infecting ancestor or, for lab strains, an isogenic mutant with its corresponding wild-type. Each pair of biofilms is grown in parallel, on the same batch of agar plates, and measured on the same day, in immediate succession, to minimize differences in the culture conditions and measurement environment.

3.2.2 In Biofilms Grown from Clinical isolates, Psl Maximizes the Energy Cost for Biofilm Disruption

Energy is the currency of biological processes including phagocytic engulfment, and toughness is a measure of the energy cost, per unit volume, to break or yield a material. To address how evolutionary changes in the production of alginate and Psl impact biofilm toughness, we use oscillatory bulk rheology to measure the shear mechanics of biofilms grown from *P. aeruginosa* strains that were isolated from the sputum of four cystic fibrosis patients [25] (Figure 3.1-3.5). These isolates were taken at well-resolved timepoints over ~200-3000 days of infection, and have been genetically and phenotypically characterized to determine the changes arising from in vivo evolution, in particular increases in Psl and/or alginate production (Figure 3.1, Table 3.2) [25,121]. We group isolates by whether production of alginate, Psl, or both has increased from that of the initially-isolated ancestor. For each biofilm studied, both elastic and viscous moduli depend only weakly on the rheometer tool's frequency of oscillation (Figure 3.2A, 3.3A, 3.4A, 3.5A). Strain sweeps at 3.14 radians/s (Figure 3.2B, 3.3B, 3.4B, 3.5B) were used to measure the biofilm toughness by integrating stress as a function of strain. We measure changes in

toughness by taking the ratio (Toughness of evolved clinical isolate)/(Toughness of initially-isolated ancestor) for each pair of biofilms. We find that increasing Psl production is associated with little change in toughness compared with the ancestor, but increasing alginate reduces biofilm toughness to approximately a third of that of the ancestor (Figure 3.6A). However, increasing Psl production in combination with alginate production entirely rescues the loss of toughness caused by increased alginate.

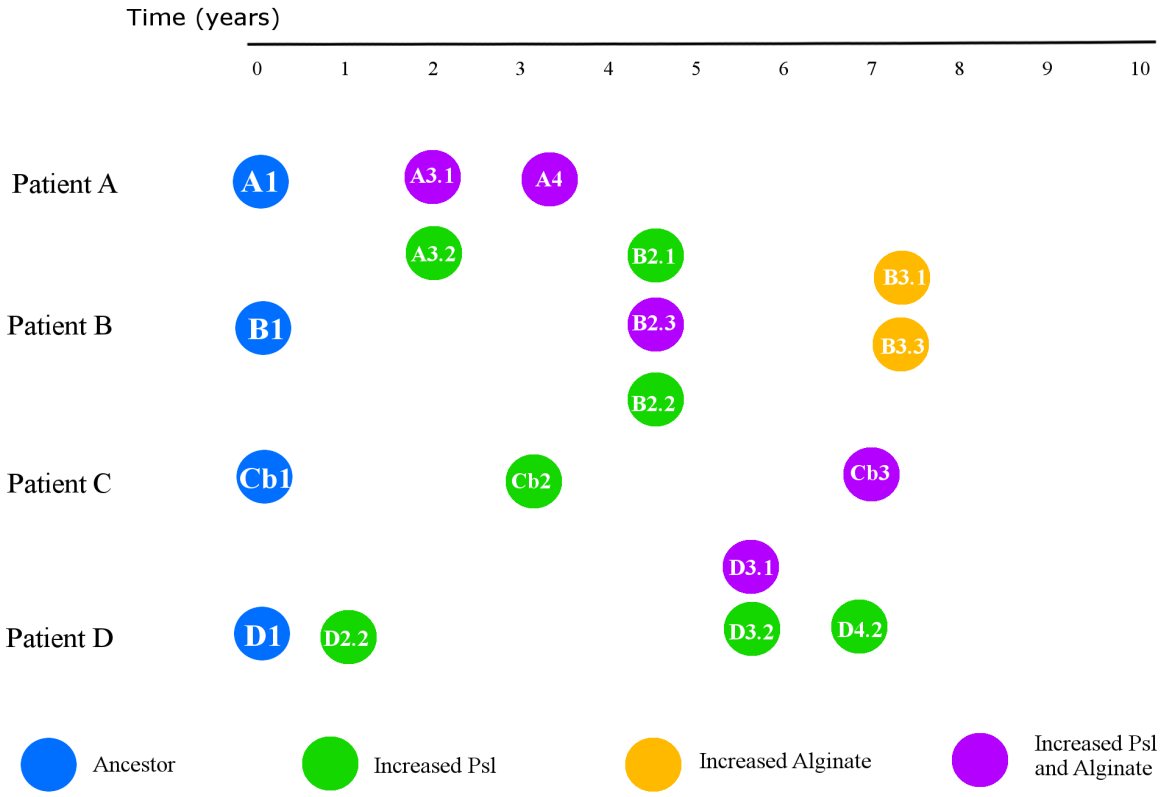

Figure 3.1 Timeline of clinical *P. aeruginosa* strains isolated from 4 CF patients

Timeline of Patients A-D, CF patients with infection isolated from sputum or throat collections. EPS content of the *P. aeruginosa* isolates characterized as producing increased alginate (orange), increased Psl (green), or increased production of Psl and alginate (purple) in comparison to the initial ancestor isolate (blue).

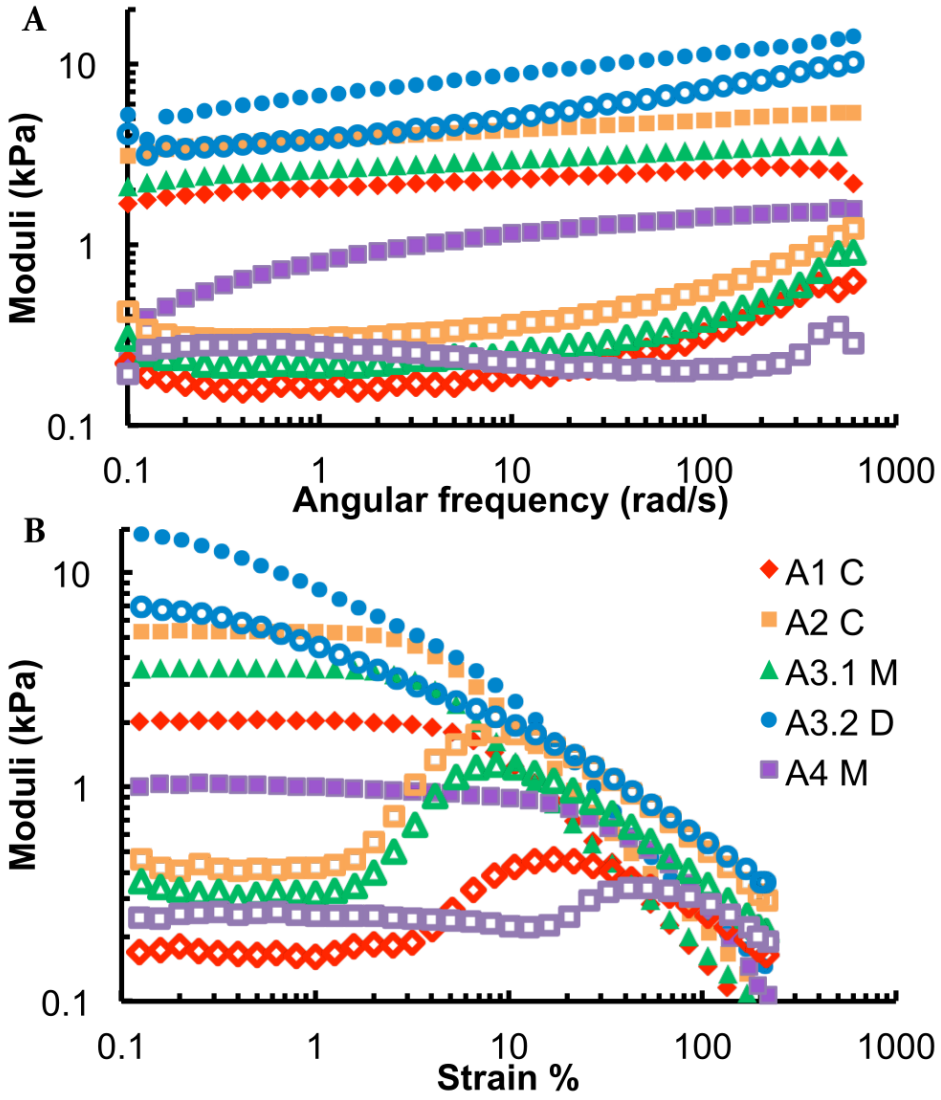

Figure 3.2 Patient A representative frequency sweep and strain sweep curves

(A) Frequency and (B) strain sweeps for one day's worth of measurements on biofilms grown from the five infecting strains isolated from Patient A at different points in time. Frequency sweeps were done at 1% strain and strain sweeps were done at 3.14 radians/s. The elastic moduli (G') are shown with solid symbols and the viscous moduli (G") are shown with hollow symbols of corresponding shape and color. Strains are listed in order of isolation – see Table 3.1 and Figure 3.1 for timepoints of isolation. Isolates from later timepoints tend to have higher elastic moduli, except for the two mucoid isolates, A3.1 M and A4 M, which have high alginate production and lower elastic moduli than their immediate ancestors.

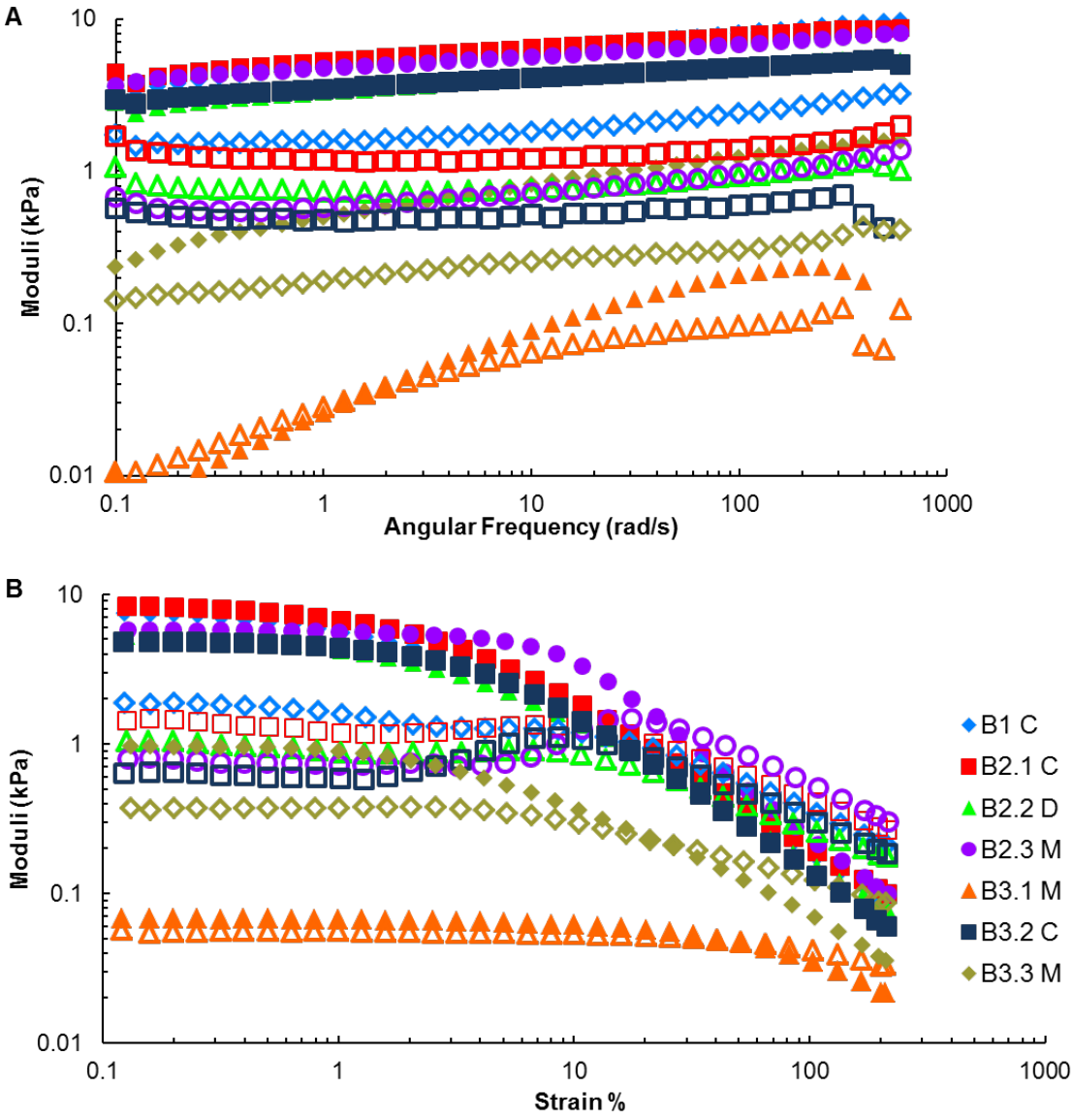

Figure 3.3 Patient B representative frequency sweep and strain sweep curves

Figure 3.3 Representative (A) frequency sweeps and (B) strain sweeps at 3.14 radians/s for biofilms regrown from clinical isolates taken from Patient B. Elastic moduli are shown by filled symbols and viscous moduli are shown by the corresponding hollow symbols. For most of these clinical isolates, the elastic modulus G′ of is greater than its viscous modulus G″. However, the ratio G″/G′, and therefore tan(δ), where δ is the phase constant in Equation 1, is much more varied for clinical isolates than for PAO1 lineages, and for B3.1 M and B3.3 M at some frequencies and strains, G″/G′ is approximately unity and our approximation that biofilms are predominantly solid-like breaks down.
The legend lists strains in order of isolation – see Table 3.1 for timepoints of isolation. Isolates from later timepoints in the infection's history that have converted to the mucoid phenotype (designated by M) tend to have lower elastic moduli than do isolates from earlier timepoints. Exceptions are found for isolates that also have increased Psl expression.
Data points for the elastic response of bacterial strain B1 C are hidden under data points for bacterial strain B2.1 C, and data points for the elastic response of bacterial strain B2.2 C are hidden under data points for bacterial strain B3.2 C. Data points for the viscous response of bacterial strain B2.2 C are largely hidden under data points for bacterial strains B2.3 M and B3.3 M.

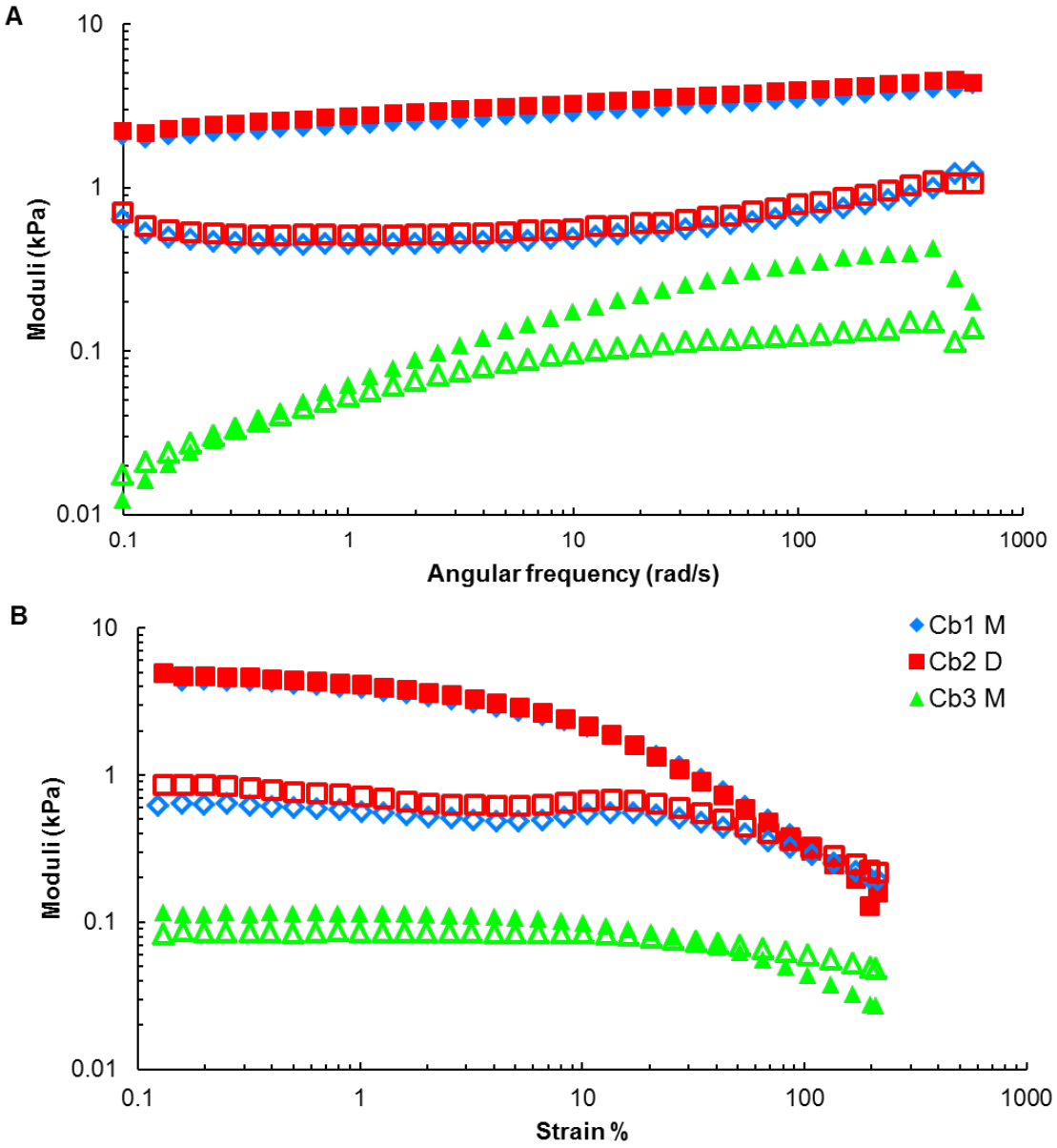

Figure 3.4 Patient C representative frequency sweep and strain sweep curves

Representative (A) frequency sweeps and (B) strain sweeps at 3.14 radians/s for biofilms regrown from clinical isolates taken from Patient C. Elastic moduli are shown by filled symbols and viscous moduli are shown by the corresponding hollow symbols. Data points for the elastic response of bacterial strain Cb1 M are largely hidden under data points for bacterial strain Cb2 D. For bacterial strain Cb3 M, the ratio G″/G′ is of order unity, indicating that our approximation of biofilms as elastic solids breaks down for this clinical isolate.

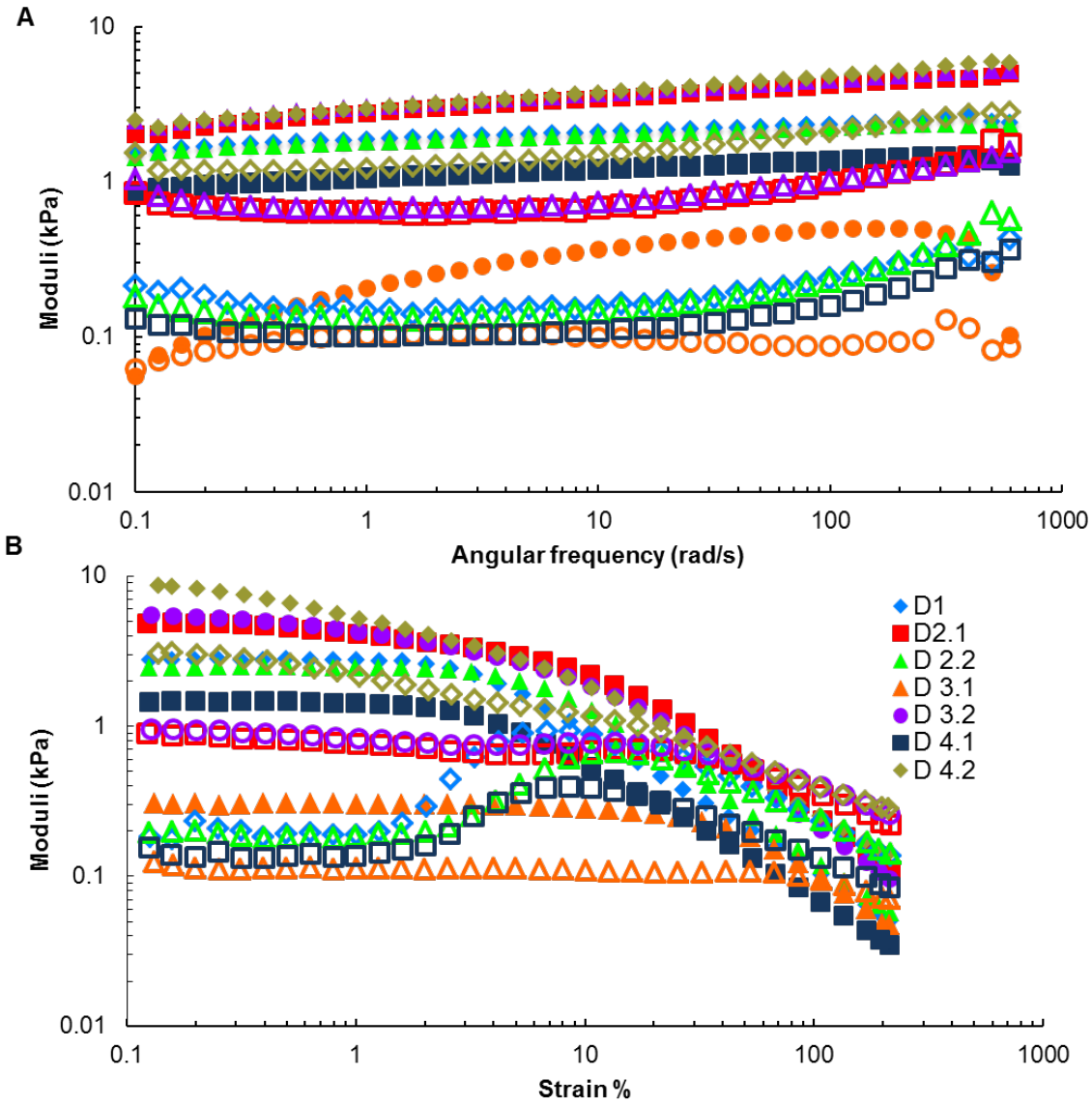

Figure 3.5 Patient D representative frequency sweep and strain sweep curves

Representative (A) frequency sweeps and (B) strain sweeps at 3.14 radians/s for biofilms regrown from clinical isolates taken from Patient D. Elastic moduli are shown by filled symbols and viscous moduli are shown by the corresponding hollow symbols. Data points for the elastic response of bacterial strain D1 are largely hidden under data points for bacterial strain D2.2.

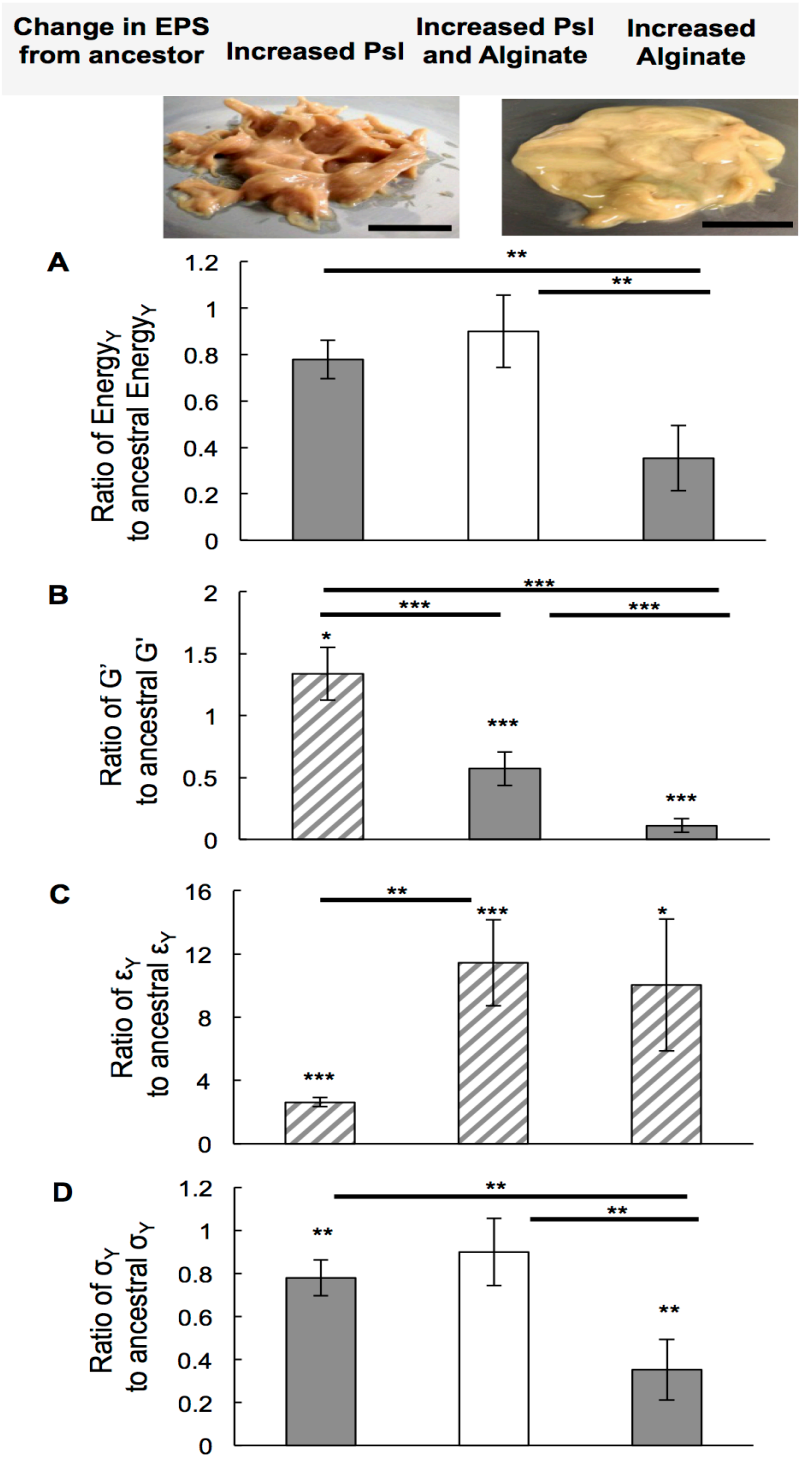

Figure 3.6 Increased production of Psl, alginate, or both enhances specific mechanical properties dependent on polymer production in evolved clinical isolates

Figure 3.6 Evolutionary changes in the mechanical properties of biofilms grown from clinical bacterial isolates, distinguished by whether the isolate strain evolved to increase Psl production, increase production of both Psl and alginate, or increase production of alginate, compared with its initially-isolated ancestor. Mechanical changes from the biofilm grown by each strain's ancestor are measured by taking the ratio of the mechanical property measured for the evolved strain to the corresponding property measured for the ancestor. Thus, a ratio of 1 indicates no change, a ratio greater than one indicates an increase with evolution, and a ratio less than 1 indicates a decrease with evolution. Grey highlights diminished mechanics and striped indicates enhanced mechanics. Inset photos show representative images of pooled biofilms that over-express Psl (left) and alginate (right). The mechanical difference between these two types of biofilms is readily apparent, as increased Psl results in a biofilm that holds the shape of stiff peaks resulting from loading onto the rheometer, but increased alginate results in a biofilm that flows under its own weight to form a smooth surface. (A) Increasing production of Psl maintains toughness (the net energy cost to cause the biofilm to yield), regardless of whether the biofilm more than increasing either polysaccharide alone. Increasing production of alginate but not Psl reduces toughness by more than a factor of two. (B) Increasing production of Psl, but not alginate, slightly increases the plateau elastic moduli G'. Increasing production of alginate but not Psl reduces the plateau elastic moduli G' by more than 10x. Increasing production of both Psl and alginate results in an intermediate case - biofilms are 1.7x softer than their ancestors but over 6x stiffer than biofilms grown by isolates with increased alginate without increased Psl. (C) Increased alginate production increases biofilm yield strains ε_Y by an order of magnitude, regardless of whether Psl production also increases. Increased production of Psl but not alginate raises yield strain only a few-fold. (D) Increased Psl production maintains the yield stress σ_Y, a measure of biofilm strength, at nearly the ancestral value – regardless of whether or not alginate production is also increased. In the absence of increased Psl expression, increased alginate reduces the average yield stress by 2.8x.

These data include: seven isolates with increased Psl (but not alginate) production, five isolates with increased production of both Psl and alginate, and four isolates with increased alginate (but not Psl). Each isolate, and its corresponding initially-isolated ancestor, was measured in three independent trials (so n=3) except for strains from patient C, which were measured in two independent trials (n=2). Only two descendent isolates came from patient C – one with increased Psl (but not alginate) and one with both Psl and alginate increased.

The energy cost to cause biofilms to yield is on the order of 10,000 k_BT/m^3 for biofilms with increased Psl production, and an order of magnitude less for biofilms with increased alginate production (Figure 3.7). For biofilms with increased Psl production, more than 80% of this energy cost is paid in the form of stored, elastic energy (Figure 3.7C), which reflects the fact that these biofilms have plateau elastic moduli G′ that are typically ~10× greater than their plateau viscous moduli G″ (Figure 3.2B, 3.3B, 3.4B, 3.5B).

3.2.3 Psl and Alginate Have Distinct Mechanical Contributions

Therefore, we dissect the distinct mechanical contributions of each polymer. If Psl production does not increase, we find that increased alginate production decreases the plateau elastic modulus G′ by 90% (Figure 3.6B). The yield stress σ_Y is the product of G′ and yield strain ε_Y, which increased alginate increases (Figure 3.6C) – but not by enough to prevent the net effect of increased alginate on yield stress being reduction by over 60% (Figure 3.6D). However, if both alginate and Psl production increase, G′ decreases by only 40% (Figure 3.6B). For isolates with increased Psl expression, σ_Y is maintained at roughly the ancestral value, regardless of alginate expression (Figure 3.6D). Please note that some of the Psl-overexpressing biofilms begin to yield at the lowest strain measured (e.g. A3.3, D4.2 in Figure 3.2, 3.5), and as a result our measurements under-estimate the actual stiffening effects of Psl.

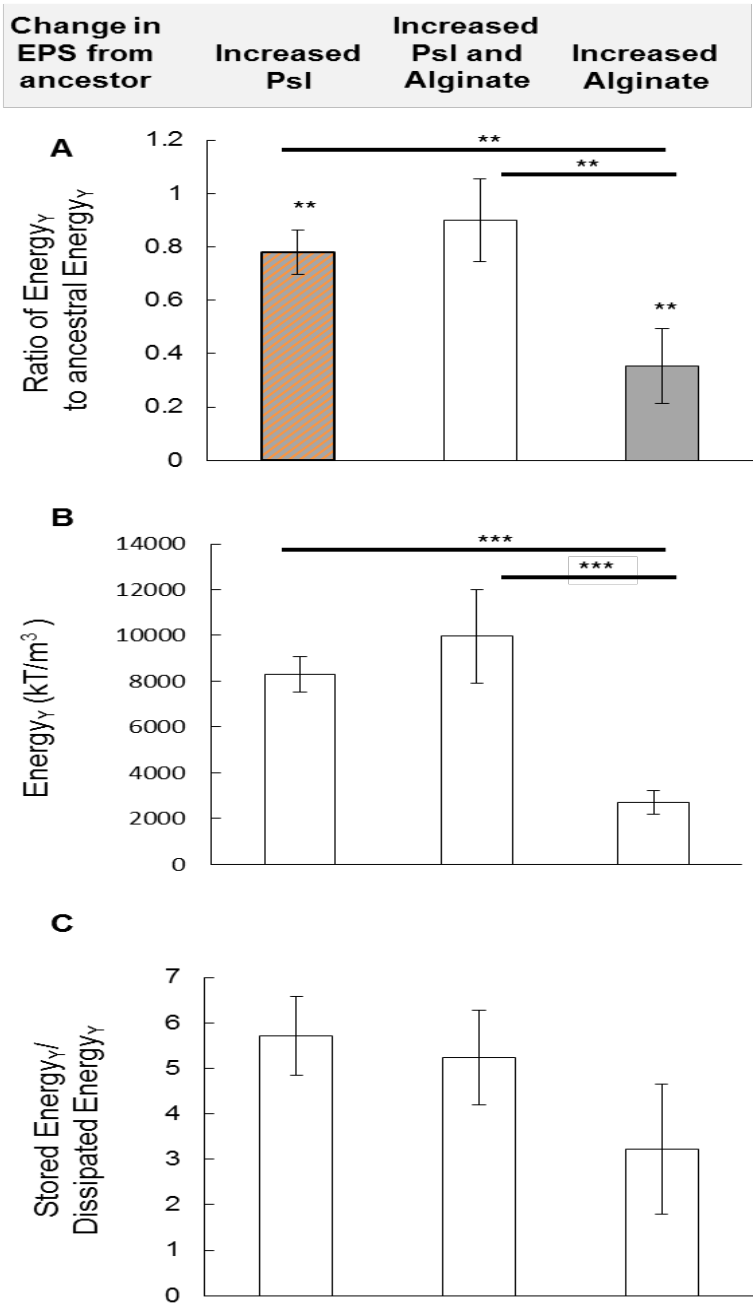

Figure 3.7 Increasing production of both Psl and alginate increases the energy cost to break the biofilm

Figure 3.7 Evolutionary changes in the toughness of biofilms grown from clinical bacterial isolates, broken down by increased Psl and alginate production. Isolates from timepoints after the first are categorized as having increased Psl expression, increased expression of both Psl and alginate, or increased alginate expression. Grey highlights diminished mechanics, and orange-and-grey striped indicates diminished mechanics that are greater than for increased alginate alone. (A) Increasing production of both Psl and alginate increases the energy cost to break the biofilm more than increasing either polysaccharide alone. (B) Biofilms grown from strains that have increased production of Psl have greater breaking energy density than biofilms that increase production of alginate only. (C) The contribution to breaking energy that comes from elastic (stored) energy contributions is typically 3-6× greater than the contribution that comes from viscous (dissipated) energy contributions.

Alginate softening biofilms is consistent with others' work and our own comparison of Δ*mucA*, an alginate over-producer in the PAO1 background, with the PAO1 wild-type (Figure 3.8) [6,96]. We infer that increasing Psl production can partially counteract softening (decreased G′) and entirely counteract weakening (decreased σ_Y) and loss of toughness (decreased $Energy_Y$) caused by increased alginate expression.

3.2.4 Single-Bacteria Cohesion Energies Increase with Increased Psl Production

To probe the role of Psl in biofilm mechanics more directly and at the smallest fundamental unit of the biofilm, we use the cantilever of an atomic force microscope (AFM) to measure force-displacement curves (example shown in Figure 3.9) associated with separating matched pairs of isogenic variants of the lab strain PAO1 with well-defined patterns of EPS expression (Table 3.2). Earlier, we used a similar approach to measure the force of detaching a single bacterium from a surface [28]. PAO1 *in vitro* produces Psl and another extracellular polysaccharide, Pel, but does not produce significant amounts of alginate [33]. We use the Δ*wspF* mutant background of PAO1. The Δ*wspF* mutation results in constitutive high levels of Psl and Pel production due to increased production of the biofilm-promoting, intracellular signal cyclic-di-GMP.

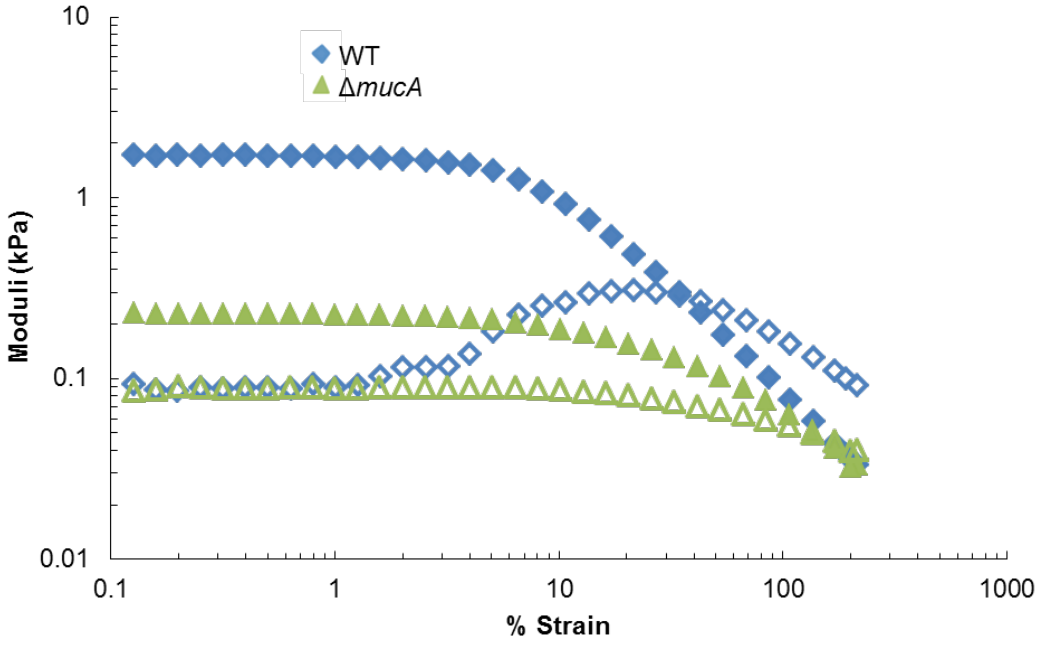

Figure 3.8 Δ*mucA* biofilms that produce alginate are softer than WT

Representative strain sweeps at 3.14 radians/s for WT and Δ*mucA* biofilms. Elastic moduli are shown by filled symbols and viscous moduli are shown by corresponding hollow symbols. Notably, for Δ*mucA*, the ratio G′/G″, while still greater than unity, is much less than for WT or for the non-alginate lab strains measured in Figures 3.7 and 3.17. This suggests that alginate expression is likely to be a factor in the variability of the ratio of elastic modulus to viscous modulus for clinical isolates (Figure 3.2-3.5).

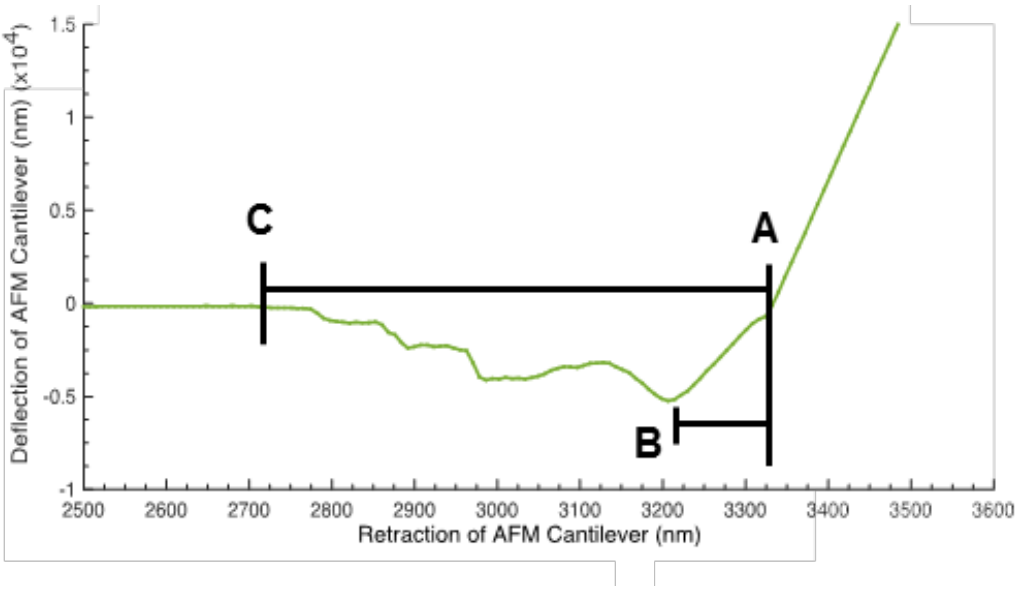

Figure 3.9 Representative force-displacement curve associated with detaching two Psl over-producing bacteria.

At (A), the AFM cantilever tip begins to lift from the surface. At (B), the greatest force magnitude is measured; the distance between (B) and (A) is the separation at maximum force. At (C), the bacterium detaches completely. The distance between (C) and (A) is the interaction range.

Integrating force over position yields the mechanical work of separation, which measures the energy cost paid to separate two bacteria. The energy cost to separate Psl-overexpressing Δ*wspF* Δ*pel* bacteria is 4-6 times greater than the work to separate wild-type 2 (Figure 3.10A, 3.11A). The increase in energy cost arises secondarily from the larger maximum force applied during detachment (Figure 3.10B, 3.11B) and primarily from the larger distance over which the inter-bacterial cohesive force is exerted (Figure 3.10C, 3.11 C and D).

3.2.5 Increased Psl Expression Stiffens and Toughens Biofilms Grown from the Lab Strain PAO1

To confirm the connection between single-bacteria cohesion mechanics to bulk biofilm rheology, we performed rheological tests on biofilms grown using the isogenic lab strains used for AFM measurements (Figure 3.12) and on their isogenic single-gene-knockout counterparts (Figure 3.13). We quantify changes in mechanical properties associated with changes in EPS production by taking ratios comparing an isogenic variant with PAO1 WT (Figure 3.14). We find that increased production of Psl consistently increases the energy cost to break the biofilm – i.e., the biofilm toughness is increased - with the lowest p-value value of any of our tests on any lab strain (Figure 3.14A. The energy cost to break these lab-strain biofilms is approximately 1,000 k_BT/m^3, less than for biofilms grown from clinical isolates (Figure 3.15A). This largely reflects our finding that some clinical-strain biofilms have higher viscous moduli than do lab-strain biofilms (Figures 3.2-3.5, 3.12-3.13). The elastic energy cost paid to cause lab-strain biofilms to yield is typically 10× greater than the viscous energy cost (Figure 3.15B).

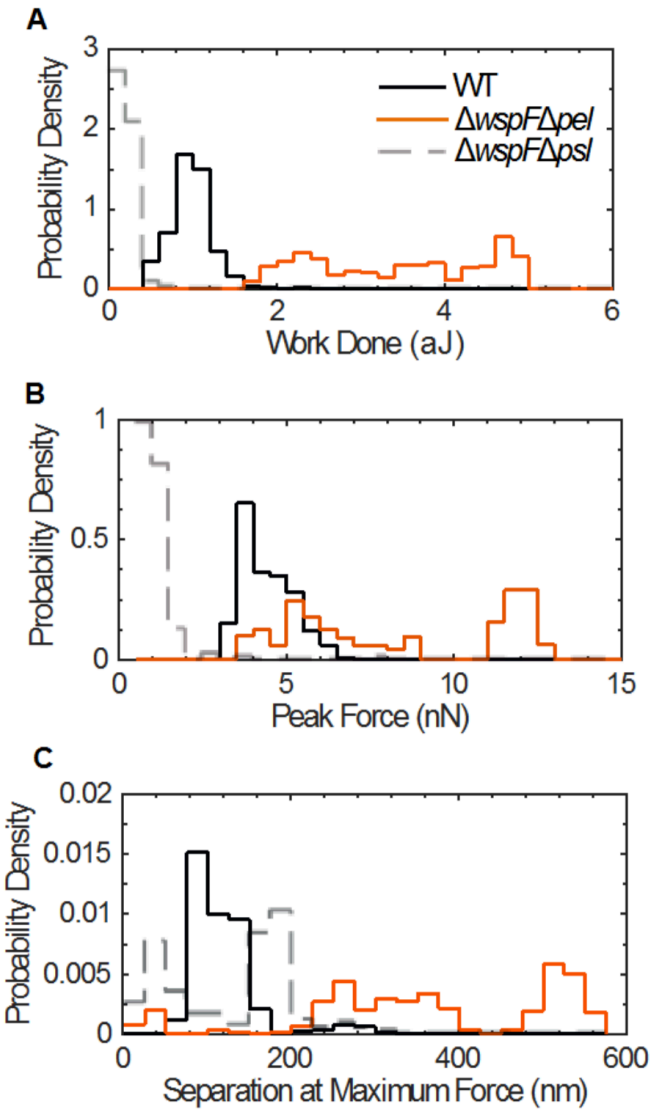

Figure 3.10 Increased Psl production increases inter-bacterial cohesion.

(A) Numerical integration of AFM force-displacement curves gives the net mechanical work of detachment. The work for Δ*wspF* Δ*pel* (solid orange line) is ~4× greater, on average, than for WT (solid black line) and ~10× greater than for Δ*wspF* Δ*psl* (dashed grey line). (B) The peak force is the maximum force measured for each detachment curve. Peak forces for Δ*wspF* Δ*pel* are greater than for WT and Δ*wspF* Δ*psl*. (C) The separation at maximum force is the displacement at which the peak force is found, and is greater for Δ*wspF* Δ*pel* than for WT and Δ*wspF* Δ*psl*. The rate of retraction of the AFM cantilever for the data shown here is 1 μm/s. The trends shown here agree with the trends found when the retraction rate is 10 μm/s (Figure 3.15). (n=200-400).

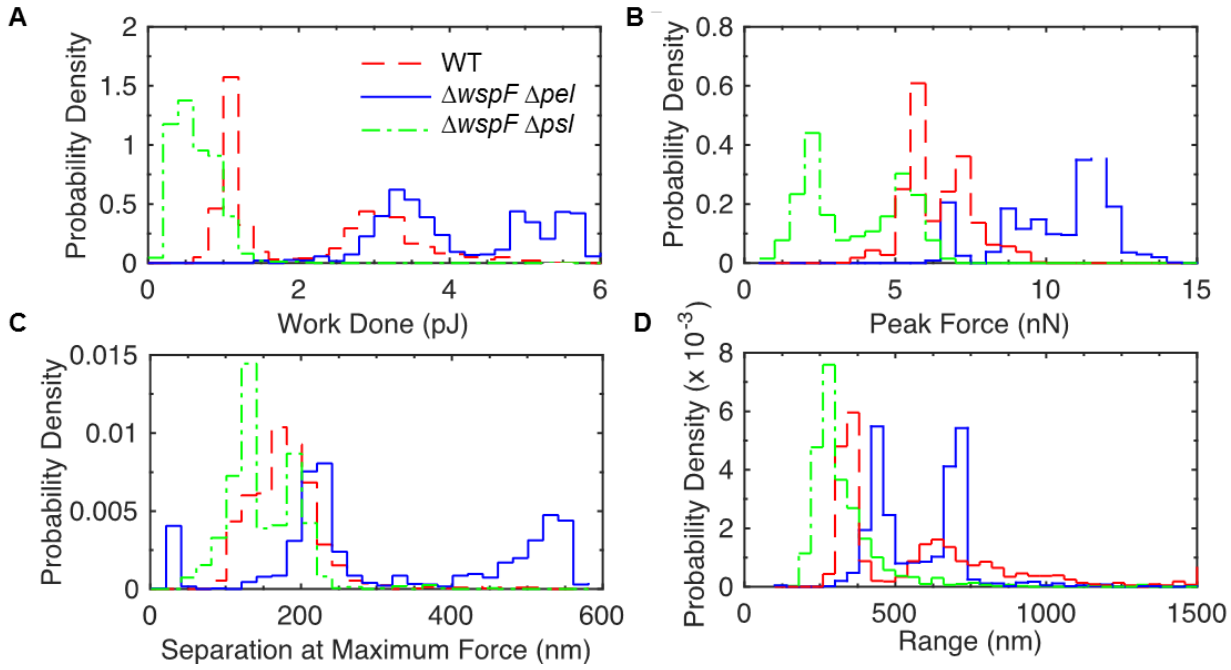

Figure 3.11 Histograms of quantities measured by separating two matched bacteria with an AFM.

The rate of retraction of the AFM cantilever is 10 μm/s. As with the data in Figure 3.10, taken with a retraction speed of 1 μm/s, overall, Δ*wspF* Δ*pel* show stronger mechanical interaction and greater variability than WT and Δ*wspF* Δ*psl*. (A) Numerical integration of force-displacement curves gives the net mechanical work of detachment. (B) The peak force is the maximum force measured for each detachment curve. (C) The separation at maximum force is the displacement at which the peak force is found. (D) The range measures the size of the displacement undergone before the force returns to its baseline, zero value. This measures the lengthscale over which two bacteria can be separated but still mechanically interacting.

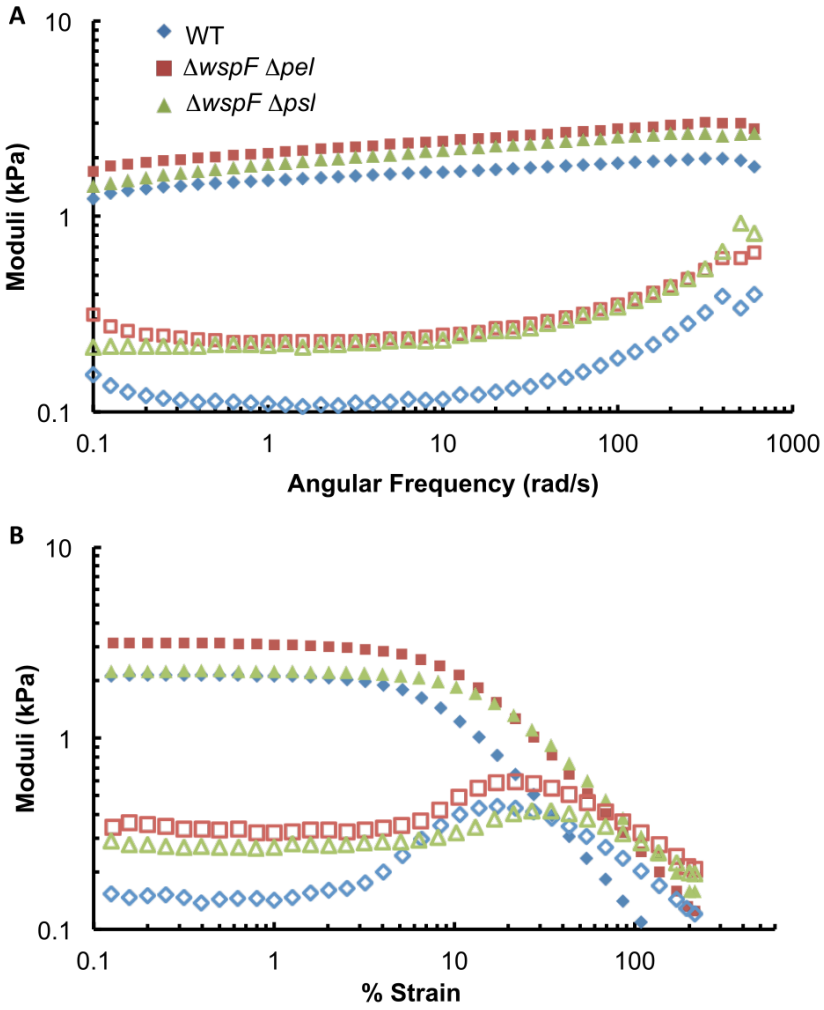

Figure 3.12 Representative frequency and strain sweep for lab strain biofilm measurements

Representative (A) frequency and (B) strain sweeps from one days' worth of measurements on biofilms grown from lab strains of bacteria. Frequency sweeps are at 1% strain and strain sweeps are at 3.14 radians/s. Elastic moduli (G') are shown with solid symbols and viscous moduli (G") are shown with hollow symbols of the corresponding color and shape. Compared with the wild-type bacteria, Δ*wspF* Δ*pel* produces higher amounts of Psl (and does not produce Pel) and Δ*wspF* Δ*psl* produces higher amounts of Pel (and does not produce Psl). Increased Psl production results in an increase in the plateau elastic modulus. Increased Pel production results in an increase in the yield strain.

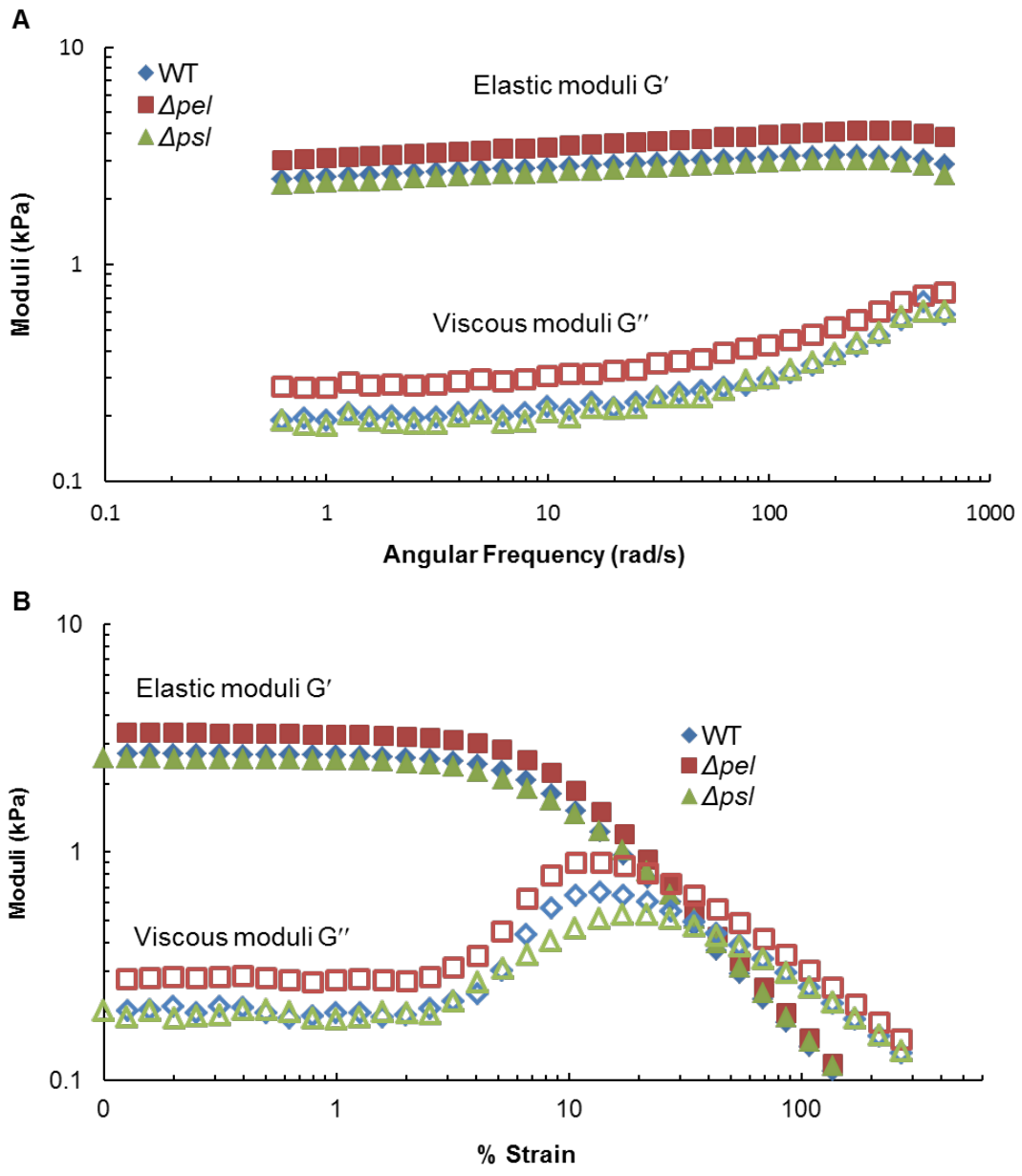

Figure 3.13 Representative frequency and strain sweeps measuring elastic and viscous moduli for WT, Δ*pel*, and Δ*psl* biofilms.

Elastic moduli are shown by filled symbols and viscous moduli are shown by the corresponding hollow symbols. (A) Frequency sweep run at 1% strain. (B) Strain sweep run at 3.14 radians/s.

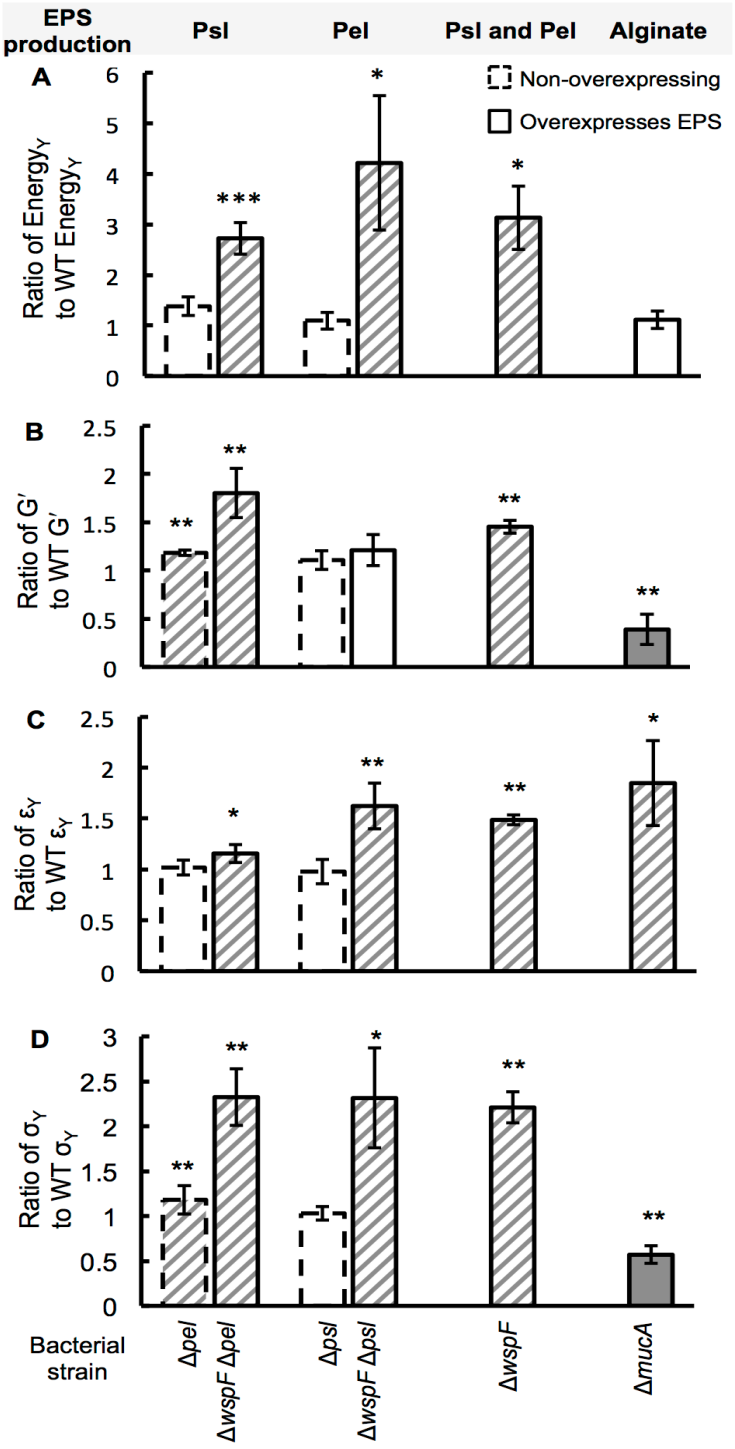

Figure 3.14 Ratio of isogenic knockout mechanical properties to WT based on EPS expression

Figure 3.14 Changes in PAO1 biofilm mechanics associated with changes in EPS expression are measured by taking the ratio of the value for a mutant biofilm to the value for the WT biofilm. Striped highlights enhanced mechanics and grey highlights diminished mechanics. Error bars are standard error of the mean. (A) Increasing the production of Psl or Pel, as seen in Δ*wspF* Δ*psl* (n=4), Δ*wspF* Δ*pel* (n=4), and Δ*wspF* (n=2), increases biofilm toughness. Increasing the production of alginate (Δ*mucA*) has no net effect on biofilm toughness (n=3). Please note that our measurement of toughness as the energy required to cause the biofilm to yield includes both elastic and viscous contributions, while the properties in panels (B-D) are all elastic properties. (B) Increased production of Psl (Δpel (n=3), Δ*wspF* Δ*pel* (n=4), and Δ*wspF* (n=2)) causes biofilms to have higher plateau elastic moduli G' than does the WT biofilm. Increased production of alginate reduces plateau value of G'. Increased production of Pel without a concomitant increase in Psl (Δ*psl* (n=3), Δ*wspF* Δ*psl* (n=4)) does not impact G'. (C) Increased production of Pel or alginate increases the yield strain ε_Y. Over-expression of Psl results in, at most, a minor increase in yield strain. (D) Over-expression of Psl and/or Pel increases biofilm yield stress σ_Y. Over-expression of alginate reduces yield stress.

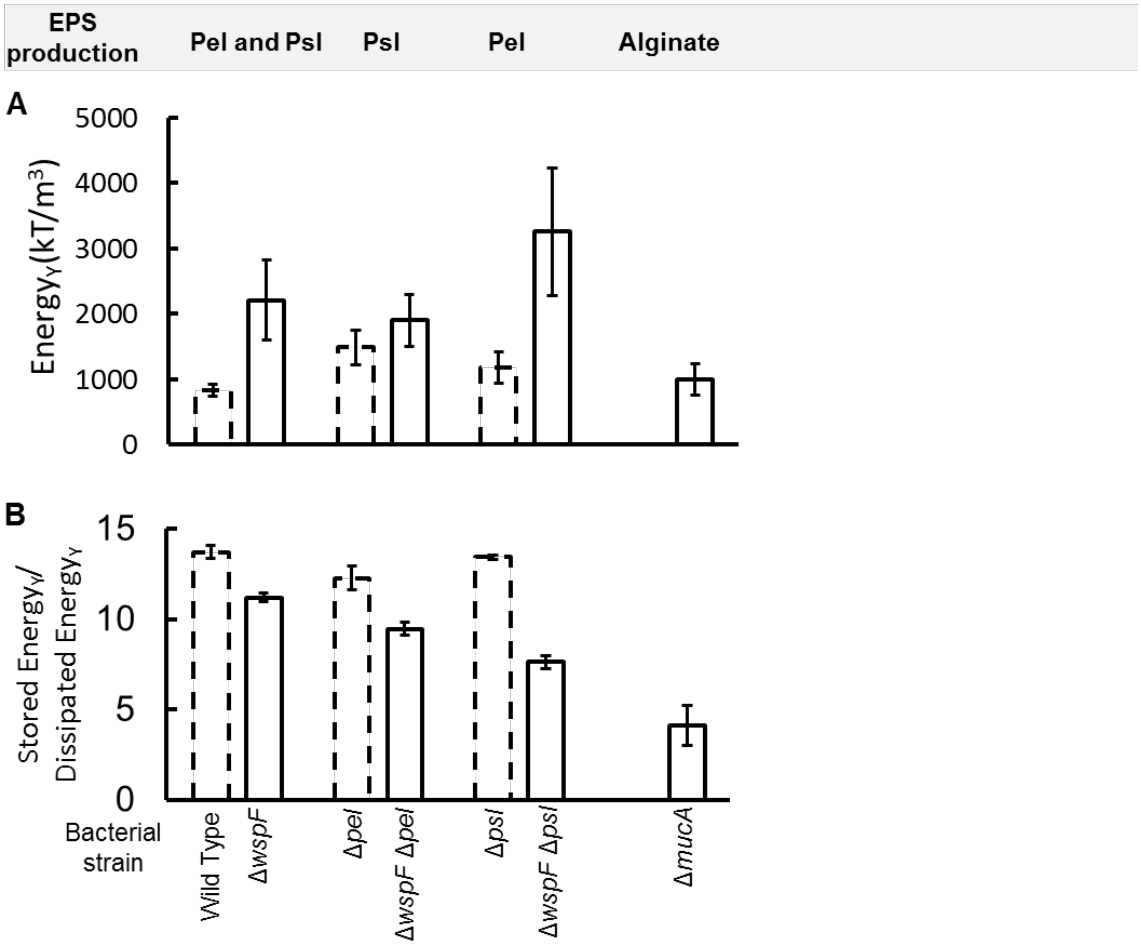

Figure 3.15 Energy required to break isolates grown from lab strains

(A) Energy density required to cause yielding of biofilms grown from lab strains with different patterns of polysaccharide production. (B) For all lab-strain biofilms except Δ*mucA*, the contribution to breaking energy that comes from elastic (stored) energy contributions is ~10× greater than the contribution that comes from viscous (dissipated) energy contributions.

3.2.6 Increased Psl of Pel Expression Strengthens PAO1 Biofilms

Therefore, we examine the contributions of each polymer to specific elastic mechanical properties of biofilms. We find that Δ*wspF* Δ*pel* biofilms, with high amounts of Psl, have plateau G′ 80% greater than that of biofilms grown from WT (Figure 3.14B). Furthermore, biofilms of Δ*pel* have plateau G′ 20% greater than that of the WT biofilm. It is likely that the higher plateau G′ for Δ*pel* reflects an increase in Psl production when Pel production is eliminated [122]. In contrast, we find that over-expression of Pel increases the biofilm's yield strain ε_Y by 60% (Figure 3.14C), while leaving the plateau value of G′ unchanged. These changes are unlike those found for increased alginate, which increases yield strain while decreasing elastic modulus. Increased Psl production has some impact on yield strain, but not as much as increased Pel. Biofilms grown from Δ*wspF* bacteria, which over-express both Psl and Pel, have G′ that is 50% greater than that of WT biofilms and a yield strain that is 44% greater than that of WT biofilms.

For WT PAO1 biofilms, yield stress is typically ≈15 kPa. We find that the yield stress is 130% greater for both Δ*wspF* Δ*pel* and Δ*wspF* Δ*psl* (Figure 3.14D). Δ*wspF* biofilms have yield stress that is, on average, 50% greater than that of biofilms grown from WT. From this we conclude that increased expression of either Psl or Pel can increase the material strength of *P. aeruginosa* biofilms, although Psl does so by stiffening the biofilm and Pel does so by making the biofilm more ductile. Over-expression of both (by Δ*wspF*) results in comparable strengthening to that for either one alone.

3.2.7 Psl Likely Stiffens Biofilms Because It is Cross-linked by the Protein CdrA

It is striking that, of the three EPS materials examined, Psl is the only one that acts to stiffen the biofilm when its production increases. Furthermore, examining mature biofilms (grown in flow cells) under confocal and phase contrast microscopes shows a low volume fraction of discrete bacteria bound in a large, continuous, primarily-polymer matrix that is well over 50% of the volume of the biofilm. Therefore, we expect that changes in biofilm mechanics are most likely to represent changes in the polymer matrix of the biofilm, not changes in the interactions between bacteria and the matrix.

It is well-known that increasing the concentration of polymer (c) in a gel will increase the gel's stiffness, $G' \propto cA$, where A is a scaling factor that is 2.25 for entangled polymer in good solvent [105]. Stiffening by increasing polymer concentration is a physical effect that does not depend on polymer chemistry. However, increasing Pel and alginate production does not stiffen biofilms. Moreover, our biofilms are grown in contact with a large water reservoir (the agar gel), which should act to minimize differences in polymer concentration. Thus, we infer that specific chemical characteristics of the EPS types govern their different effects on biofilm mechanics. Psl is a neutral, branched pentasaccharide made of D-glucose, D-mannose, and L-rhamnose [42]. Psl contains several mannose groups, including a mannose side-chain, to which the protein CdrA, which has been suggested by other researchers as a possible crosslinker, binds [117,122]. CdrA is co-regulated with Pel and Psl through c-di-GMP induction, and is therefore over-produced in all the Δ*wspF* backgrounds. To examine the role of CdrA in contributing to stiffening by Psl, we measure the shear mechanics of

biofilms grown from Δ*pel* Δ*cdrA*, which does not produce CdrA, and compare with Δ*pel* biofilms. When the capacity to make CdrA is lost, the stiffening effect found for Δ*pel* is lost and the elastic modulus and toughness return to approximately those of the WT (Figure 3.16). From this, we conclude that CdrA likely crosslinks Psl and that this is the cause of Psl-induced stiffening. Furthermore, our AFM measurements imply that stiffening by Psl should result from a process that can occur over the one second during which the two bacteria are in contact before we begin separation. Chemical processes, such as protein binding, are faster than physical process such as polymer entanglement. Indeed, if reptation of entangled polymers were important for our systems over the timescales of measurement, we would expect to see a crossover in viscous and elastic moduli at the inverse of the reptation time; instead, no such crossover is seen for frequencies from 0.1 to 1000 Hz (Figure 3.12A, 3.13A).

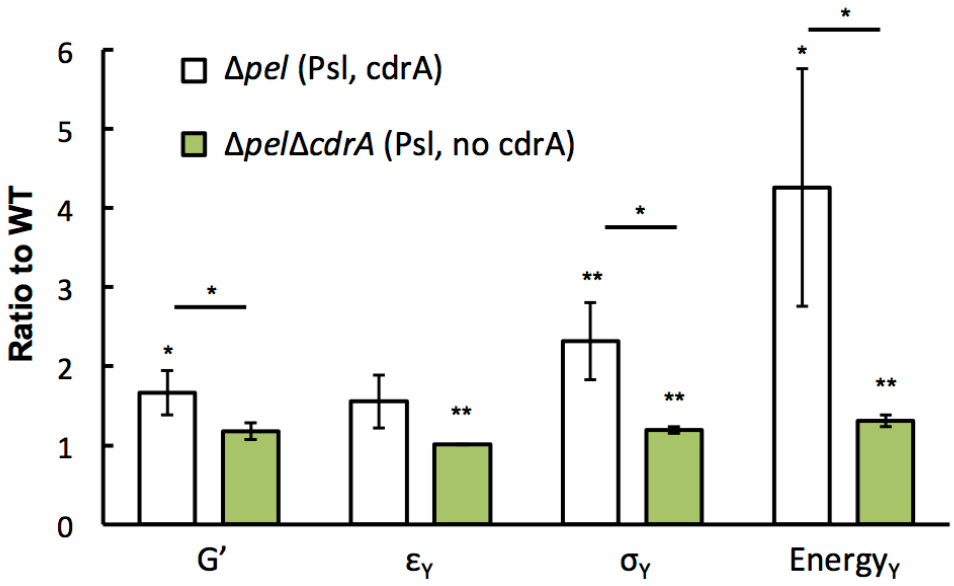

Figure 3.16 Psl conferred mechanics are lost without production of CdrA

Production of the protein CdrA is needed for the stiffening (increased G′), strengthening (increased σ_Y), and toughening (increased yield energy) effects of Psl. For Δ*pel* strains that produce Psl but not Pel, biofilm mechanics are enhanced compared to the WT only if CdrA is also produced. (n=3).

3.3 DISCUSSION

3.3.1 Summary of Results

Increasing the expression of the extracellular polysaccharide Psl increases the stiffness and the mechanical strength and toughness of *P. aeruginosa* biofilms. This must arise from molecular specifics of Psl because increasing the expression of other extracellular polysaccharides Pel and alginate, or increasing Psl without the presence of the Psl-binding protein CdrA, have different effects on biofilms mechanics. Increasing the expression of Pel also strengthens the biofilm, but by increasing yield strain rather than increasing stiffness. In clinical isolates, increasing alginate expression softens and weakens the biofilm, but this can be counteracted by also increasing Psl expression, which synergizes with increased alginate expression to increase the energy cost to break the biofilm. Thus we have shown that, in CF lungs, biofilms have a tendency to evolve in such a way that mechanical toughness and stiffness are maintained, despite a parallel tendency to evolve increased alginate production, which weakens and softens biofilms.

3.3.2 Potential Impact on Clearance by the Immune System

Neutrophils are phagocytic immune cells that densely surround biofilm infections without actually entering the biofilm [53,54]. It has been recently pointed out that, because ~10 μm neutrophils are an order of magnitude smaller than ~100 μm biofilm infections, the only way that neutrophils will be able to engulf biofilm bacteria will be if they can break off a small piece of the biofilm [123]. During phagocytosis, neutrophils exert estimated attractive stresses of ~1kPa [69]. The elastic moduli G′ that we measure are also on the order of ~1kPa (Figure 3.2

– 3.5). Since the elastic moduli we measure are comparable to the stresses exerted by neutrophils during phagocytosis, it is plausible that the tenfold difference in G′ and the over-twofold difference in yield stress that we measure for biofilms with different patterns of matrix production could impact their susceptibility to phagocytosis and that increasing Psl production could help to protect against phagocytosis through its impact on G′ and yield stress. In addition to overall susceptibility, biofilm mechanics are likely to impact the timescale of phagocytosis. Alterations in timescale matter because bacterial biofilms can express virulence factors that kill neutrophils and other immune cells – so that delays that give more time for these biochemical factors to act should be protective for the biofilm, even if the mechanical changes per se do not altogether prevent phagocytosis. Thus, biofilms may act as a fortress to resist mechanical attack.

This will be explored and discussed in greater detail in the following chapter, Chapter 4.

3.3.3 Mapping *In vitro* Properties Onto *In vivo* Properties

It is widely thought that the mucus in cystic fibrosis (CF) airways is more concentrated, with less water, compared with the mucus in normal, healthy airways (for examples of an extensive literature containing a great deal of controversy, see Garland *et al*., 2013 PNAS 110:15973-15978 and Mall *et al.,* 2004 Nature Medicine 10:487-493 [124,125]). Although *P. aeruginosa* biofilms are not typically found in healthy lungs, it is possible that if they were, they would be more hydrated than *P. aeruginosa* biofilms of the same strain in CF lungs. The degree of such difference in hydration, if any, is not known.

The lungs consist of the respiratory zone, which does not have submucosal glands, and the conductive zone, where mucus is produced and the mucociliary escalator provides a defense against pathogens by removing them [64]. This removal is hindered in CF because of the high viscosity of concentrated mucus. In terms of CF lung infections, *P. aeruginosa* biofilms are rarely found in the respiratory zone of mature patients (like the ones from which our clinical isolates were drawn), likely owing to the intensive antibiotic treatment commonly used for this disease [64]. Sputum, from which all the clinical isolates we study were taken, is coughed up from the conductive zone of the lungs, so that any biofilms growing in it are embedded in mucus. Because the mucus volume is much greater than the volume of the ~100 μm biofilm spheroids found in CF lungs [53], the mucus acts as a fluid reservoir for the biofilms just as does the nutrient agar gel in our petri dishes on which we grow biofilms. Therefore, to zeroth order, we expect the degree of hydration for all biofilms growing within the conductive zone to be roughly the same, modulo any inter-patient differences in mucus composition and any intra-patient changes in mucus composition over time. We therefore expect the shifts in mechanics we measure in vitro to result from different biofilm matrix compositions to correspond to similar trends of biofilm mechanics *in vivo*.

3.4 Related and Future work

3.4.1 Microrheology

Our finding that Psl stiffens biofilms and Pel makes biofilms more ductile are reasonably congruent with a recent microrheological study that examined the effects of Pel and Psl on the creep compliance of biofilms grown in flow cells

using an alginate-overexpessing background [126]. Creep compliance describes the deformation of a material under a constant load and it includes both elastic (solid-like) and viscous (fluid-like) interactions. In contrast, our use of oscillatory bulk rheology allows us to distinguish the elastic modulus G' and the viscous modulus G''. Passive microrheology is well-adapted to studies of local heterogeneities, which our bulk measurements cannot probe, but passive thermal motions are insufficient to cause biofilms to yield. Therefore, passive microrheology cannot obtain information about yielding and toughness. Thus, our measurements also allow us to compare the elastic modulus and yield stress of biofilms grown from clinical strains with the stresses other researchers have estimated that phagocytosing neutrophils exert, to show that the mechanical changes we measure and associate with different evolutionary changes in polysaccharide production are likely to have a significant impact on the biofilm infections' susceptibility to phagocytosis. This is the first hint of evolution to adapt biofilm mechanics under pressure from the immune system.

3.4.2 Pel Electrostatic Binding to DNA

Unlike our bulk measurements of Pel-overexpressing biofilms, our AFM studies of cell-cell cohesion show that Pel over-expression actually decreases the distance over which inter-bacterial cohesion forces are exerted (Figure 3.10C, Figure 3.11 C and D) and the work of detachment (Figure 3.10A, 3.11A), compared with the WT. Thus, unlike Psl, the effects of Pel on biofilm mechanics are inconsistent with its effects at the single-cell level. This implies that the increased ductility and the resulting increased yield stress of Pel-overexpressing biofilms is an emergent property of the biofilm state. Recent work has shown

that Pel is cationic and binds extracellular DNA [48]. Extracellular DNA is a significant component of the polymeric matrix in biofilms [36], but not for the planktonic bacteria in our AFM studies. Therefore, we speculate that the increased biofilm yield strain, and resulting greater yield stress, associated with increased Pel production arise from Pel binding to extracellular DNA. For example, in so-called "double network" gels made of two kinds of interacting polymers, the yield strain can be greater than that of a gel made of either polymer alone, as a result of mobile inter-polymer junctions and of one polymer acting as "hidden length" within the network[108,127].

3.4.3 Heterogeneity

Other researchers have shown that the spatial distribution of polysaccharide types in biofilms is heterogeneous [16,48,128]. Integrating this with our results implies that biofilm mechanics are likely to be heterogeneous, as seen for *E. coli* [101]. Thus, the localized effects of specific polymers may be much greater than our bulk rheology measurements are able to characterize. Future work, using microrheology[101,126] in combination with staining for specific EPS materials, could address this. Furthermore, although our studies have focused on monoclonal biofilms, real biofilm infections are often poly-clonal and poly-species, which increases the number of ways in which biofilms could be heterogeneous and tuned for optimum fitness.

3.5 METHODS

3.5.1 Bacterial Strains and Growth Conditions

The strains of *P. aeruginosa* used in this study are described in Table 3.1 (for clinical isolates [25,129]) and Table 3.2 (for lab strains [47,117,130-133]). Each lab strain constitutively expresses green fluorescent protein (GFP). GFP expression was intended as future-proofing so that we could later examine the relationship between single-cell behavior imaged using fluorescence microscopy and the bulk biofilm rheology that we measure here.

We grew all bacterial cultures in Luria broth (LB). For rheology, strains were grown overnight in 4 mL LB, shaking at 37 ˚C. Then we spread the overnight culture onto agar plates at 250μL/plate. The biofilm grew overnight on the agar plates.

Label	Sample ID	Days *in vivo*	Colony morphology	EPS classification
A1	C2773C	0	Classic	Ancestor
A2	C3470C	570	Classic	Not used
A3.1	C3639M	703	Mucoid	Increased Psl and Alginate
A3.2	C3640D	703	Small	Increased Psl
A4	C4278M	1194	Mucoid	Increased Psl and Alginate
B1	C1913C	0	Classic	Ancestor
B2.1	C4218C	1669	Classic	Increased Psl
B2.2	C4219D	1669	Small	Increased Psl
B2.3	C4220M	1669	Mucoid	Increased Psl and Alginate
B3.1	C5912M	2790	Mucoid	Increased Alginate
B3.2	C5913C	2790	Classic	Not used
B3.3	C5914M	2790	Mucoid	Increased Alginate
Cb1	C2159M	0	Mucoid	Ancestor
Cb2	C3488D	1025	Small	Increased Psl
Cb3	C5623M	2545	Mucoid	Increased Psl and Alginate
D1	C3881C	0	Classic	Ancestor
D2.1	C4197D	252	Small	Not used
D2.2	C4198C	252	Classic	Increased Psl
D3.1	C6926M	1988	Mucoid	Increased Psl and Alginate
D3.2	C6927C	1988	Classic	Increased Psl
D4.1	C7514E	2394	Entire	Not used
D4.2	C7515D	2394	Small	Increased Psl

Table 3.1 Clinical isolates used in this study

Chronological clinical isolates from four cystic fibrosis patients with chronic *P. aeruginosa* infections (Patients A-C [1]; Patient D [2]) were used in this study. To bin data for the analysis shown in Figure 3.6, each strain used except for the initially-isolated ancestor strain was classified as having increased Psl, increased alginate, or both, compared with the ancestor. Increased alginate was determined by visual identification of mucoid colonies. Determination of increased Psl was taken from [134]. Isolates that had neither increased Psl nor increased alginate were not used because the purpose of this study was to examine the effect of changes in EPS production on biofilm mechanics.

Strain	Description	Ref.
PAO1 GFP	Wild Type [6] makes Psl and some Pel, no alginate	[130]
Δ*pel* GFP	Makes Psl, no Pel, no alginate	[117,135]
Δ*psl* GFP	Makes Pel, no Psl, no alginate	[131]
D*mucA* GFP	Over-expresses alginate	[132]
Δ*wspF* Δ*pel* GFP	Over-expresses Psl, no Pel, no alginate	[133]
Δ*wspF* Δ*psl* GFP	Over-expresses Pel, no Psl, no alginate	This paper (for GFP addition)

Table 3.2 Lab strains used in this study**.**

3.5.2 Background Rheology

Mechanically, biofilms are viscoelastic materials [91], with both solid-like (elastic) and fluid-like (viscous) properties. We measure the bulk mechanics of biofilms by applying an oscillatory shear strain, $\varepsilon = \varepsilon_0 \sin(\omega t)$ (where ω is the angular frequency of oscillation and t is time) and measuring the resulting shear stress using a rheometer [92]. Shear strain is the lateral deformation of a material divided by its thickness in the non-deformed direction (Figure 3.17 A&B).

Stress is force per unit area and is the product of the strain and the elastic modulus. When a strain is applied, the material's stress response, $\sigma = \sigma_0 \sin(\omega t + \delta) = \varepsilon_0 [G' \sin(\omega t) + G'' \cos(\omega t)]$, (1) gives the elastic modulus G' and the viscous modulus G''. The viscous modulus characterizes the material's fluid-like resistance to flow. The elastic modulus characterizes the material's solid-like resistance to deformation in the elastic regime where the stress-strain relationship is linear and reversible (Figure 3.17 C&D). When a material is deformed past the elastic regime, the material is irreversibly deformed and begins to mechanically fail. The yield strain is the strain at which material failure begins, and the yield stress is the stress at which material failure begins (Figure 3.17 C&D).

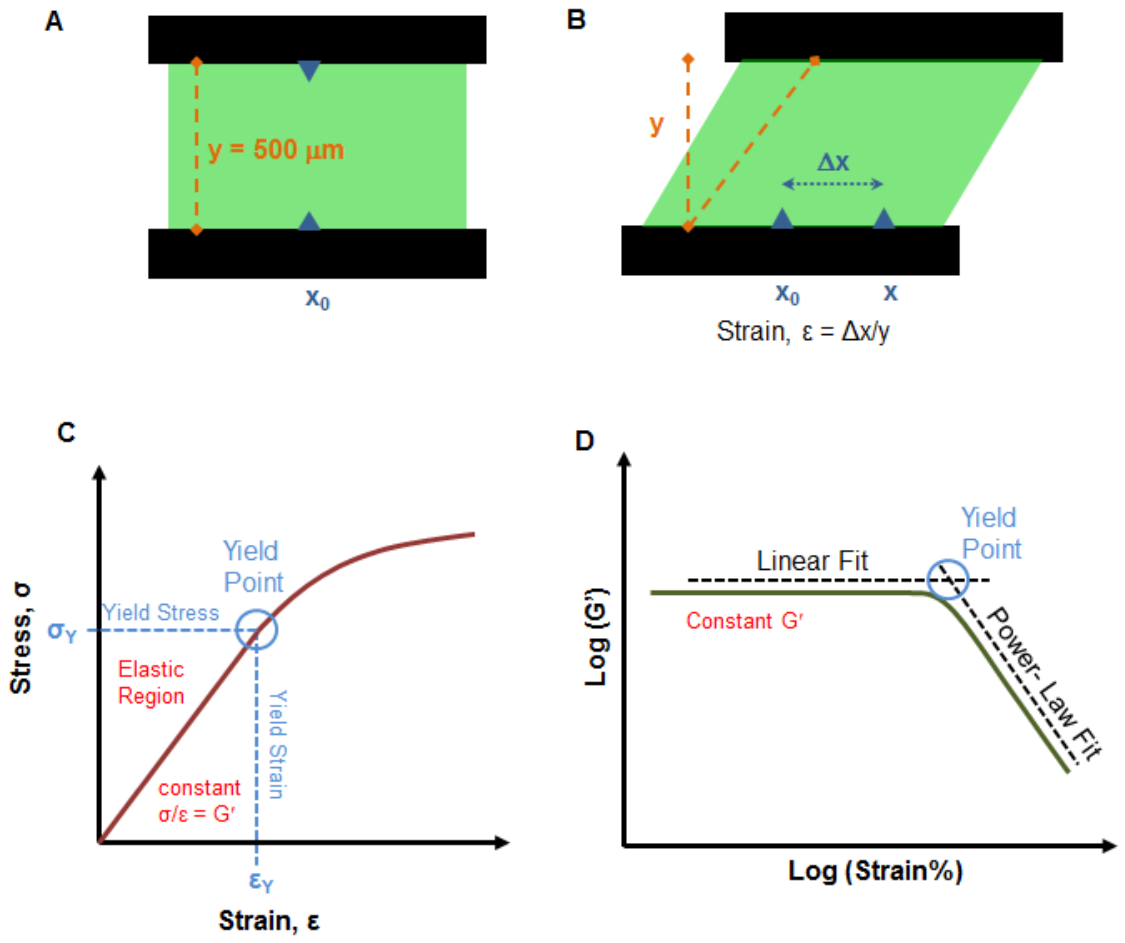

Figure 3.17 Schematics of rheology measurements and measurements taken from stress-strain curves.

(A and B) The rheometer tool (two parallel, black plates) applies a mechanical shear to the biofilm (green). (A) shows the unstrained state; (B) shows displacement of the top plate to impose a shear strain $\varepsilon = \Delta x/y$. (C) For elastic solids, the slope of the linear regime of the stress-strain curve gives the material's elastic modulus G′. The end of the linear regime marks the yield point, which correlates with a yield strain and yield stress. (D) Using our strain-sweep rheology measurements, we determined biofilm yield as the point of intersection between a linear fit to the plateau elastic modulus G′ and a power-law fit to the region of decreasing G′ with strain.

3.5.3 Rheology Measurements

We used a stress-controlled TA Instruments AR-G2 Magnetic Bearing Rheometer for bulk rheology measurements. We used a parallel-plate tool geometry, with a roughened surface to prevent slippage. The biofilm from multiple agar plates (grown from the same strain) was scraped directly onto the rheometer using a metal spatula. We typically used 10-15 plates' worth of biofilm per measurement. Biofilm was loaded into the rheometer tool as quickly as possible, with two people working together, to minimize evaporation. Then, the geometry of the rheometer was lowered to a 500 μm gap height, and any excess biofilm was trimmed, if needed, so that sample material did not extend beyond the edge of the tool. Filling the tool with this gap required approximately 0.6 mL of biofilm. Since the 500 μm gap height is smaller than recommended for this rheometer, we tested the output of the rheometer at this gap height in the regime of our measurements with a calibration oil to verify that this gap is acceptable. To prevent drying of the biofilm during measurement, a cylindrical solvent trap was made from polycarbonate, lined with moist cotton balls, and placed around the geometry and base of the rheometer. An image of the solvent trap and time-sweeps contrasting the effects of drying, in the absence of the solvent trap, with no drying, when the solvent trap is used, are shown in Figure 3.18.

Oscillatory frequency sweeps from 0.1 to 600 rad/s at 1% strain and strain sweeps from 0.1 to 200% at 3.14 rad/s were performed on each sample on each day of measurement. The plateau modulus G′ was taken as the elastic modulus at 1% strain for biofilms grown from lab strains of bacteria, and at 0.5% strain for biofilms grown from clinical isolates. These strain values are below the yield

stress for the biofilms measured – a lower strain was used for biofilms grown from clinical isolates because many of these yielded before 1% strain.

Representative frequency and strain sweeps are shown for 1 day's worth of measurements on clinical isolates (from one patient) in Figure 3.2 - 3.5, and for WT and EPS over-expressing lab strains in Figure 3.12, 3.8 and 3.13.

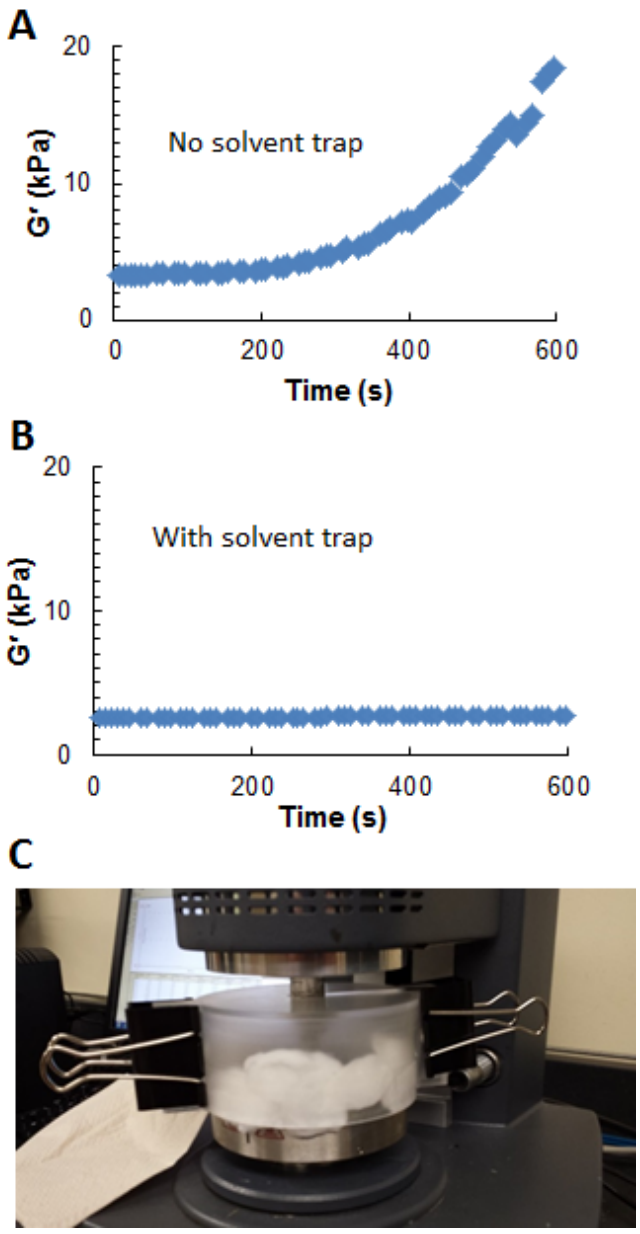

Figure 3.18 Biofilm drying in the presence and absence of a solvent trap

Time sweep of WT to evaluate drying with and without solvent trap. Elastic modulus G′ was measured for 10 minutes at constant strain and frequency. (A) Without the solvent trap, the stiffness of the biofilm increases with time as a result of water loss. (B) With the solvent trap, biofilm stiffness stays constant in time. The solvent trap alleviates the stiffness increase due to drying. (C) Image of the rheometer tool with the solvent trap in place.

3.5.4 Determination of Yield Stress and Yield Strain

The yield strain of each biofilm was determined from strain-sweep data. The plateau region on the left part of each strain-sweep graph, where stress and strain are linearly related, was fit to a linear equation. The region on the right part of each strain-sweep graph, after the biofilm has "broken" and the modulus quickly decreases with increasing strain, was fit to a power law. The strain at which these equations intersect was taken to be the yield strain (Figure 3.17D). The corresponding yield stress was then determined from the raw rheology data.

3.5.5 Statistical Significance

P-values are calculated using a Student one-tailed T-test. Each p-value associated with a single bar tests the null hypothesis that the ratio should be unity. Each p-value that compares two bars tests the null hypothesis that the compared values are the same. P-values are indicated on the figures as follows: * $p<0.1$, ** $p<0.05$, *** $p<0.005$. Error bars are standard error of the mean. The sample size and number of repetitions was chosen to give p-values of 0.05 or less for our central conclusions (Figures 3.6, 3.14, and 3.16). In figures, error bars are standard error of the mean.

3.5.6 AFM Force Measurements

We used a BioScope Catalyst BioAFM (Bruker) for atomic force microscopy (AFM) measurements. This instrument combines both fluorescence and atomic force microscopy. We used triangular silicon nitride cantilevers (Bruker, MSNL-10, spring constant 0.07 N/m) for all measurements. Thermal tuning was used to confirm the cantilever spring constant. The cantilevers were loaded into a fluid probe holder.

To prepare the probe for attachment of bacteria, we dipped the probe into a droplet of 0.1% w/v poly-L-lysine solution for approximately 30 minutes. The probe was removed from the droplet and the excess solution was wicked from the cantilever using a Kimwipe. Poly-L-lysine is a polycation that electrostatically attaches bacteria to the probe. We allowed the probe to dry for 10 minutes and then dipped it into a droplet of bacterial suspension. The probe was in the bacterial suspension for ~30 minutes and was then gently rinsed with deionized water. We verified the presence of bacteria on the cantilever using a Plan Apo 60x oil objective (Nikon) with bright-field microscopy.

While the cantilever was being prepared, a glass slide was prepared similarly. We placed a droplet of 0.1% w/v poly-L-lysine onto the glass slide for 30 minutes; we wicked away excess solution with a Kimwipe; the slide was allowed to dry for 10 minutes. A droplet of bacterial suspension was then placed onto the same location, left there for 30 minutes, and then rinsed. We then placed a fresh droplet of de-ionized water on the fixed bacteria.

We used the AFM probe, with attached bacteria, to image the surface in contact mode. While the presence of bacteria on the probe decreases image quality, the location of bacteria on the surface can still be discerned from the resulting image. Once bacteria were located on the surface, the probe was positioned over a single bacterium on the surface. We lowered the cantilever tip onto a bacterium, held the tip on the bacterium for 1s, and then retracted the probe. This cycle was repeated 200-400 times over a vertical distance of 4 μm at speeds of both 10 μm/s (Figure 3.15) and 1 μm/s (Figure 3.10). We used the deflection of the cantilever upon retraction to measure the adhesion force

between the bacterium on the surface and the bacterium on the cantilever. An annotated representative force-displacement curve is shown in Figure 3.9.

3.5.7 Analysis of Force Displacement Curves

We used MATLAB to analyze the data from the retraction curves obtained using the AFM. Frequently, bacteria were removed from the surface during over the course of hundreds of approach-contact-retraction cycles, and sometimes the AFM tip would break over the course of cycles. To distinguish true inter-bacterial force-separation curves, we discarded all the curves which had an interaction region less than 150nm (that of the "control curve" taken with a tip attached to bacteria, and a surface free of bacteria). We also discarded all the plots which have a consistent slope till the minima in the interaction region; if we are measuring a polymer interaction rather than the sensitivity of the cantilever, we would expect the slope to change once the tip begins to pull off the surface.

Using the measured spring constant of the cantilever, the slope extracted from the contact region is used to calculate the force exerted on the cantilever during retraction. The work done during retraction was calculated by numerical integration in Matlab. The quantities measured are roughly the same for a cantilever tip retraction speed of 1 μm/s (Figure 3.10) or 10 μm/s (Figure 3.15).

Chapter 4: Neutrophil Phagocytosis of Large Viscoelastic Hydrogels With Varying Mechanics

4.1 Introduction

Neutrophils are short-lived phagocytic immune cells and the most abundant white blood cell in humans. Neutrophils, an integral part of the innate immune system, rapidly respond during the initial inflammatory response to infection and migrate from the bloodstream into infected or damaged tissue where they can clear away pathogens and debris.

Phagocytosis is one of a neutrophil's main defenses against pathogens. The shape and size of the phagocytic target are known to impact the initiation and completion of phagocytosis – others have shown that neutrophils are unable to engulf rigid particles over ~10μm in size, which is roughly the size of a neutrophil [69,72]. Single bacteria are ~1μm in size and are readily engulfed by neutrophils. However, biofilm infections in soft tissue are made up of aggregates that are ~5-200μm in size – too big to be cleared by neutrophils if the biofilm acts like a solid, rigid target [110]. Imaging studies of chronic biofilm infections show bacterial aggregates that are densely surrounded by neutrophils that are unable to clear the infection [53].

However, biofilms are not rigid solids but instead are composite viscoelastic materials. We have shown that biofilms re-grown from clinical isolates have elastic moduli in the range 0.1-10 kPa [76]. We also found that *in vivo* evolution in chronic Cystic Fibrosis (CF) infections changed the production of matrix polymers in a way that promoted mechanical toughness. Others have found that neutrophils can exert an attractive force of 1kPa during phagocytosis[69]; this is consistent with the forces exerted by macrophages during

phagocytosis[72,136]. Since the mechanical stress exerted during phagocytosis is within the range of mechanical properties characterizing biofilms, we have hypothesized that the mechanical robustness promoted by changes in polymer production in clinical isolates is an evolutionary adaptation that increases the biofilm's ability to avoid phagocytosis by neutrophils. Our hypothesis also suggests that treatments that weaken biofilms mechanically could help to promote clearance by the body's innate defenses, without involving antibiotic mechanisms or antibiotic resistance.

It was recently shown that neutrophils were able to use trogocytosis, a process that allows neutrophils to engulf parts of neighboring cells, to break off fragments of and kill *Trichomonas vaginalis* [70,137-139]. *T. vaginalis* is a large pathogen that surpasses the size of particles neutrophils can engulf during phagocytosis. Neutrophils were able to kill the parasite by taking bites, leading to the death of the parasite. Killing via trogocytosis was shown to be actin-dependent and contact-dependent, but independent of phagocytosis and external microbicidal factors such as reactive oxygen species (ROS)[70]. The nibbling process of trogocytosis and the neutrophil's ability to engulf smaller pieces of a large target could be linked to whether or not neutrophils can break off pieces of and clear a bacterial biofilm. We know that neutrophils can take these "small bites" of a large target, but it's unclear how target mechanical properties may influence this process and if these toughened biofilms are at an advantage when targeted by biofilms. However, our hypothesis about the effect of biofilm mechanics on the phagocytosis of biofilms cannot be tested using the current state of the art, because protocols for determining how a large, viscoelastic target's mechanics impacts its susceptibility to phagocytosis, by neutrophils or by

any other phagocytic cell, do not exist. This prevents both our basic understanding of neutrophil phagocytosis and the development of novel anti-biofilm treatments.

To fill this gap and have the ability to elucidate the mechanical limitations of phagocytic engulfment, we developed a relatively cheap and quick method to determine neutrophils' ability to successfully engulf large, viscoelastic targets. Abiotic hydrogels with tunable mechanics were exposed to neutrophils, and successful engulfment was visualized using μm-sized fluorescent beads, previously incorporated in the gel. We find that as the elastic modulus of the target gel varies across the range we previously measured for biofilms, the success of engulfment changes. Most neutrophils are able to engulf part of targets with low elasticity, but at high elasticity almost no neutrophils engulf part of the targets. Thus, we demonstrate that a mechanical property of the target is correlated with the degree of successful engulfment, and that this experimental design is appropriate for probing the effects of viscoelastic mechanics on phagocytosis by neutrophils. Therefore, this work constitutes both a step forward in basic understanding and a methodological development that can be used to advance the field.

4.2 RESULTS

4.2.1 Hydrogel Mechanical Properties

To determine the effect of increasing elastic modulus (G') of a viscoelastic target on the success of neutrophil phagocytosis, we utilized two abiotic hydrogels to determine if gels with similar mechanical properties but different chemical compositions were engulfed with similar success. In order to assess the

mechanical properties of the hydrogels, we used oscillatory bulk rheology as described in chapters two and three.

4.2.2 Agarose Hydrogel Mechanics

As mentioned in earlier chapters, it is well-known that increasing the concentration of polymer in a gel will increase the gel's stiffness and in turn increase the elastic modulus[105]. We used agarose gels as our abiotic hydrogel model for manipulation of target G' in relation to polymer concentration. The G' of agarose gels was not found to be frequency dependent within relevant biological ranges (Figure 4.1A). Agarose gels did not yield with a distinctive break and definitive drop in G' as the bacterial strains did in chapter 3, so we will focus on G' of the plateau region for hydrogel mechanics (Figure 4.1B). Agarose concentrations from 0.3% agarose to 2% agarose replicated G' values comparable to the G' measured in *P. aeruginosa* clinical isolates in chapter 3. The softest gel, 0.3% agarose, had a measured G' between 120-130Pa. The stiffest gel, 2% agarose, had a measured G' between 9,000-12,000Pa. The value for G' used for analysis was picked at the midpoint of the plateau region or, if the material was already yielding, at the earliest point measured.

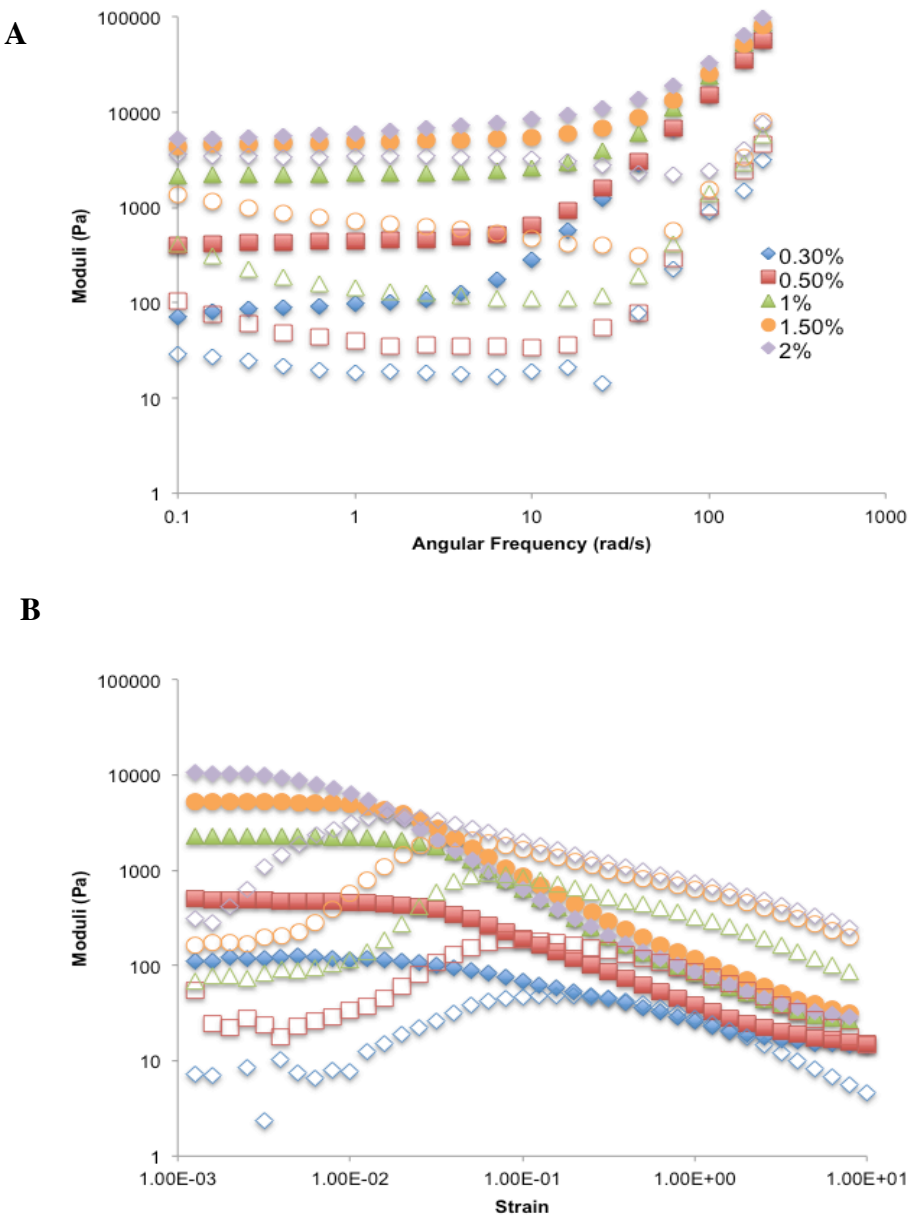

Figure 4.1 Representative frequency sweep and strain sweep curves of agarose hydrogels

(A) Frequency and (B) strain sweeps for one day's worth of agarose gels ranging in concentration from 0.3% agarose to 2% agarose. Frequency sweeps were done at 1% strain and strain sweeps were done at 3.14 radians/s. The elastic moduli (G') are shown with solid symbols and the viscous moduli (G") are shown with hollow symbols of corresponding shape and color.

4.2.3 Alginate Hydrogel Mechanics

Unlike agarose gels, alginate gels have increasing G' that scale in relation to the calcium concentration [140]. Alginate is made up of β-D-mannuronate (M) and α-L-guluronate (G) residues; calcium increases the elastic modulus of alginate by crosslinking with the G residues of alginate. By increasing the length of the G-block of alginate, mechanical properties can be enhanced [141]. The ratio of M:G residues varies across species that produce alginate therefore mechanics will vary for alginate gels depending on the source of alginate. We used sodium alginate isolated from brown algae and while it is a cheaper, more accessible source of alginate, its G-block composition is more variable than others. Alginate gels consistently were made of 4% alginate and 5% of calcium carbonate solution, with the concentration of $CaCO_3$ in water varying to change the calcium concentration. 5% D-(+)-Gluconic acid δ-lactone (GDL) was added to cause internal gelation by slowly lowering the pH of the gel causing calcium ions to be released from $CaCO_3$ into solution [142].

Alginate gel G' was measured using oscillatory bulk rheology and G' consistently increased with increasing calcium concentration (Figure 4.2). Alginate gels with 10mM calcium did display frequency dependence; however, for the frequency of neutrophil phagocytosis that we estimated, the G' of alginate gels remained under 100Pa, an order of magnitude lower than the lowest G' measured for 20mM calcium (Figure 4.2B). Alginate gels cross-linked with 20mM calcium and 30mM calcium did not display the frequency dependence that was seen in 10mM. The reported G' for the 10mM alginate gels used for the remainder of the paper will be the sustained G' measured during the strain sweep at a frequency of 3.14 radians/s.

The complex behavior of alginate gels is likely due to the hour the gels are incubated at 37˚C immediately prior to when the rheological measurements are taken in order to replicate experimental conditions when exposed to the interview. It has been previously shown that the elastic modulus of G' is temperature dependent [143]. Gels are put in the incubator so that the mechanics measured more closely mirror those while the neutrophils are incubated with the gels at 37˚C. During these experiments, while the 20mM and 30mM gels had visually consistent properties before and after incubation, the 10mM gel would become much more fluid-like during incubation. All rheology and experiments were done after the gels were allowed to sit at 37˚C to ensure the properties being measured were biologically relevant to a neutrophil's environment.

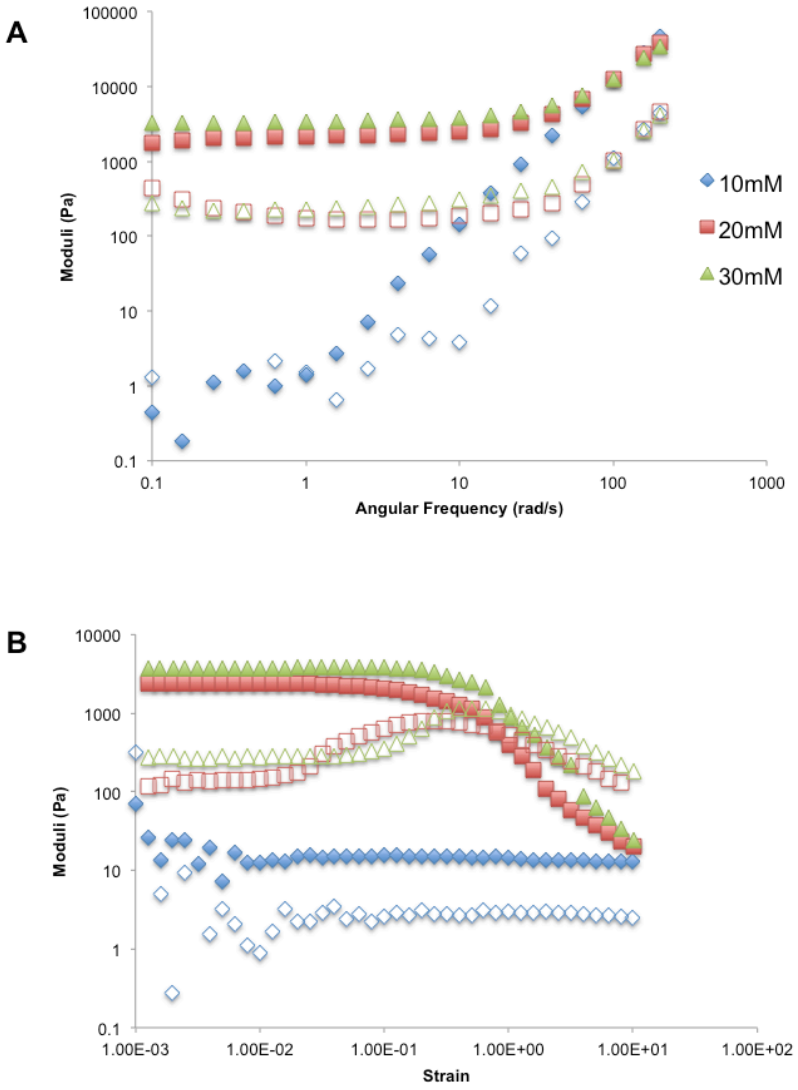

Figure 4.2 Representative frequency sweep and strain sweep curves of alginate hydrogels

A) Frequency and (B) strain sweeps for one day's worth of alginate gels. Gels are 4% alginate with 10, 20, or 30mM $CaCO_3$. Frequency sweeps were done at 1% strain and strain sweeps were done at 3.14 radians/s. The elastic moduli (G') are shown with solid symbols and the viscous moduli (G'') are shown with hollow symbols of corresponding shape and color.

4.2.4 Neutrophil Engulfment of Agarose Hydrogels

Neutrophil phagocytosis success was measured by successful engulfment of fluorescent beads embedded within the hydrogels as visualized with phase contrast microscopy. Percent engulfment, or the percent of neutrophils observed within an experiment that had successfully internalized beads, was calculated by dividing the total number of neutrophils with internalized beads by the total number of neutrophils and then multiplying by 100. At least 100 neutrophils were counted per sample. The fluorescent beads were under 1μm in size and a much lower volume fraction of the gel than the polymers themselves so they would not be the predominate factor in determining mechanics of the gels. The hydrogels were in the bottom of 24-well plates and much larger than the neutrophils themselves, therefore, the relative shape compared to the neutrophil would be a flat surface representative of a much larger spherical target.

Neutrophil engulfment of agarose gels has a sharp decrease in phagocytosis and the number of cells per sample that can successfully engulf beads from the 0.3% agarose trials to 0.5% agarose trials (Figure 4.3). At 0.3% agarose, between 15-62% of neutrophils had successfully internalized fluorescent particles from the gels. Hydrogels with polymer concentrations of 0.5% agarose and above have much lower engulfment rates with less than 2% of neutrophils able to successfully engulf the stiffer gels.

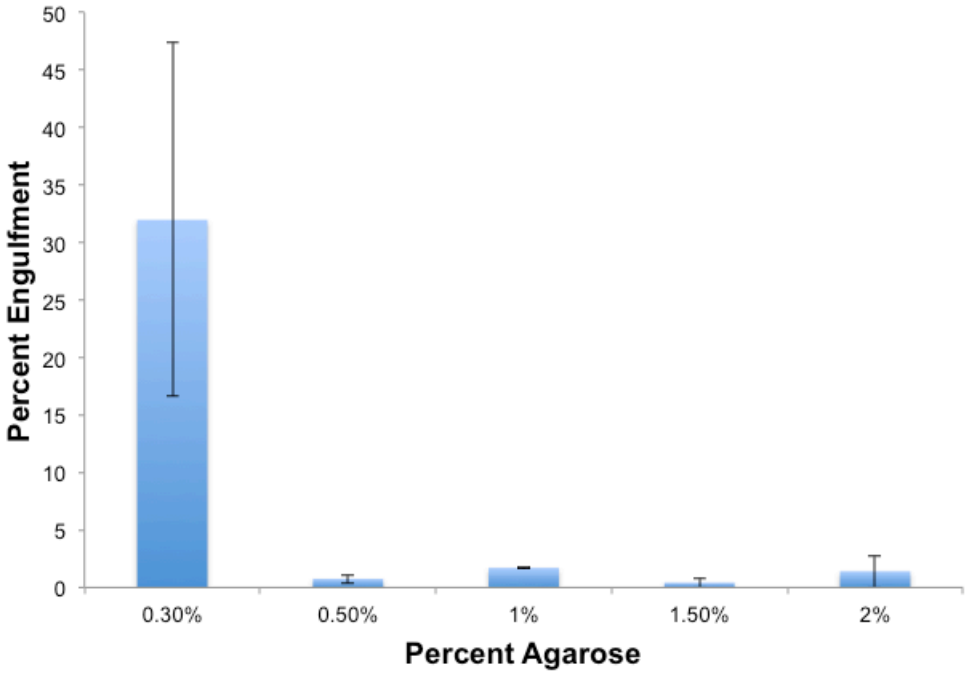

Figure 4.3 Neutrophils more successfully engulf lower percentage agarose gels

At 0.3% agarose, an average of 31% of neutrophils had internalized beads and successfully engulfed part of the agarose gel. All other gels had percent engulfment of above 2%. 0.3% agarose has a large standard deviation of the mean, but more trials are being done to narrow results. Percent engulfment represents the percent of neutrophils out of the counted sample with internalized beads. P-value for 0.3% gel versus every other gel% is < 0.1, no other gels statistically significant.

4.2.5 Neutrophil Engulfment of Alginate Hydrogels

Alginate hydrogels with varying calcium concentration and containing μm-sized fluorescent beads were subjected to neutrophil phagocytosis in the same way as agarose gels. Percent engulfment measuring successful bead internalization was measured the same way using phase contrast microscopy to visualize internalization (Figure 4.4). 65-77% of neutrophils were able to engulf beads within alginate gels cross-linked with 10mM calcium (Figure 4.5). When 20mM calcium was used to cross-link alginate, the amount of neutrophils that were able to engulf beads dropped to 1.6-14% of neutrophils. The highest calcium concentration used, 30mM, resulted in gels that could only be engulfed by fewer than 4% of neutrophils.

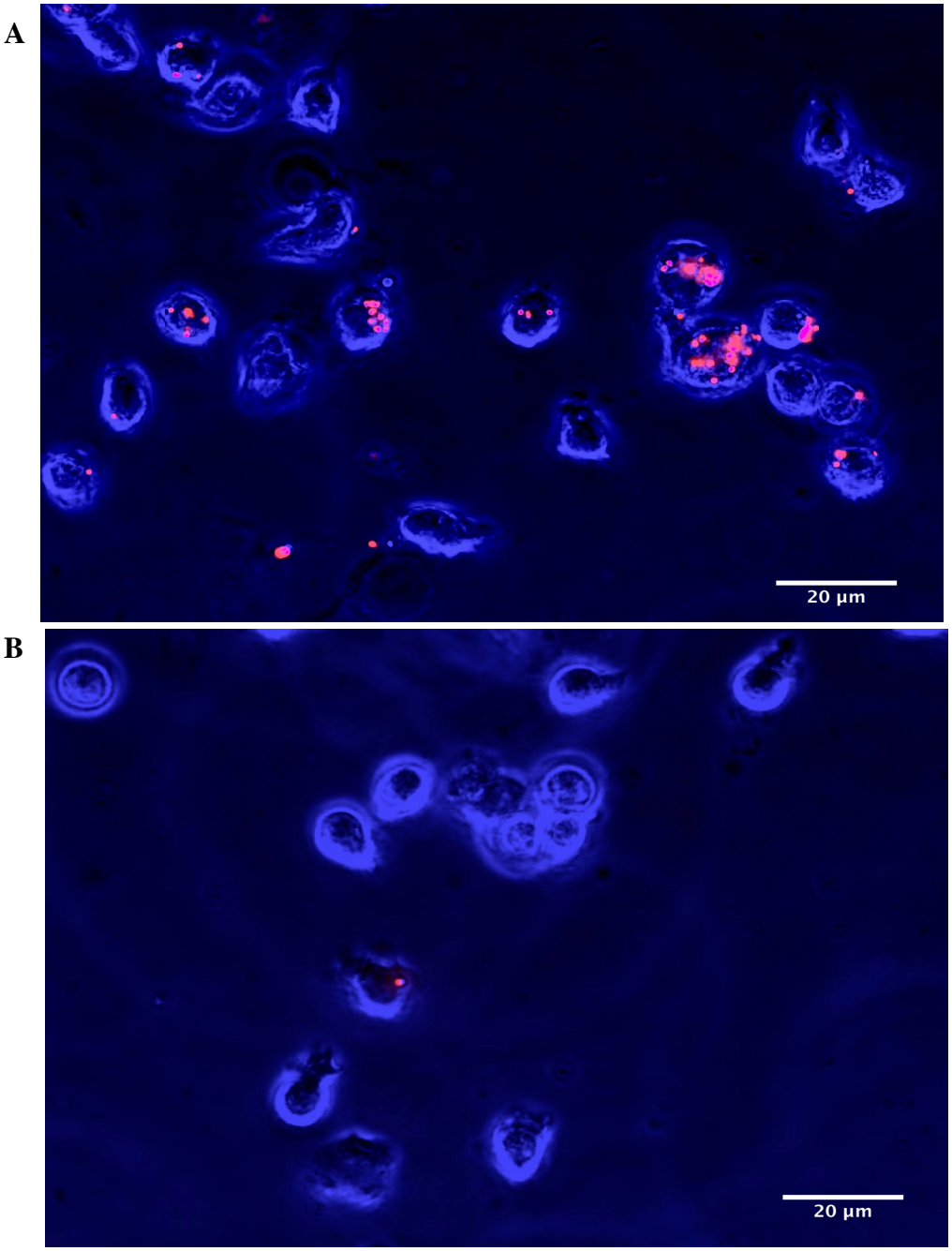

Figure 4.4 Phase contrast microscopy of neutrophils with internalized fluorescent beads from alginate gels

Figure 4.4 False colored phase contrast images of neutrophils after incubation with alginate gels cross- linked with 10mM calcium (A) and 30mM calcium (B). Neutrophils are blue and fluorescent beads are red. Internalization of the beads within a 10mM gel occurs at a much higher rate than 30mM gel.

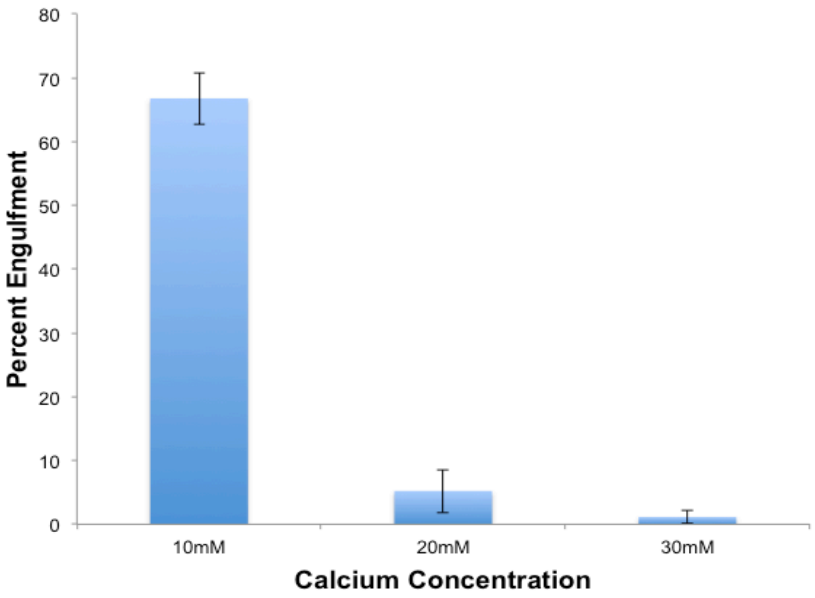

Figure 4.5 Neutrophils more successfully engulf alginate gels cross-linked with lower concentrations of calcium

As the concentration of calcium increases and therefore calcium cross-linking increases, the ability of neutrophils to successfully engulf the gels and internalize beads decreases. Percent engulfment represents the percent of neutrophils out of the counted sample with internalized beads. 10mM gels were significantly different from both 20mM and 30mM alginate gels with a P value less the 0.05.

4.2.6 Neutrophil Engulfment Increases as Elastic Modulus of Hydrogel Target Decreases

Alginate and agarose gels were both used as abiotic models to illuminate if gels with similar elastic moduli but different chemical compositions were engulfed with similar success. The percent of neutrophils that successfully engulfed beads was dependent on the G' of the hydrogels for both alginate and agarose gels with an increase in G' resulting in a decrease in successful phagocytosis and internalized beads regardless of gel composition (Figure 4.6).

20mM Ca^{2+} alginate gels resulted in more successful neutrophil engulfment than 0.5% agarose gels despite having a higher G' so there are likely other contributing factors that result in a change in neutrophil engulfment, such as yielding behavior and neutrophil adhesion. Neutrophils also engulfed more beads per cell from the 10mM alginate gels than any other gel which is not taken into account in overall percent engulfment. However, there is still a distinct trend that shows G' alters the success of phagocytosis in neutrophils and that a reduction in G' leads to increased neutrophil phagocytosis.

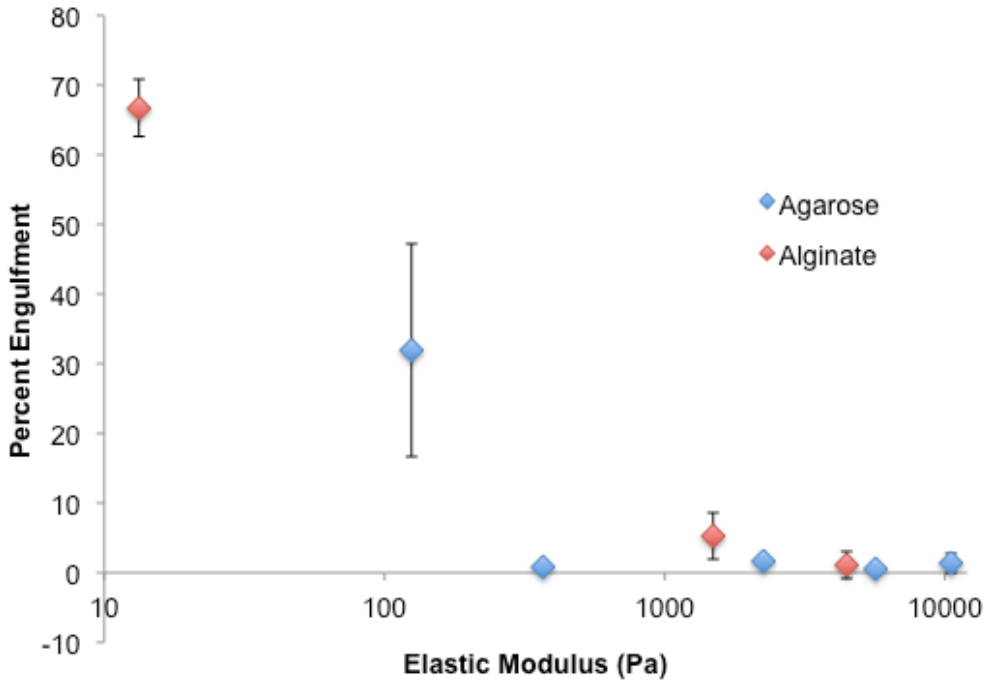

Figure 4.6 Percent engulfment lowers as elastic modulus of hydrogel increases

Elastic modulus includes moduli measured from both alginate and agarose. Data points from alginate engulfment experiments are in red and agarose experiments are blue. There is a general trend of a decrease in the number of neutrophils that have internalized beads as elastic modulus increases, regardless of hydrogel material. X axis in a log scale to aid in visualization of the lower elastic moduli points.

4.3 DISCUSSION

4.3.1 Summary of Results

Increasing the elastic modulus of a large, viscoelastic target decreases the ability of neutrophils to successfully engulf the target. Both alginate and agarose hydrogels with G' above 100Pa were minimally engulfed with less than 5% of neutrophils able to complete phagocytosis of the target. Even though alginate and agarose gels enhance their mechanical properties and G' through different interactions, by increasing cross-linking via calcium concentration or increasing polymer concentration respectively, neutrophils were still able to engulf both abiotic gels and successful engulfment was similarly affected with increasing G'.

4.3.2 Other Influences on Neutrophil Engulfment

These studies focus on G' of the large, viscoelastic targets, but do not take into account any other mechanical properties. While G' does influence a neutrophil's phagocytic ability, yield strain, stress, and the energy needed to break up the target likely influence the overall outcome as well. Unlike G' however, these properties do not scale as easily in hydrogels nor do the yielding properties stay consistent so this model currently works best for studying the affect of G' of hydrogels and abiotic targets on phagocytosis.

In order to engulf particles, neutrophils must bind to the target as it extends its cell membrane across to engulf it. The more binding sites, the stronger a neutrophil can adhere and wrap itself around the target. To make the abiotic gels recognizable to the neutrophils, BSA was added into the gel and was then incubated with an anti-BSA antibody before exposure to the neutrophils. Most previous studies of the mechanical limitations of neutrophil phagocytosis

have been measured only with antibody-mediated phagocytosis. This method has been used to study neutrophil mechanics when the target is a stiff, polystyrene bead. In our studies, we saw that the presence or absence of antibodies did not affect percent engulfment of alginate gels. BSA was still added to the gels, but as engulfment of the gels occurs without the antibodies present, phagocytosis of the abiotic alginate gel is not necessarily mediated through the Fc receptors.

4.3.3 Health Implications

The elastic modulus of bacterial biofilms has been measured to be far above 100Pa in *P. aeruginosa* clinical isolates. During long-term infections, the bacteria evolve to enhance their physical properties. With these results, it can be shown that the increasing G' of biofilms would render them resistant to neutrophil phagocytosis. Increased elastic modulus could negatively impact infection outcome because bacteria within the biofilm resist engulfment, causing delayed or frustrated phagocytosis—which leads to an increase in ROS damage to the host as mentioned in chapter 1—and also allowing more time for bacterial virulence factors, such as pyocyanin and rhamnolipids by *Pseudomonas aeruginosa*, to be produced, damaging the neutrophils themselves.

In order to render these biofilms susceptible to phagocytosis, the biofilms would need to be mechanically weakened. Studies show that neutrophils are still attracted to mechanically intact biofilms, surrounding them, but unable to engulf them. By finding ways to weaken G', biofilms could be broken up into pieces by neutrophils, likely in a manner similar to trogocytosis.

4.3.4 Future Work

This methodology is a first step in elucidating the impacts of a viscoelastic target mechanics on an attacking immune cell. In order to create new therapies, more studies must be done on the mechanical limitations of immune cells and the mechanics of infections that resist phagocytosis. Other mechanical properties such as yielding and binding mechanics need to be taken into account. Diverse gel types and more molecularly precise polymer gels should be studied to precisely pinpoint the threshold of neutrophil mechanical limitations. It is known that the shape and initial angle of contact between a macrophage and its target determines whether or not phagocytosis is successful, but this has yet to be confirmed in neutrophils. This study has developed a method to begin these studies to carry forward the mechanical studies of neutrophils, and there is still much work to be done in this burgeoning field.

4.4 METHODS

4.4.1 Hyrdogel preparation

Abiotic hydrogels were produced using alginic acid sodium salt powder or low-gelling temperature agarose (both Sigma-Aldrich). Alginate gels were made by dissolving 4% sodium alginate in distilled water and subsequently adding 5% calcium carbonate and 5% GDL. Alginate gels were made using 10, 20, and 30mM $CaCO_3$, leading to differential mechanics due to increasing crosslinking density within the alginate gels. Agarose gels were made using low-gelling temperature agarose, with increasing agarose concentration used to alter gel mechanics. 0.3%, 0.5%, 1%, 1.5%, and 2% gels were used. Both alginate and agarose gels contained 10µg/ml bovine serum albumin (BSA) (HycClone, GE Lifesciences) for immune activation and a 1:100 dilution of fluorescent beads (0.955µm polystyrene Dragon Green beads, Bangs Laboratories) for microscopic visualization. Hydrogels used for microscopy experiments were stored overnight at 4˚C in 500µl aliquots in 24-well flat-bottom plates. Hydrogels used for rheological measurements were poured into small petri dishes at 1000-2000µm deep and stored overnight at 4˚C.

4.4.2 Hydrogel Bulk Rheology Measurements

Measurement of hydrogel bulk mechanics was done using oscillatory bulk rheology as previously described [76]. In summary, hydrogel samples were taken out of 4˚C on the morning of the experiment and placed at 37˚C for one hour. After, hydrogel sections were placed on the rheometer and cut down to the size of the 8mm parallel plate head. Oscillatory frequency sweeps from 0.1 to 600 rad/s at 1 % strain and strain sweeps from 0.1 to 200 % at 3.14 rad/s were

performed on each sample on each day of measurement. Elastic modulus was reported as the midsection of the G' plateau region during strain sweeps.

4.4.3 Neutrophil Isolation

Human neutrophils were isolated from adult volunteer blood donors following protocol from Neutrophil Methods and Protocols [59]. Briefly, blood was collected in heparin-coated tubes, mixed with a 3% dextran and 0.9% sodium solution, and red blood cells fell out of solution. Supernatant was centrifuged for 10 minutes at 500g and resultant pellet was resuspended in 10ml of Hanks Buffered Salt Solution (HBSS) (Sigma-Aldrich) without calcium or magnesium. Cells were separated using a Ficoll-Paque (GE Healthcare) density gradient solution, spun at 400g for 40 minutes. The pellet was resuspended in distilled water for 30 seconds to lyse remaining red blood cells and solution isotonicity was restored using 1.8% NaCl. Cells were centrifuged for 5 minutes and 500g and the final neutrophil pellet was resuspended in 1ml HBSS with calcium and magnesium (Sigma-Aldrich) and 20% human serum (Sigma-Aldrich).

4.4.4 Neutrophil Engulfment Assay and Microscopy

On the day of phagocytic engulfment experiments, neutrophils were isolated as described above. During the course of isolation, 100µl of rabbit anti-BSA antibody (Invitrogen; Thermo-Fisher Scientific) was added to each hydrogel and incubated at 4˚C for 30 minutes. Plates were then washed three times with DPBS. After neutrophil isolation was complete, 200µl of cell suspension in HBSS and serum was added to each well. The hydrogel plate with neutrophils was then incubated at 37˚C for one hour. After one hour, cells were collected from off the top of the hydrogel. Cells collected from the alginate hydrogel samples were

concentrated and resuspended in 50µl of HBSS while agarose samples were not concentrated. Cell suspension was put on microscope slide with a coverslip that had been coated in 0.1% poly-l-lysine (Sigma-Aldrich). Cells were imaged using phase contrast microscopy and engulfment of beads using GFP fluorescence. 100 neutrophils per sample were counted for presence or absence of beads to calculate percent engulfment.

Chapter 5: Conclusion

5.1.1 Mechanics of Bacterial Biofilms

Bacterial biofilms are a ubiquitous problem in ranging from environments from industry to healthcare. Debridement and other physical removal methods are common ways to help eliminate biofilms,. In order to make biofilms more susceptible to antibiotics, biofilms can be broken down and once physically broken up, bacteria are again as susceptible to antibiotics as planktonic cells. All these physical treatments highlight a need to study the mechanical properties of bacterial biofilms in order to make treatment more effective.

Pseudomonas aeruginosa is one of the most commonly studied biofilm-forming bacteria. It's been shown that during long-term infections *P. aeruginosa* increases production of EPS that make up their bacterial matrix, specifically Psl and alginate. Exploring the chemical benefits of the increase in polymer is a popular area of study to help pinpoint why these adaptations lead to increased and prolonged survival of *P. aeruginosa* in immunocompromised patients. The mechanical properties conferred by the increase in EPS and the potential mechanical benefits of this increase have yet to be studied in a comprehensive manner until now.

Alginate production is associated with chronic *P. aeruginosa* infections and poor patient outcomes. It has been shown that alginate does make the biofilm softer, but the properties of other EPS materials must also be taken into account. In the majority of the clinical isolates studied within the work presented here, Psl production was increased concomitantly with alginate, so studying only

one polymer in isolation is not sufficient to describe the EPS and mechanical characteristics of clinical biofilms.

In this study, we show that each polymer in the biofilm matrix confers unique mechanical properties to the biofilm. In clinical isolates and lab strains of *P. aeruginosa*, Psl stiffens the biofilm and increases mechanical strength of the biofilm. Alginate and Pel increase yield strain but alginate reduces mechanical toughness. Increased Psl and Pel both increase yield strain. These properties were maintained throughout lab strain and clinical isolates although the amount of Pel produced in the clinical isolates is not known. Psl also increases the inter-bacterial cohesion of *P. aeruginosa* single cells.

Rather than the bacteria could be making energetically unfavorable redundant polymers, we see that these polymers confer their own unique mechanical properties to the biofilms. These properties may help the biofilm evade antibiotic clearance and immune cell clearance. If the biofilms are tougher and more resistant to being physically broken down, they will retain their biofilm state and remain inherently resistant to antibiotics. The stiffness may also aid the biofilms in avoiding immune cell phagocytosis.

5.2 Mechanics of Neutrophil Phagocytosis

Neutrophils are known to be difficult to genetically manipulate or culture. In general, neutrophils are isolated from fresh blood samples and die after several hours, making them an unpopular cell line with which to work. Macrophages and neutrophils are both professional phagocytes, and so much of what we know about neutrophils is inferred from studies on macrophages. However, while

sharing many similarities, there are distinct differences in neutrophils that are often overlooked and most likely differences that are as yet unknown.

Neutrophils have an arsenal of antimicrobial defenses if pathogens get around the body's physical barriers, but some of these defenses are damaging to the cells themselves or damaging to the host, such as NETosis and ROS production. Phagocytosis results in the killing of pathogens or foreign particles without their own cell death or damage to the host (ROS can be released during phagocytosis, but phagocytosis itself does not harm the host). If phagocytosis is unsuccessful or becomes frustrated, neutrophils will keep releasing molecules damaging to the host so efficient phagocytosis is crucial for clearance of infection and more positive patient outcomes.

It was suggested that neutrophils are able to apply a force of 1000Pa during phagocytosis and can engulf stiff particles generally smaller than the 10-15μm diameter of neutrophils. Neutrophil phagocytosis could be avoided if a target was larger than 10μm and stiffer than the 1000Pa threshold of force a neutrophil could apply, but the ability of neutrophils to engulf large, soft targets had never been measured.

Here we develop a method to measure how elastic modulus of an abiotic hydrogel target impacts the success of neutrophil phagocytosis. Using both alginate and agarose gels, we see significant engulfment of gel and the fluorescent beads within closer to a G' threshold of around 100Pa. Above 100 Pa, phagocytosis is unsuccessful over several orders of magnitude of increasing elastic modulus.

5.3 Future Work

As I wrap up this work, one of my final but immediate next steps is confirming neutrophil bead engulfment using flow cytometry, of which trials are currently ongoing. I fully expect the results of flow cytometry to support the more qualitative measurements of hydrogel engulfment taken using phase contrast microscopy.

Ongoing research in our lab is focused on identifying how to target mechanical integrity of bacterial biofilm polymers as a way to compromise biofilms, rendering them more susceptible to clearance. In addition, biofilm structural properties and mechanics need to be measured in microscale to elucidate heterogeneities within the biofilm and in *in vivo* environments to ensure the bulk rheological measurements are not an *in vitro* artifact or an artifact of disruption of the biofilm during bulk rheology.

Complete studies of bacterial biofilms with known EPS production and mechanics *in vivo* and their interaction with neutrophils would more fully help elucidate the biophysical relationship in this host-pathogen arms race From there, antimicrobial therapies that target pathogen mechanical integrity would open a new door of study and treatment that could help make traditional antibiotics more effective or help move away from those treatments as antibiotic resistance is on the rise, while also allowing the host's own immune response to be more successful.

Bibliography

1 Flemming, H. C. & Wingender, J. The biofilm matrix. *Nature reviews. Microbiology* **8**, 623-633, doi:10.1038/nrmicro2415 (2010).

2 Monroe, D. Looking for chinks in the armor of bacterial biofilms. *PLoS Biol* **5**, e307, doi:10.1371/journal.pbio.0050307 (2007).

3 Cotter, P. A. & Stibitz, S. c-di-GMP-mediated regulation of virulence and biofilm formation. *Curr Opin Microbiol* **10**, 17-23, doi:10.1016/j.mib.2006.12.006 (2007).

4 Gupta, K., Liao, J., Petrova, O. E., Cherny, K. E. & Sauer, K. Elevated levels of the second messenger c-di-GMP contribute to antimicrobial resistance of Pseudomonas aeruginosa. *Molecular microbiology* **92**, 488-506, doi:10.1111/mmi.12587 (2014).

5 Perencevich, E. N. *et al*. Health and economic impact of surgical site infections diagnosed after hospital discharge. *Emerging infectious diseases* **9**, 196-203, doi:10.3201/eid0902.020232 (2003).

6 Ramsey, S. D. *et al*. Incidence, outcomes, and cost of foot ulcers in patients with diabetes. *Diabetes Care* **22**, 382-387 (1999).

7 Wolcott, R. & Dowd, S. The role of biofilms: are we hitting the right target? *Plast Reconstr Surg* **127 Suppl 1**, 28S-35S, doi:10.1097/PRS.0b013e3181fca244 (2011).

8 Bjarnsholt, T. *et al*. Pseudomonas aeruginosa biofilms in the respiratory tract of cystic fibrosis patients. *Pediatric pulmonology* **44**, 547-558, doi:10.1002/ppul.21011 (2009).

9 Bjarnsholt, T., Tolker-Nielsen, T., Givskov, M., Janssen, M. & Christensen, L. H. Detection of bacteria by fluorescence in situ hybridization in culture-negative soft tissue filler lesions. *Dermatol Surg* **35 Suppl 2**, 1620-1624, doi:10.1111/j.1524-4725.2009.01313.x (2009).

10 Bjarnsholt, T. *et al*. Why chronic wounds will not heal: a novel hypothesis. *Wound Repair Regen* **16**, 2-10, doi:10.1111/j.1524-475X.2007.00283.x (2008).

11 Fexby, S. *et al*. Biological Trojan horse: Antigen 43 provides specific bacterial uptake and survival in human neutrophils. *Infect Immun* **75**, 30-34, doi:10.1128/IAI.01117-06 (2007).

12 Wessel, A. K. *et al*. Oxygen limitation within a bacterial aggregate. *Mbio* **5**, e00992, doi:10.1128/mBio.00992-14 (2014).

13 Walters, M. C., Roe, F., Bugnicourt, A., Franklin, M. J. & Stewart, P. S. Contributions of antibiotic penetration, oxygen limitation, and low metabolic activity to tolerance of Pseudomonas aeruginosa biofilms to ciprofloxacin and tobramycin. *Antimicrob Agents Ch* **47**, 317-323, doi:Doi 10.1128/Aac.47.1.317-323.2003 (2003).

14 Wolcott, R. D. *et al*. Biofilm maturity studies indicate sharp debridement opens a time- dependent therapeutic window. *J Wound Care* **19**, 320-328, doi:10.12968/jowc.2010.19.8.77709 (2010).

15 Winner, C. in *Oceanus Magazine* Vol. 50 8-12 (2013).

16 Alhede, M. *et al*. Phenotypes of non-attached Pseudomonas aeruginosa aggregates resemble surface attached biofilm. *PloS one* **6**, e27943, doi:10.1371/journal.pone.0027943 (2011).

17 Donlan, R. M. & Costerton, J. W. Biofilms: survival mechanisms of clinically relevant microorganisms. *Clinical microbiology reviews* **15**, 167-193 (2002).
18 Aloush, V., Navon-Venezia, S., Seigman-Igra, Y., Cabili, S. & Carmeli, Y. Multidrug-resistant Pseudomonas aeruginosa: risk factors and clinical impact. *Antimicrob Agents Chemother* **50**, 43-48, doi:10.1128/AAC.50.1.43-48.2006 (2006).
19 Murphy, T. F. *et al*. Pseudomonas aeruginosa in chronic obstructive pulmonary disease. *Am J Respir Crit Care Med* **177**, 853-860, doi:10.1164/rccm.200709-1413OC (2008).
20 Winstanley, C., O'Brien, S. & Brockhurst, M. A. Pseudomonas aeruginosa Evolutionary Adaptation and Diversification in Cystic Fibrosis Chronic Lung Infections. *Trends Microbiol* **24**, 327-337, doi:10.1016/j.tim.2016.01.008 (2016).
21 Tang, A. C. *et al*. Current concepts: host-pathogen interactions in cystic fibrosis airways disease. *Eur Respir Rev* **23**, 320-332, doi:10.1183/09059180.00006113 (2014).
22 Palmer, K. L., Mashburn, L. M., Singh, P. K. & Whiteley, M. Cystic fibrosis sputum supports growth and cues key aspects of Pseudomonas aeruginosa physiology. *J Bacteriol* **187**, 5267-5277, doi:10.1128/JB.187.15.5267-5277.2005 (2005).
23 Palmer, K. L., Aye, L. M. & Whiteley, M. Nutritional cues control Pseudomonas aeruginosa multicellular behavior in cystic fibrosis sputum. *J Bacteriol* **189**, 8079-8087, doi:10.1128/JB.01138-07 (2007).
24 Pressler, T. *et al*. Chronic Pseudomonas aeruginosa infection definition: EuroCareCF Working Group report. *J Cyst Fibros* **10 Suppl 2**, S75-78, doi:10.1016/S1569-1993(11)60011-8 (2011).
25 Huse, H. K. *et al*. Pseudomonas aeruginosa Enhances Production of a Non-Alginate Exopolysaccharide during Long-Term Colonization of the Cystic Fibrosis Lung. *PloS one* **8**, doi:ARTN e82621
DOI 10.1371/journal.pone.0082621 (2013).
26 Pedersen, S. S., Kharazmi, A., Espersen, F. & Hoiby, N. Pseudomonas aeruginosa alginate in cystic fibrosis sputum and the inflammatory response. *Infect Immun* **58**, 3363-3368 (1990).
27 Gilligan, P. H. Microbiology of Airway Disease in Patients with Cystic-Fibrosis. *Clinical microbiology reviews* **4**, 35-51 (1991).
28 Cooley, B. J. *et al*. The extracellular polysaccharide Pel makes the attachment of P. aeruginosa to surfaces symmetric and short-ranged. *Soft Matter* **9**, 3871-3876, doi:Doi 10.1039/C3sm27638d (2013).
29 Ryder, C., Byrd, M. & Wozniak, D. J. Role of polysaccharides in Pseudomonas aeruginosa biofilm development. *Curr Opin Microbiol* **10**, 644-648, doi:Doi 10.1016/J.Mib.2007.09.010 (2007).
30 Friedman, L. & Kolter, R. Two genetic loci produce distinct carbohydrate-rich structural components of the Pseudomonas aeruginosa biofilm matrix. *J Bacteriol* **186**, 4457-4465, doi:10.1128/JB.186.14.4457-4465.2004 (2004).
31 Jackson, K. D., Starkey, M., Kremer, S., Parsek, M. R. & Wozniak, D. J. Identification of psl, a locus encoding a potential exopolysaccharide that is essential for Pseudomonas aeruginosa PAO1 biofilm formation. *J Bacteriol* **186**, 4466-4475, doi:10.1128/JB.186.14.4466-4475.2004 (2004).
32 Friedman, L. & Kolter, R. Genes involved in matrix formation in Pseudomonas aeruginosa PA14 biofilms. *Molecular microbiology* **51**, 675-690 (2004).

33 Wozniak, D. J. *et al*. Alginate is not a significant component of the extracellular polysaccharide matrix of PA14 and PAO1 Pseudomonas aeruginosa biofilms. *Proceedings of the National Academy of Sciences of the United States of America* **100**, 7907-7912, doi:10.1073/pnas.1231792100 (2003).
34 Jakubovics, N. S., Shields, R. C., Rajarajan, N. & Burgess, J. G. Life after death: the critical role of extracellular DNA in microbial biofilms. *Lett Appl Microbiol* **57**, 467-475, doi:10.1111/lam.12134 (2013).
35 Gloag, E. S. *et al*. Self-organization of bacterial biofilms is facilitated by extracellular DNA. *Proceedings of the National Academy of Sciences of the United States of America* **110**, 11541-11546, doi:10.1073/pnas.1218898110 (2013).
36 Whitchurch, C. B., Tolker-Nielsen, T., Ragas, P. C. & Mattick, J. S. Extracellular DNA required for bacterial biofilm formation. *Science* **295**, 1487, doi:10.1126/science.295.5559.1487 (2002).
37 Valentini, M. & Filloux, A. Biofilms and Cyclic di-GMP (c-di-GMP) Signaling: Lessons from Pseudomonas aeruginosa and Other Bacteria. *The Journal of biological chemistry* **291**, 12547-12555, doi:10.1074/jbc.R115.711507 (2016).
38 Hengge, R. Principles of c-di-GMP signalling in bacteria. *Nature reviews. Microbiology* **7**, 263-273, doi:10.1038/nrmicro2109 (2009).
39 Hickman, J. W., Tifrea, D. F. & Harwood, C. S. A chemosensory system that regulates biofilm formation through modulation of cyclic diguanylate levels. *Proceedings of the National Academy of Sciences of the United States of America* **102**, 14422-14427, doi:10.1073/pnas.0507170102 (2005).
40 Ma, L. M. *et al*. Assembly and Development of the Pseudomonas aeruginosa Biofilm Matrix. *Plos Pathog* **5**, doi:Artn E1000354
Doi 10.1371/Journal.Ppat.1000354 (2009).
41 Ma, L. Y., Lu, H. P., Sprinkle, A., Parsek, M. R. & Wozniak, D. J. Pseudomonas aeruginosa PSl is a galactose- and mannose-rich exopolysaccharide. *J Bacteriol* **189**, 8353-8356, doi:Doi 10.1128/Jb.00620-07 (2007).
42 Byrd, M. S. *et al*. Genetic and biochemical analyses of the Pseudomonas aeruginosa Psl exopolysaccharide reveal overlapping roles for polysaccharide synthesis enzymes in Psl and LPS production. *Molecular microbiology* **73**, 622-638, doi:10.1111/j.1365-2958.2009.06795.x (2009).
43 Ma, L., Jackson, K. D., Landry, R. M., Parsek, M. R. & Wozniak, D. J. Analysis of Pseudomonas aeruginosa conditional psl variants reveals roles for the psl polysaccharide in adhesion and maintaining biofilm structure postattachment. *J Bacteriol* **188**, 8213-8221, doi:10.1128/JB.01202-06 (2006).
44 Irie, Y. *et al*. Self-produced exopolysaccharide is a signal that stimulates biofilm formation in Pseudomonas aeruginosa. *Proceedings of the National Academy of Sciences of the United States of America* **109**, 20632-20636, doi:10.1073/pnas.1217993109 (2012).
45 Tseng, B. S. *et al*. The extracellular matrix protects Pseudomonas aeruginosa biofilms by limiting the penetration of tobramycin. *Environ Microbiol* **15**, 2865-2878, doi:10.1111/1462-2920.12155 (2013).
46 Mishra, M. *et al*. Pseudomonas aeruginosa Psl polysaccharide reduces neutrophil phagocytosis and the oxidative response by limiting complement-mediated opsonization. *Cellular microbiology* **14**, 95-106, doi:10.1111/j.1462-5822.2011.01704.x (2012).

47 Starkey, M. *et al*. Pseudomonas aeruginosa rugose small-colony variants have adaptations that likely promote persistence in the cystic fibrosis lung. *J Bacteriol* **191**, 3492-3503, doi:10.1128/JB.00119-09 (2009).
48 Jennings, L. K. *et al*. Pel is a cationic exopolysaccharide that cross-links extracellular DNA in the Pseudomonas aeruginosa biofilm matrix. *Proceedings of the National Academy of Sciences of the United States of America* **112**, 11353-11358, doi:10.1073/pnas.1503058112 (2015).
49 Govan, J. R. W. & Deretic, V. Microbial pathogenesis in cystic fibrosis: Mucoid Pseudomonas aeruginosa and Burkholderia cepacia. *Microbiol Rev* **60**, 539-+ (1996).
50 Simpson, J. A., Smith, S. E. & Dean, R. T. Scavenging by Alginate of Free-Radicals Released by Macrophages. *Free Radical Bio Med* **6**, 347-353, doi:Doi 10.1016/0891-5849(89)90078-6 (1989).
51 Pedersen, S. S., Hoiby, N., Espersen, F. & Koch, C. Role of Alginate in Infection with Mucoid Pseudomonas-Aeruginosa in Cystic-Fibrosis. *Thorax* **47**, 6-13, doi:Doi 10.1136/Thx.47.1.6 (1992).
52 Bylund, J., Burgess, L. A., Cescutti, P., Ernst, R. K. & Speert, D. P. Exopolysaccharides from Burkholderia cenocepacia inhibit neutrophil chemotaxis and scavenge reactive oxygen species. *The Journal of biological chemistry* **281**, 2526-2532, doi:10.1074/jbc.M510692200 (2006).
53 Kragh, K. N. *et al*. Polymorphonuclear leukocytes restrict growth of Pseudomonas aeruginosa in the lungs of cystic fibrosis patients. *Infect Immun* **82**, 4477-4486, doi:10.1128/IAI.01969-14 (2014).
54 Kirketerp-Moller, K. *et al*. Distribution, organization, and ecology of bacteria in chronic wounds. *J Clin Microbiol* **46**, 2717-2722, doi:Doi 10.1128/Jcm.00501-08 (2008).
55 Borregaard, N. Neutrophils, from marrow to microbes. *Immunity* **33**, 657-670, doi:10.1016/j.immuni.2010.11.011 (2010).
56 Aulakh, G. K. Neutrophils in the lung: "the first responders". *Cell Tissue Res* **371**, 577-588, doi:10.1007/s00441-017-2748-z (2018).
57 Mantovani, A., Cassatella, M. A., Costantini, C. & Jaillon, S. Neutrophils in the activation and regulation of innate and adaptive immunity. *Nature reviews. Immunology* **11**, 519-531, doi:10.1038/nri3024 (2011).
58 Kobayashi, S. D., Voyich, J. M., Buhl, C. L., Stahl, R. M. & DeLeo, F. R. Global changes in gene expression by human polymorphonuclear leukocytes during receptor-mediated phagocytosis: cell fate is regulated at the level of gene expression. *Proceedings of the National Academy of Sciences of the United States of America* **99**, 6901-6906, doi:10.1073/pnas.092148299 (2002).
59 Mark T. Quinn, F. R. D. *Neutrophil Methods and Protocols*. (Humana Press, 2014).
60 Hartl, D. *et al*. Innate immunity in cystic fibrosis lung disease. *J Cyst Fibros* **11**, 363-382, doi:10.1016/j.jcf.2012.07.003 (2012).
61 Lacy, P. Mechanisms of degranulation in neutrophils. *Allergy Asthma Clin Immunol* **2**, 98-108, doi:10.1186/1710-1492-2-3-98 (2006).
62 Brinkmann, V. *et al*. Neutrophil extracellular traps kill bacteria. *Science* **303**, 1532-1535, doi:10.1126/science.1092385 (2004).
63 Nguyen, G. T., Green, E. R. & Mecsas, J. Neutrophils to the ROScue: Mechanisms of NADPH Oxidase Activation and Bacterial Resistance. *Front Cell Infect Microbiol* **7**, 373, doi:10.3389/fcimb.2017.00373 (2017).

64 Hoiby, N., Ciofu, O. & Bjarnsholt, T. Pseudomonas aeruginosa biofilms in cystic fibrosis. *Future Microbiol* **5**, 1663-1674, doi:Doi 10.2217/Fmb.10.125 (2010).
65 Clark, R. A. Activation of the neutrophil respiratory burst oxidase. *J Infect Dis* **179 Suppl 2**, S309-317, doi:10.1086/513849 (1999).
66 Underhill, D. M. & Ozinsky, A. Phagocytosis of microbes: complexity in action. *Annual review of immunology* **20**, 825-852, doi:10.1146/annurev.immunol.20.103001.114744 (2002).
67 Lee, V. M., Quinn, P. A., Jennings, S. C. & Ng, L. L. Neutrophil activation and production of reactive oxygen species in pre-eclampsia. *J Hypertens* **21**, 395-402, doi:10.1097/01.hjh.0000052416.12292.7d (2003).
68 Thanabalasuriar, A. *et al*. Bispecific antibody targets multiple Pseudomonas aeruginosa evasion mechanisms in the lung vasculature. *The Journal of clinical investigation* **127**, 2249-2261, doi:10.1172/JCI89652 (2017).
69 Herant, M., Heinrich, V. & Dembo, M. Mechanics of neutrophil phagocytosis: experiments and quantitative models. *J Cell Sci* **119**, 1903-1913, doi:Doi 10.1242/Jcs.02876 (2006).
70 Mercer, F., Ng, S. H., Brown, T. M., Boatman, G. & Johnson, P. J. Neutrophils kill the parasite Trichomonas vaginalis using trogocytosis. *PLoS Biol* **16**, e2003885, doi:10.1371/journal.pbio.2003885 (2018).
71 Champion, J. A. & Mitragotri, S. Role of target geometry in phagocytosis. *Proceedings of the National Academy of Sciences of the United States of America* **103**, 4930-4934, doi:10.1073/pnas.0600997103 (2006).
72 Champion, J. A., Walker, A. & Mitragotri, S. Role of particle size in phagocytosis of polymeric microspheres. *Pharm Res* **25**, 1815-1821, doi:10.1007/s11095-008-9562-y (2008).
73 Allen, L. *et al*. Pyocyanin production by Pseudomonas aeruginosa induces neutrophil apoptosis and impairs neutrophil-mediated host defenses in vivo. *J Immunol* **174**, 3643-3649 (2005).
74 Jensen, P. O. *et al*. Rapid necrotic killing of polymorphonuclear leukocytes is caused by quorum-sensing-controlled production of rhamnolipid by Pseudomonas aeruginosa. *Microbiol-Sgm* **153**, 1329-1338, doi:Doi 10.1099/Mic.0.2006/003863-0 (2007).
75 Vernita D Gordon, M. D.-F., Kristin Kovach, and Christopher A Rodesney. Biofilms and mechanics: a review of experimental techniques and findings. *Journal of Physics D: Applied Physics* **50** (2017).
76 Kovach, K. *et al*. Evolutionary adaptations of biofilms infecting cystic fibrosis lungs promote mechanical toughness by adjusting polysaccharide production. *npj Biofilms and Microbiomes* **3**, 1 (2017).
77 Wilking, J., T. Angelini, A. Seminara, M. Brenner, and D. Weitz. Biofilms as Complex Fluids. *MRS Bulletin* **36**, 385-391 (2011).
78 Tuson, H. H. *et al*. Measuring the stiffness of bacterial cells from growth rates in hydrogels of tunable elasticity. *Molecular microbiology* **84**, 874-891, doi:10.1111/j.1365-2958.2012.08063.x (2012).
79 Loskill, P. *et al*. Reduction of the peptidoglycan crosslinking causes a decrease in stiffness of the Staphylococcus aureus cell envelope. *Biophys J* **107**, 1082-1089, doi:10.1016/j.bpj.2014.07.029 (2014).
80 Rupp, C. J., Fux, C. A. & Stoodley, P. Viscoelasticity of Staphylococcus aureus biofilms in response to fluid shear allows resistance to detachment and facilitates rolling migration. *Appl Environ Microbiol* **71**, 2175-2178, doi:10.1128/AEM.71.4.2175-2178.2005 (2005).

81 Bol, M., Ehret, A. E., Bolea Albero, A., Hellriegel, J. & Krull, R. Recent advances in mechanical characterisation of biofilm and their significance for material modelling. *Crit Rev Biotechnol* **33**, 145-171, doi:10.3109/07388551.2012.679250 (2013).
82 Billings, N. *et al*. The extracellular matrix Component Psl provides fast-acting antibiotic defense in Pseudomonas aeruginosa biofilms. *Plos Pathog* **9**, e1003526, doi:10.1371/journal.ppat.1003526 (2013).
83 Chew, S. C. *et al*. Dynamic Remodeling of Microbial Biofilms by Functionally Distinct Exopolysaccharides. *Mbio* **5**, doi:ARTN e01536-14
DOI 10.1128/mBio.01536-14 (2014).
84 Lau, P. C., Dutcher, J. R., Beveridge, T. J. & Lam, J. S. Absolute quantitation of bacterial biofilm adhesion and viscoelasticity by microbead force spectroscopy. *Biophys J* **96**, 2935-2948, doi:10.1016/j.bpj.2008.12.3943 (2009).
85 Ahimou, F., Semmens, M. J., Novak, P. J. & Haugstad, G. Biofilm cohesiveness measurement using a novel atomic force microscopy methodology. *Appl Environ Microbiol* **73**, 2897-2904, doi:10.1128/AEM.02388-06 (2007).
86 Aggarwal, S., Poppele, E. H. & Hozalski, R. M. Development and testing of a novel microcantilever technique for measuring the cohesive strength of intact biofilms. *Biotechnol Bioeng* **105**, 924-934, doi:10.1002/bit.22605 (2010).
87 Chen, M. J., Zhang, Z. & Bott, T. R. Effects of operating conditions on the adhesive strength of Pseudomonas fluorescens biofilms in tubes. *Colloids Surf B Biointerfaces* **43**, 61-71, doi:10.1016/j.colsurfb.2005.04.004 (2005).
88 Cense, A. W. *et al*. Mechanical properties and failure of Streptococcus mutans biofilms, studied using a microindentation device. *J Microbiol Methods* **67**, 463-472, doi:10.1016/j.mimet.2006.04.023 (2006).
89 Poppele, E. H. & Hozalski, R. M. Micro-cantilever method for measuring the tensile strength of biofilms and microbial flocs. *J Microbiol Methods* **55**, 607-615 (2003).
90 H. M. Wyss, R. J. L., D. A. Weitz. Oscillatory Rheology. *G.I.T. Laboratory Journal* (2007).
91 Stoodley, P., Cargo, R., Rupp, C. J., Wilson, S. & Klapper, I. Biofilm material properties as related to shear-induced deformation and detachment phenomena. *J Ind Microbiol Biotechnol* **29**, 361-367, doi:10.1038/sj.jim.7000282 (2002).
92 Lieleg, O., Caldara, M., Baumgartel, R. & Ribbeck, K. Mechanical robustness of Pseudomonas aeruginosa biofilms. *Soft Matter* **7**, 3307-3314, doi:Doi 10.1039/C0sm01467b (2011).
93 Colvin, K. M. *et al*. The pel polysaccharide can serve a structural and protective role in the biofilm matrix of Pseudomonas aeruginosa. *Plos Pathog* **7**, e1001264, doi:10.1371/journal.ppat.1001264 (2011).
94 Wloka, M., H. Rehage, H.-C. Flemming, and J. Wingender. Rheological properties of viscoelastic biofilm extracellular polymeric substances and comparison to the behavior of calcium alginate gels. . *Colloid and Polymer Science* **50**, 1067-1076 (2004).
95 Drescher, K., Shen, Y., Bassler, B. L. & Stone, H. A. Biofilm streamers cause catastrophic disruption of flow with consequences for environmental and medical systems. *Proceedings of the National Academy of Sciences of the United States of America* **110**, 4345-4350, doi:10.1073/pnas.1300321110 (2013).
96 Stoodley, P., Lewandowski, Z., Boyle, J. D. & Lappin-Scott, H. M. Structural deformation of bacterial biofilms caused by short-term fluctuations in fluid shear: an in situ investigation of biofilm rheology. *Biotechnol Bioeng* **65**, 83-92 (1999).

97 Stoodley, P., Dodds, I., Boyle, J. D. & Lappin-Scott, H. M. Influence of hydrodynamics and nutrients on biofilm structure. *J Appl Microbiol* **85 Suppl 1**, 19S-28S, doi:10.1111/j.1365-2672.1998.tb05279.x (1998).
98 Crocker, J. a. D. G. Methods of digital video microscopy for colloidal studies. *J Colloid Interf Sci* **179**, 298-310 (1996).
99 Birjiniuk, A. *et al*. Single particle tracking reveals spatial and dynamic organization of the E. coli biofilm matrix. *New J Phys* **16**, 085014, doi:10.1088/1367-2630/16/8/085014 (2014).
100 Rogers, S. S., van der Walle, C. & Waigh, T. A. Microrheology of bacterial biofilms in vitro: Staphylococcus aureus and Pseudomonas aeruginosa. *Langmuir* **24**, 13549-13555, doi:10.1021/la802442d (2008).
101 Galy, O. *et al*. Mapping of bacterial biofilm local mechanics by magnetic microparticle actuation. *Biophys J* **103**, 1400-1408, doi:10.1016/j.bpj.2012.07.001 (2012).
102 Rani, S. A. *et al*. Spatial patterns of DNA replication, protein synthesis, and oxygen concentration within bacterial biofilms reveal diverse physiological states. *J Bacteriol* **189**, 4223-4233, doi:10.1128/JB.00107-07 (2007).
103 de Beer, D., Stoodley, P., Roe, F. & Lewandowski, Z. Effects of biofilm structures on oxygen distribution and mass transport. *Biotechnol Bioeng* **43**, 1131-1138, doi:10.1002/bit.260431118 (1994).
104 Stewart, P. S. & Franklin, M. J. Physiological heterogeneity in biofilms. *Nature reviews. Microbiology* **6**, 199-210, doi:10.1038/nrmicro1838 (2008).
105 Degennes, P. G. Dynamics of Entangled Polymer-Solutions .1. Rouse Model. *Macromolecules* **9**, 587-593, doi:Doi 10.1021/Ma60052a011 (1976).
106 Hild, G. Model networks based on "endlinking" processes: synthesis, structure and properties. *Progress in Polymer Science* **23**, 1019-1149 (1998).
107 Treloar, L. *Physics of Rubber Elasticity*. (Clarendon Press., 1975).
108 Tirumala, V. R. *et al*. Molecular model for toughening in double-network hydrogels. *J Phys Chem B* **112**, 8024-8031, doi:10.1021/jp8002454 (2008).
109 Pamp, S. J., Sternberg, C. & Tolker-Nielsen, T. Insight into the microbial multicellular lifestyle via flow-cell technology and confocal microscopy. *Cytometry A* **75**, 90-103, doi:10.1002/cyto.a.20685 (2009).
110 Bjarnsholt, T. *et al*. The in vivo biofilm. *Trends Microbiol* **21**, 466-474, doi:Doi 10.1016/J.Tim.2013.06.002 (2013).
111 Watters, C. *et al*. Pseudomonas aeruginosa biofilms perturb wound resolution and antibiotic tolerance in diabetic mice. *Med Microbiol Immunol* **202**, 131-141, doi:10.1007/s00430-012-0277-7 (2013).
112 Rickard, A. H., Gilbert, P., High, N. J., Kolenbrander, P. E. & Handley, P. S. Bacterial coaggregation: an integral process in the development of multi-species biofilms. *Trends Microbiol* **11**, 94-100 (2003).
113 Leriche, V., Briandet, R. & Carpentier, B. Ecology of mixed biofilms subjected daily to a chlorinated alkaline solution: spatial distribution of bacterial species suggests a protective effect of one species to another. *Environ Microbiol* **5**, 64-71 (2003).
114 Burmolle, M. *et al*. Enhanced biofilm formation and increased resistance to antimicrobial agents and bacterial invasion are caused by synergistic interactions in multispecies biofilms. *Appl Environ Microbiol* **72**, 3916-3923, doi:10.1128/AEM.03022-05 (2006).

115 Stacy, A. *et al*. Bacterial fight-and-flight responses enhance virulence in a polymicrobial infection. *Proceedings of the National Academy of Sciences of the United States of America* **111**, 7819-7824, doi:10.1073/pnas.1400586111 (2014).
116 Colvin, K. M. *et al*. The Pel and Psl polysaccharides provide Pseudomonas aeruginosa structural redundancy within the biofilm matrix. *Environ Microbiol* **14**, 1913-1928, doi:10.1111/j.1462-2920.2011.02657.x (2012).
117 Borlee, B. *et al*. *Pseudomonas aeruginosa* uses a cyclic-di-GMP-regulated adhesin to reinforce the biofilm extracellular matrix. *Molecular Microbiology* **75**, 827-842 (2010).
118 Gordon, J. *The new science of strong materials*. (Walker and COmpany, 1968).
119 Korstgens, V., Flemming, H. C., Wingender, J. & Borchard, W. Uniaxial compression measurement device for investigation of the mechanical stability of biofilms. *J Microbiol Methods* **46**, 9-17 (2001).
120 Jones, W. L., Sutton, M. P., McKittrick, L. & Stewart, P. S. Chemical and antimicrobial treatments change the viscoelastic properties of bacterial biofilms. *Biofouling* **27**, 207-215, doi:10.1080/08927014.2011.554977 (2011).
121 Huse, H. K. *et al*. Parallel evolution in Pseudomonas aeruginosa over 39,000 generations in vivo. *Mbio* **1**, doi:10.1128/mBio.00199-10 (2010).
122 Franklin, M. J., Nivens, D. E., Weadge, J. T. & Howell, P. L. Biosynthesis of the Pseudomonas aeruginosa Extracellular Polysaccharides, Alginate, Pel, and Psl. *Front Microbiol* **2**, 167, doi:10.3389/fmicb.2011.00167 (2011).
123 Stewart, P. S. Biophysics of biofilm infection. *Pathog Dis* **70**, 212-218, doi:Doi 10.1111/2049-632x.12118 (2014).
124 Garland, A. L. *et al*. Molecular basis for pH-dependent mucosal dehydration in cystic fibrosis airways. *Proceedings of the National Academy of Sciences of the United States of America* **110**, 15973-15978, doi:10.1073/pnas.1311999110 (2013).
125 Mall, M., Grubb, B. R., Harkema, J. R., O'Neal, W. K. & Boucher, R. C. Increased airway epithelial Na+ absorption produces cystic fibrosis-like lung disease in mice. *Nat Med* **10**, 487-493, doi:10.1038/nm1028 (2004).
126 Chew, S. C. *et al*. Dynamic remodeling of microbial biofilms by functionally distinct exopolysaccharides. *Mbio* **5**, e01536-01514, doi:10.1128/mBio.01536-14 (2014).
127 Brown, G. D. & Gordon, S. Immune recognition. A new receptor for beta-glucans. *Nature* **413**, 36-37, doi:10.1038/35092620 (2001).
128 Ma, L. *et al*. Assembly and development of the Pseudomonas aeruginosa biofilm matrix. *Plos Pathog* **5**, e1000354, doi:10.1371/journal.ppat.1000354 (2009).
129 Mahenthiralingam, E., Campbell, M. E. & Speert, D. P. Nonmotility and phagocytic resistance of Pseudomonas aeruginosa isolates from chronically colonized patients with cystic fibrosis. *Infect Immun* **62**, 596-605 (1994).
130 Holloway, B. Genetic recombination in *Pseudomonas aeruginosa*. *Journal of General Microbiology* **13**, 572-581 (1955).
131 Kirisits, M., Prost, L., Starkey, M. & Parsek, M. Characterization of colony morphology variants isolated from *Pseudomonas aeruginosa* biofilms. *Applied and Environmental Microbiology* **71**, 4809-4821 (2005).
132 Jacobs, M. *et al*. Comprehensive transposon mutant library of Pseudomonas aeruginosa. *Proceedings of the National Academy of Sciences of the USA* **100**, 14339–14344 (2003).
133 Hutchison, J. *et al*. Single-cell control of initial spatial structure in biofilm development using laser trapping. *Langmuir* **30**, 4522-4530 (2014).

134 Walters, M. C., 3rd, Roe, F., Bugnicourt, A., Franklin, M. J. & Stewart, P. S. Contributions of antibiotic penetration, oxygen limitation, and low metabolic activity to tolerance of Pseudomonas aeruginosa biofilms to ciprofloxacin and tobramycin. *Antimicrob Agents Chemother* **47**, 317-323 (2003).
135 Starkey, M. *et al*. Pseudomonas aeruginosa rugose small-colony variants have adaptations that likely promote persistence in the cystic fibrosis lung. *Journal of Bacteriology* **191**, 3492-3503 (2009).
136 Tabata, Y. & Ikada, Y. Effect of the size and surface charge of polymer microspheres on their phagocytosis by macrophage. *Biomaterials* **9**, 356-362 (1988).
137 Li, K. J. *et al*. Membrane Transfer from Mononuclear Cells to Polymorphonuclear Neutrophils Transduces Cell Survival and Activation Signals in the Recipient Cells via Anti-Extrinsic Apoptotic and MAP Kinase Signaling Pathways. *PloS one* **11**, e0156262, doi:10.1371/journal.pone.0156262 (2016).
138 Valgardsdottir, R. *et al*. Human neutrophils mediate trogocytosis rather than phagocytosis of CLL B cells opsonized with anti-CD20 antibodies. *Blood* **129**, 2636-2644, doi:10.1182/blood-2016-08-735605 (2017).
139 Taylor, R. P. & Lindorfer, M. A. Fcgamma-receptor-mediated trogocytosis impacts mAb-based therapies: historical precedence and recent developments. *Blood* **125**, 762-766, doi:10.1182/blood-2014-10-569244 (2015).
140 Kaklamani, G., Cheneler, D., Grover, L. M., Adams, M. J. & Bowen, J. Mechanical properties of alginate hydrogels manufactured using external gelation. *J Mech Behav Biomed Mater* **36**, 135-142, doi:10.1016/j.jmbbm.2014.04.013 (2014).
141 BLANSHARD, J. R. M. J. M. V. RHEOLOGICAL PROPERTIES OF ALGINATE GELS. *Journal of Texture Studies* (1976).
142 Schmitt, A. *et al*. Calcium alginate gels as stem cell matrix-making paracrine stem cell activity available for enhanced healing after surgery. *PloS one* **10**, e0118937, doi:10.1371/journal.pone.0118937 (2015).
143 Størker T.Moe, K. I. D., Gudmund Skjåk-Bræk, Olav Simdsrød. Temperature dependence of the elastic modulus of alginate gels. *Carbohydrate Polymers* **19**, 279-284 (1992).